



UNIVERSITY OF NAIROBI

**EVALUATION OF EFFECTIVENESS OF NON DESTRUCTIVE TESTING
TECHNIQUES FOR INSPECTION OF CRITICAL AIRCRAFT COMPONENTS:
A CASE OF THE KENYAN AVIATION INDUSTRY**

By

Benedetta Margaret Kikechi, BSc(Chem)

A thesis submitted to the Graduate School in partial fulfillment of the requirements for the award
of Master of Science degree in Nuclear Science of the University of Nairobi

January 2020

DECLARATION

This Thesis is my original work and has not been presented for a degree in any other University.

Benedetta Margaret Kikechi, **S56/84530/2016**
Institute of Nuclear Science and Technology, University of Nairobi

Sign -----

Date -----

SUPERVISORS' APPROVAL

This thesis has been submitted with our knowledge as university supervisors:

- 1) Mr Michael J. Mangala,
Lecturer, Institute of Nuclear Science and Technology, University of Nairobi.

Sign

Date

- 2) Dr Lydia A. Olaka,
Lecturer, Department of Geology, University of Nairobi.

Sign.....

Date.....

- 3) Dr John N. Kimani,
Director General/Chief Executive Officer, Kenya Space Agency

Sign.....

Date.....

DEDICATION

This research work is dedicated to; my late dad, Joseph Kikechi, my mum, Petronillah Nafula Kikechi, my late brother, Cleophas Wekesa Kikechi, my son , Pavel Joseph Kikech Wasike and my daughter, Pearl Nafulah Wasike.

ACKNOWLEDGMENT

I would like to express my sincere appreciation and gratitude, for the help and support I got from all that made this work a success. I thank Mr Michael Mangala, Dr Lydia Olaka and Dr John Kimani, my project supervisors for their guidance, encouragement, advice, support and criticism. I thank Lieutenant General (Rtd), S. N. Thuita and Major General, F. O. Ogolla for their overwhelming support in my studies. I give gratitude to the staff of the Institute of Nuclear Science and Technology for their support, during the project research period. I thank the Non- Destructive Testing (NDT) personnel of a Commercial Airline at Jomo Kenyatta International Airport (JKIA) and at the security department, for their support during my research work. I am grateful to the commercial airline and the security department for allowing me to use their equipment in the Non Destructive Testing Laboratory. I thank the University of Nairobi for granting me the scholarship for the study.

I want to express gratitude to my family; brothers, sisters, cousin Agrippina, husband and children for their unfailing support while I was studying. I also thank my classmates, year 2016, for their social and moral support. Finally, I am grateful to God for the gift of life, good health, wisdom and protection which enabled me to study without disruptions.

ABSTRACT

Aircraft structural defects account for 33.3% of the aviation accidents in Kenya. This study evaluated the effectiveness of four types of NDT methods; ultrasonic inspection, radiography, visual testing and magnetic particle inspection being used in aviation industry, specifically for their sensitivity, accuracy, and reliability. It involved the use of in-service aircraft engine and landing gear components to evaluate structural defects during scheduled and unscheduled maintenance. This study was motivated by the need to improve our understanding and application of different NDT methods in defect identification in critical aircraft components. One hundred and one (101) aircraft samples were inspected at the following NDT Laboratories; Institute of Nuclear Science and Technology, University of Nairobi, a commercial airline in JKIA and in the security department, between July 2017 – April 2019. The results show that 50% of all the components inspected for landing gears assemblies had crack defects (1.9 mm-14.8 mm), while the engine components, had the cracks defects (1.00 mm- 220 mm), with highest proportion in combustion chamber and the turbine sections at (24.4% each), followed by the exhaust section at 14.6%. Other engines components had less than 10% of other defects; corrosion, disbond and delamination. In this study, the following defects were found; cracks (60%), corrosion (6%), delamination (2%), disbond defects (2%). Twenty nine samples (30%) had no defects. In conclusion, the study identified the structural defects in the landing gears and engine components; fatigue cracks, corrosion, delamination and disbond defects, using four NDT methods. The most effective NDT method for use in routine inspection of aircraft is boroscopic, which was sensitive to small size defects (> 2.5 mm) with the highest Probability of Detection (POD) at the 95% confidence limits. Visual inspection by magnifying glass is generally sensitive to larger size defects (>56.2 mm). MPI method is appropriate in defect detection of both surface and subsurface defects of ferrous materials. The application of UT method was appropriate for use to subsurface defects. The study recommends; to increase the frequency of aircraft inspections and further research on corrosion related defects upon recommendation to and approval by Original Equipment Manufacturers (OEM). The results of this study will contribute to improved safety regime and maintenance regime in the aviation industry in Kenya for extended aircraft service life, considering that aircrafts operate in the tropical climatic conditions and are prone to high rates of wear and tear of components.

LIST OF ABBREVIATIONS AND ACRONYMS

AAIB	Air Accidents Investigation Branch
AAID	Air Accident Investigation Department
AIMI	African Inland Mission International
ASME	American Society of Mechanical Engineer
ASNT	American Society of Non Destructive Testing
BHEC	Bolt Hole Eddy Current
BVID	Barely Visible Impact Damage
EC	Eddy Current
EP	Engine Part
FOD	Foreign Object Damage
GE	General Electric
GASP	Global Aviation Safety Plan
HKJK	ICAO Aerodrome Designation for JKIA
HKWL	ICAO Aerodrome Designation for WL
ICAO	International Civil Aviation Organization
JKIA	Jomo Kenyatta International Airport
LGP	Landing Gear Part
LCF	Low Cycle Fatigue
KCAA	Kenya Civil Aviation Authority
KQ	Kenya Air Ways
MLG	Main Landing Gear
MPT	Magnetic Particle Testing
MM	Millimeters
NASA	National Aeronautics and Space Administration
NDE	Non Destructive Evaluation
NDI	Non Destructive Inspection

NTSB	National Transportation Safety Board
NLG	Nose Landing Gear
NDT	Non Destructive Testing
OEM	Original Equipment Manufacturer
POD	Probability of Detection
PTO	Power Take-Off
PT	Penetrant Testing
ROK	Republic Of Kenya
RT	Radiographic Testing
TBO	Time Between Overhaul
UKCAA	United Kingdom Civil Aviation Authority
UT	Ultrasound Testing
VT	Visual Testing

TABLE OF CONTENT

DECLARATION	i
DEDICATION	ii
ACKNOWLEDGMENT	iii
ABSTRACT	iv
LIST OF ABBREVIATIONS AND ACRONYMS	v
TABLE OF CONTENT	vii
LIST OF FIGURES	xi
LIST OF TABLES	xiii
CHAPTER ONE: INTRODUCTION.....	1
1.1 Background.....	1
1.2 Problem Statement	3
1.3 Objectives	4
1.3.1 General Objective	4
1.3.2 Specific Objectives	4
1.4 Justification of the Study	4
1.5 Scope, Limitations and Assumptions	5
CHAPTER TWO: LITERATURE REVIEW.....	7
2.1 Overview.....	7
2.2 Theory of Non- Destructive Testing Methods for Inspection.....	7
2.2.1 Visual Testing.....	7
2.2.2 Radiographic Testing	8
2.2.3 Liquid Penetrant Testing	8
2.2.4 Magnetic Particle Testing	9
2.2.5 Eddy Current Testing.....	9
2.2.6 Ultrasonic Testing.....	9
2.2.7 Thermography	10
2.3 POD Analysis for NDI method effectiveness	10
2.4 Types of Structural Defects in aircraft components.....	11
2.4.1 What causes structural failure?.....	11
2.4.2 Fatigue Defects.....	11

2.4.3 Delamination Defects	12
2.4.4 Corrosion Defects	13
2.5 Review of Studies on Evaluation of Structural Defects in Aircraft: NDT Applications	13
2.6 Summary of the Literature Review	19
CHAPTER THREE: METHODOLOGY	21
3.1 Introduction.....	21
3.2 Description of the Landing Gear Assembly	22
3.3 Description of Engine Assembly	25
3.4 The Equipment, Instrument and Inspection Procedures.....	25
3.4.1 Stationary Magnetic Particle Inspection Unit	25
3.4.2 Ultrasonic Inspection Machine- Phased Array.....	28
3.4.3 Visual Inspection by Magnifying glass	29
3.4.5 Radiographic Inspection Machine	33
3.4.6 Other Facilities and Accessories	35
3.5 Inspection Methods Used in identification of Aircraft structural Defects	35
3.6 Data collection: NDT Inspections of aircraft components	36
3.7 Statistical Data Analysis	37
3.8 Criteria for Acceptance.....	38
CHAPTER FOUR: RESULTS AND DISCUSSIONS	39
4.1 Introduction.....	39
4.2 Quality Assurance Tests	39
4.3 Results of NDT Measurements and Defect Evaluations	39
4.3.1 Structural Defects Distributions in Aircraft Components.....	39
4.4 The Characterization of Aircraft Components Structural Defects.....	44
4.4.1 Fatigue Cracks	44
4.4.2 Corrosion Defects	46
4.4.3 Delamination Defects	47
4.4.4 Disbonds.....	47
4.5 Statistical analysis of the NDT Data	49
4.6 The probable causes of the defects in the aircraft parts and the corrective actions	53

CHAPTER FIVE: CONCLUSION AND RECOMMENDATIONS	55
5.1 Introduction.....	55
5.2 Conclusion	55
5.3 Recommendations	56
REFERENCES	57
APPENDICES	61
Appendix 1: Non Destructive Inspection Data Form.....	62
Appendix 2: A typical record of MPI data of a commercial airline	65
Appendix 3: Copy of UT Equipment Model; USD-15S Calibration Certificate	66
Appendix 4: Personnel Qualifications Certificates.....	67
Appendix 5 : Landing Gear Defects and Record Sheet for Stator Plates.....	69
Appendix 6: Landing Gear Defects and Record Sheet for Torque Tubes	69
Appendix 7: Landing Gear Defects and Record Sheet for Pressure Plates	70
Appendix 8: Landing Gear Defects and Record Sheet for Wheel Hub Tie Bolts	70
Appendix 9: Landing Gear Defects and Record Sheet for Wheel Hub Drive Keys using MPI method.....	71
Appendix 10: Landing Gear Defects and Record Sheet for Wheel Hub Drive Keys using UT method	71
Appendix 11: Landing Gear Defects and Record Sheet for Landing Gear.....	72
Appendix 12: Compressor Section Defects and Record Sheet.....	72
Appendix 13: Combustion Section Defects and Record Sheet	72
Appendix 14: Turbine Section Defects and Record Sheet	73
Appendix 15: Exhaust Section Defects and Record Sheet.....	73
Appendix 16: Other Sections Defects and Record Sheet	73
Appendix 17: Radiographic Inspection of Landing Gear Parts.....	74
Appendix 18: Visual (Magnifying Glass) Inspection of Engine Compressor Rotor Spool	75
Appendix 19: Photo of Compressor Spool.....	76
Appendix 20: MPI Data for Bearing Lock Nut	77
Appendix 21: Photos of Defects on The Bearing Locknut (Around the holes)	78
Appendix 22: Photos of Defects on The Bearing Locknut (Along the nut threads).....	79
Appendix 23: MPI of Engine Compressor Rotor Spacer Disc	80
Appendix 24: Photos of Engine Compressor Section.....	81
Appendix 25: Visual (Magnifying Glass) Inspection of Combustion Section.....	82

Appendix 26: Photos of Combustion Liner showing cracks	83
Appendix 27: Photos of Defects on the Combustion Liner.....	84
Appendix 28: Visual (Borosopic) Inspection of Engine Turbine Section.....	85
Appendix 29: Photos of Aircraft Engine Power Turbine	86
Appendix 30: Visual (Magnifying Glass) Inspection of Engine Turbine Section.....	87
Appendix 31: Photos of Defects on Stage Two Nozzle	88
Appendix 32: Photos of Cracks on Stage 2 Stator Blades	89
Appendix 33: Visual (Borosopic) Inspection of Engine Turbine Section.....	90
Appendix 34: Photos of the broken Free Turbine Blades	91
Appendix 35: MPI of Engine Bevel Shaft Gear	92
Appendix 36: Photos of PTO Driver Shaft Gear	93
Appendix 37: Visual (Magnifying Glass) Inspection of Engine Exhaust Section parts	94
Appendix 38: Photos of Engine Cracked Flame Holder	95
Appendix 39: Photos of Engine Cracked Flame Holder along the Weld	96
Appendix 40: Crack on Engine Flame Holder Duct.....	97
Appendix 41: Visual (Magnifying Glass) Inspection of Engine Exhaust Section Parts.....	98
Appendix 42: Photos of Cracked Afterburner Assembly.....	99
Appendix 43: Visual (Magnifying Glass) Inspection of other Engine Parts.....	100
Appendix 44: Photos of Oil Sump Crank Case Mating Surfaces (Interior surface)	101
Appendix 45: Photos of Oil Sump Crank Case Mating Surfaces (Exterior surface).....	102
Appendix 46: Visual (Magnifying Glass) Inspection of Engine Parts.....	103

LIST OF FIGURES

Figure 1.1: Threats to Aircraft Structural Safety	2
Figure 3.1: The Boeing 737 Brake Assembly 3D	22
Figure 3.2: The Boeing 737 Main Landing Gear Wheel Assembly	23
Figure 3.3: The Boeing 737 Nose Landing Gear Wheel Assembly	23
Figure 3.4: The Helicopter Landing Gear Assembly	24
Figure 3.5: The Engine Assembly	25
Figure 3.6: The Stationary MPI equipment:	26
Figure 3.7: The Magnetic Yoke.....	26
Figure 3.8: Flux Leakage from Surface and Subsurface discontinuities.....	27
Figure 3.9: The ultrasonic inspection equipment.....	28
Figure 3.10: The magnifying glass	30
Figure 3.11: Parts of everest borescope.	31
Figure 3.12: Photo of everest borescope	32
Figure 3.13: Radiography-X-Ray machine.	33
Figure 3.14: Radiography- X-Ray control unit.....	34
Figure 4.1: Distribution of Cracks in Brake Assembly Components.	40
Figure 4.2: Distribution of Cracks in Wheel Assembly Components.....	41
Figure 4.3: Distribution of Cracks in Engine Assembly Components.....	42
Figure 4.4: Distribution of Defects in Engine Assembly Components.....	43
Figure 4.5: Boroscopic Image of Longitudinal Crack defect in the Engine Exhaust Section.	45
Figure 4.6: Boroscopic Image showing Transverse Crack defect in the Engine Exhaust Section.....	45
Figure 4.7: Corrosion defect in the aircraft Engine Compressor Section	46
Figure 4.8: Filiform Corrosion under paint coating on the other parts of the Engine	46
Figure 4.9: Delamination defect in the other aircraft Engine parts.....	47
Figure 4.10: A disbond defect in the other Engine Sections.	47
Figure 4.11: Prevalence of Defects in aircraft samples.....	48
Figure 4.12: A Summary of Frequency of use of NDT Methods	49
Figure 4.13: POD Curve for Visual (Magnifying Glass).	50
Figure 4.14: POD Curve for Visual(Boroscopic) Inspection.	51

Figure 4.15: POD Curve for Magnetic Particle Inspection Method.51
Figure 4.16: POD Curve for Ultrasonic Inspection Method.52

LIST OF TABLES

Table 3.1: Landing Gear Defects and Inspection Methods	35
Table 3.2: Engine Defects and Inspection Methods	36
Table 4.1: Actual Defect Sizes from the POD Curves.....	52

CHAPTER ONE: INTRODUCTION

1.1 Background

Air transport plays a major role in driving sustainable economies and social development worldwide. According to the Global Aviation Safety Plan of 2014-2016 (GASP, 2013), air transport supports directly and indirectly, the employment of over 56.6 million, facilitates transportation of over 2.5 billion passengers and cargo and generates USD 5.3 Trillion annually. In Africa, the aviation industry is rapidly growing because, in many countries, road and rail transport network systems are not well developed in most parts, as such, many countries invest in local airlines by way of partnership. For example, Kenya Airways is a public-private partnership company in which, the Government of Kenya has 29.8% stake followed by KLM, with 26.73% stake, in the company ownership, (ROK, 2012).

The two main challenges facing the Kenyan Aviation Industry are high cost of servicing and maintenance of aircrafts. In general, stretched maintenance time intervals and extended aircraft lifetime, have resulted in development of structural defects such as cracks, corrosion, delamination and voids in the aircraft critical components over a period of time (Hagemaiier, 1990). This therefore requires inspection methods, which do not require long turnaround times for in-service inspections that are fast, cost effective and reliable.

Nondestructive testing (NDT) is an examination or test evaluation method performed on any type of object without changing or altering it in any way, in order to determine the presence of discontinuities that may have an effect on the usefulness and serviceability of that component (USAF, 2014) . Nondestructive tests may also be conducted to measure other characteristics, such as; size, dimension, configuration, or structure, including alloy content, hardness, grain size, etc (Hellier, 2003).

NDT gives information on the nature, size and location of flaws. The information obtained is then evaluated and decisions made based on severity and danger of flaws in their current state; whether to repair, to scrap, or to allow the affected component to continue in service for a given duration without any compromise on safety (Birir, 2015).

Cracks and other subsequent component failures due to fatigue and corrosion are major threats to aircraft structural safety as shown in Fig.1.1. In general, cracks originate from manufacturing

processes, material defects, high local stresses; design errors or specimen deficiencies, environmental damage and service induced maintenance deficiencies. Other minor causes are; bird strikes, unattended tools, Foreign Object Damage (FOD) and unchecked engine rotor failures (Tiffany, Gallagher, Babish, & Charles, 2010).

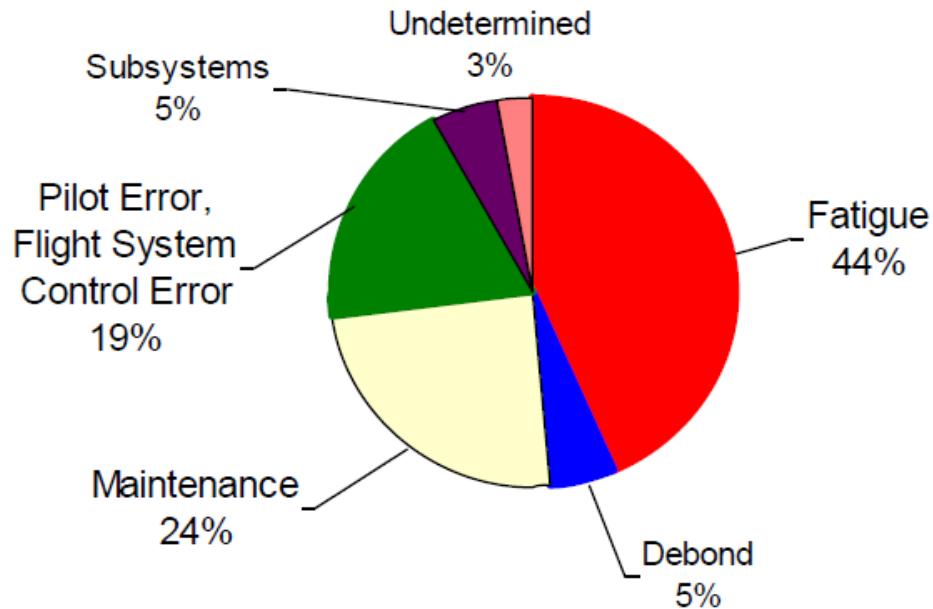


Figure 1.1: Threats to Aircraft Structural Safety (Tiffany, et al. , 2010)

The NDT methods are considered most promising tools for use in inspection of defects in critical aircraft components. The different NDT applications range from; in marine and wheeled vessels, such as fuel tankers and vehicles, to concrete structures, such as buildings and bridges.

Some of the common NDT techniques used include; visual inspection, dye penetrant testing, magnetic particle testing, radiographic testing, ultrasonic testing and eddy current testing. These methods have been used in the examination of raw materials prior to processing, evaluation of materials during processing as a means of process control examination of finished products and for evaluation of products and structures once they have been put into service ((Hellier, 2003).

Currently, the most used method to determine the effectiveness and sensitivity of any NDT technique is through the assessment of Probability of Detection (POD) curves. A POD curve estimates the capacity of detection of an inspection technique in regard to discontinuity size (Da Silva & de Padua, 2012).

The applicability and suitability of the different types of NDT methods for inspection of aircraft structures owing to its complexity of aircraft systems is critical in enhancing air transport safety, in addition to reduction in aircraft turnaround times and re-organization of their maintenance schedules. It is on this basis, that this study was undertaken in order to contribute to the local efforts to enhance air transport safety and aircraft maintenance.

1.2 Problem Statement

The need for sustainable reliable air safety and reduced aircraft turnaround time while maintaining high number of aircraft is an ever-present challenge in any aviation industry. The main cause of aviation accidents in Kenya is mechanical problems, which accounts for 33.3% of the accidents. Others include; pilot error at 19.4%, bird strikes at 2.8%, runway excursions and ground operations at 8.3%, collisions with other planes at 5.6%, cabin safety (5.6%) and weather (8.3%), (Mariera, 2013). These figures cast aspersions to the quality of maintenance of aircrafts in Kenya as well as the quality of aviation professionals such as pilots, engineers and crew, both in ground maintenance and in flight.

The conventional inspection methods currently used include; old radiographic inspection method, conventional ultrasound and non-aided visual inspection. These methods might not be able to identify the early onset of structural failure of critical aircraft components caused by operation in tropical climatic conditions and in open air aircraft parking areas within the airports. Therefore, applying appropriate complementary methods, like; digital radiography, advanced ultrasound technique optically aided inspection and incorporating statistical methods and elements of probability; R software to generate POD curves, will lead to improved maintenance standards and safety.

1.3 Objectives

1.3.1 General Objective

The general objective of this study is to evaluate the effectiveness of four Non Destructive Testing methods for the inspection of critical aircraft components for serviceability in Kenyan aviation industry.

1.3.2 Specific Objectives

The specific objectives are;

- 1) To identify structural defects in the following critical in service aircraft components; landing gears and engine parts of the aircraft using four (4) NDT methods; radiography, visual inspection, ultrasonic and magnetic particle inspection;
- 2) To characterize aircraft components structural defect ;
- 3) To assess the effectiveness of NDT methods and advise on the most effective NDT methods for use in routine aircraft inspection.

1.4 Justification of the Study

There are serious concerns over the aviation safety, maintenance standards and procedures used in the aviation industry. The expansion of the aviation sector has led to increased number of aircraft operating within the country that require strong maintenance regimes.

Air Safety is one of Kenya Airways (KQ) core mandate and it is clearly stipulated in the mission statement. The airline has invested heavily in safety training of its employees; cabin and pilots as regulated by Kenya Civic Aviation Authority. Other mandatory safety trainings are undertaken during initial training, and thereafter, yearly refresher training which include Safety Emergency and Procedure Training (SEPT), First Aid and Ditching.

Kenya Airways for instance has recorded losses for the last two consecutive years something which has not gone down well with a number of stakeholders in the industry. Although immense pressure has been on the financial performance, air safety performance is also a key area that needs serious consideration. In Kenya, there exists a gap in research given that most studies done on

airline safety performance have been done in other jurisdictions with no particular study done on airline safety in Kenya.

In addition, operation of the aircraft in country's tropical environmental conditions can make them prone to excessive corrosion and structural damage due to conventional rainfall, lightning strikes, hailstones and open air parking (IAEA, 2003). These defects, when they go undetected, which to some extent would otherwise be detected by application of appropriate NDT methods, cause fatalities and injuries related to air incidents and accidents.

The advantages of NDT inspections in aircraft maintenance are; reduced aircraft downtime, reduced maintenance costs and improved aviation safety standards. In general, the aviation safety assurance has profound economic benefit in long term potential or investment venture. The findings of this study are expected to form the basis for developing policies for a continuous improvement of the maintenance standards in the aviation industry.

To the best of my knowledge, no scientific studies have been done locally on the evaluation of effectiveness of different NDT methods in detection of defects for engine and landing gear serviceability.

1.5 Scope, Limitations and Assumptions

This study was limited to the following:

- 1) The one hundred and one (101) engine and landing gear parts from different aircraft types that were available in the commercial airline and security sector.
- 2) The timings of the various maintenance schedules because each aircraft that was inspected had its own maintenance program. The accessibility of some of the areas of inspection interests was a challenge.
- 3) Facility: All the equipment and instruments that were used in the study had been calibrated in accordance with the equipment and instrument calibration manuals.
- 4) Inspectors: The personnel that assisted in the inspection exercise were NDT trained, equivalent to level I, II and III in methods. The personnel were also regularly monitored for radiation exposures.
- 5) Specimen preparation: Focused on factors such as part cleaning, preparation and surface condition checking.

- 6) All the inspections were carried out in accordance with the requirements in the aircraft service manuals and the standard practices.
- 7) The inspections were done during scheduled and non-scheduled maintenance period between July, 2017 – April, 2019.
- 8) The actual identity of the locations and details of assistant NDT inspectors has concealed due to security concerns.
- 9) The details of the aircraft operators are also not specified due to ethical reasons.

CHAPTER TWO: LITERATURE REVIEW

2.1 Overview

This chapter presents a review and a detailed discussion on Non Destructive Testing methods being used in the aviation industry followed by a review of past and recent studies on NDT methods in support of the current study.

2.2 Theory of Non- Destructive Testing Methods for Inspection

The following seven (7) NDT techniques are discussed in the subsequent sections.

2.2.1 Visual Testing

Direct visual and optically aided inspection is applied to the surface of object to detect flaws and anomalies. Direct visual testing is defined as using “*visual aids such as mirrors, telescopes, cameras, or other suitable instruments to detect flaws*”. The direct visual examination is conducted when access allows the eye to be within 12 inches (300mm) of the surface to be examined, and at an angle not less than 30° to the surface to be examined (Hellier, 2003) (as illustrated in Fig. 2.1. Remote visual testing uses: borescopes, fiberscopes, and video technology (Hellier, 2003)

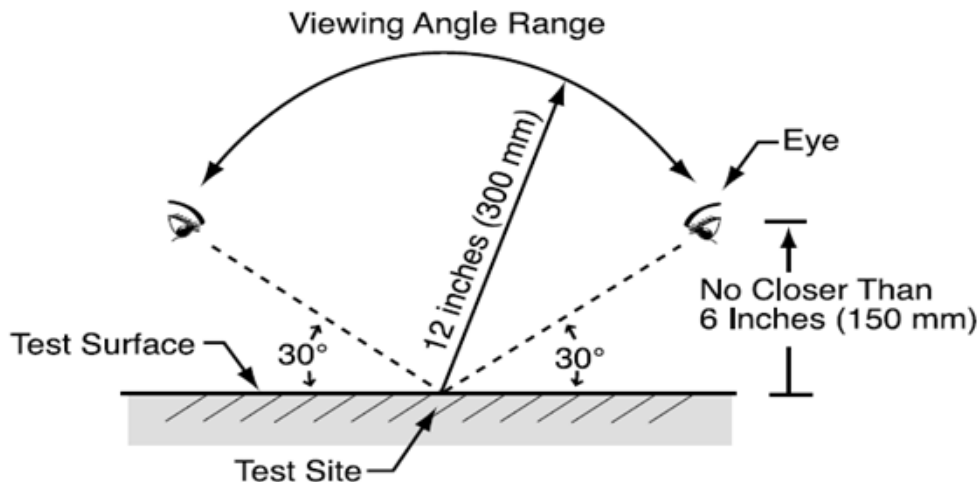


Figure 2.1 : Minimum Angle for typical Visual Testing (Hellier, 2003).

This method has a limitation of detecting only surface cracks and it is dependent on the visual and observation capabilities of the inspector. However, this procedure is mainly used as a fast monitoring method for failures particularly after the aircraft has landed and it is ready for takeoff after few minutes or hours (Hellier, 2003).

2.2.2 Radiographic Testing

Radiographic inspection is a nondestructive method suitable for inspecting materials for surface, subsurface and internal discontinuities like cracks, delamination and corrosion (Ansley, Bakanas, Castronuovo, & Grant, 1992). This method is applied during inspection of inaccessible areas in the aircraft airframe structure or other sections which do not offer themselves to inspection through other NDT methods. This is made possible by transmitting an X-Ray or Gamma-Ray beam through the aircraft part or an assembly being inspected. The transmitted beam impinges on a radiographic film or detector revealing irregularities. The essential details of the aircraft part or an assembly will be displayed by variations in density on film or a video display. This variation is then measured and recorded on a film in form of an image indicating a defect. The amount of light transmitted by a region of processed film is described by the transmittance T, where

$$T = \frac{\text{Amount light transmitted by a region of film}}{\text{Amount light received at the same location with film removed}} \dots\dots\dots (1)$$

The degree of blackening of a region of film is described as the optical density (OD) of the region while the presence of the defect means less OD:

$$OD = \log \frac{1}{T} \dots\dots\dots (2)$$

The interpretation of the radiograph will indicate discontinuities. This method has been applied in inspection of aging aircraft (Ansley et al., 1992) .

2.2.3 Liquid Penetrant Testing

Liquid Penetrant method is the most commonly used NDT method for detection of metallic surface cracks and is extensively used in aviation industry during aircraft production and maintenance (Pitropakis, 2015). It is often used on all ferrous and non-ferrous materials. The method is based on the capillary action of the liquid that penetrates in the crack at the surface of the material. The capillary action of a liquid occurs when the molecules of the liquid have the ability to move using the adhesion forces between the liquid and the solid material under inspection. In that way, the liquid can penetrate into the surface of the material without the aid of gravity and the molecules can be inserted in microscopic cracks (Pitropakis, 2015).

2.2.4 Magnetic Particle Testing

Magnetic Particle Testing has been widely utilized for decades, in detection of defects like cracks, laps, seams, voids, pits, subsurface holes, and other surface, or slightly subsurface, discontinuities in Ferro-magnetic materials. This method relies on the leakage of magnetic flux for the defect detection. Magnetization of the test specimen is done by either circular or longitudinal methods (Burke & Ditchburn, 2013).

2.2.5 Eddy Current Testing

Eddy current inspection is used to detect surface or near-surface cracks in metals, to detect thinning of metals due to corrosion and to sort metals or alloys and their heat treat conditions. High frequency eddy current techniques can be applied to airplane parts or assemblies where the defective area is accessible to contact by the eddy current probe. Low frequency techniques are used to detect cracks or corrosion on back surfaces or cracks in underlying structure. The inspection is performed by inducing eddy currents into a part and electronically observing variations in the induced field (Ansley et al., 1992).

The eddy current method is used in various major fields; In-service inspection of tubing at nuclear and fossil fuel power utilities, at chemical and petrochemical plants, on nuclear submarines, and in air conditioning systems, Inspection of aerospace structures and engines and production testing of tubing, pipe, wire, rod, and bar stock (Hellier, 2003).

2.2.6 Ultrasonic Testing

Ultrasonic Testing uses sound waves with frequencies ranges from 500 kHz to 10 MHz which travel freely in liquid and solid mediums and are more directional than audible sound waves. The waves can propagate in two modes namely; longitudinal and shear, where longitudinal wave is most common for NDT applications because of its speed and ability to travel in both mediums. Sound waves are generated when voltage difference is applied between any two of a piezo electric material. The quality of inspection relies on the sensitivity and resolution of the equipment (Jolly, et al., 2015). The UT method is used in various major fields; In-service inspection of tubing at nuclear and fossil fuel power utilities, at chemical and petrochemical plants, on nuclear submarines, and in air conditioning systems, Inspection of aerospace structures and engines and production testing of tubing, pipe, wire, rod, and bar stock (Hellier, 2003).

2.2.7 Thermography

Thermography is an NDT method that employs the principle of two dissimilar materials possessing different thermo-physical properties that produce two distinctive thermal signatures that can be revealed by an infrared sensor, for example, the thermal camera. There are two kinds of thermography inspection; the passive and the active. The passive approach tests materials and structures that have the ability to emit thermal energy and is mainly used when the materials are heterogeneous while for the active approach, an external stimulus is necessary to induce relevant thermal contrasts (Maldague, 2002). Thermography inspection as an NDT method has become more and more popular in detecting delamination in composite aircraft components (Ibarra-Castanedo, et al., 2008).

2.3 POD Analysis for NDI method effectiveness

Non-destructive Testing effectiveness is the probability of detecting a crack in a structure using the specified inspection conditions and procedures. The underlying statistical parameter is the POD, which is the measure of quantifying NDT reliability and is expressed as a function of flaw size (i.e. length or depth) as shown in Fig. 2.2. POD determinations are based on data that have already been determined by the various NDT methods on verified defects (Fahr & Forsyth, 1998)

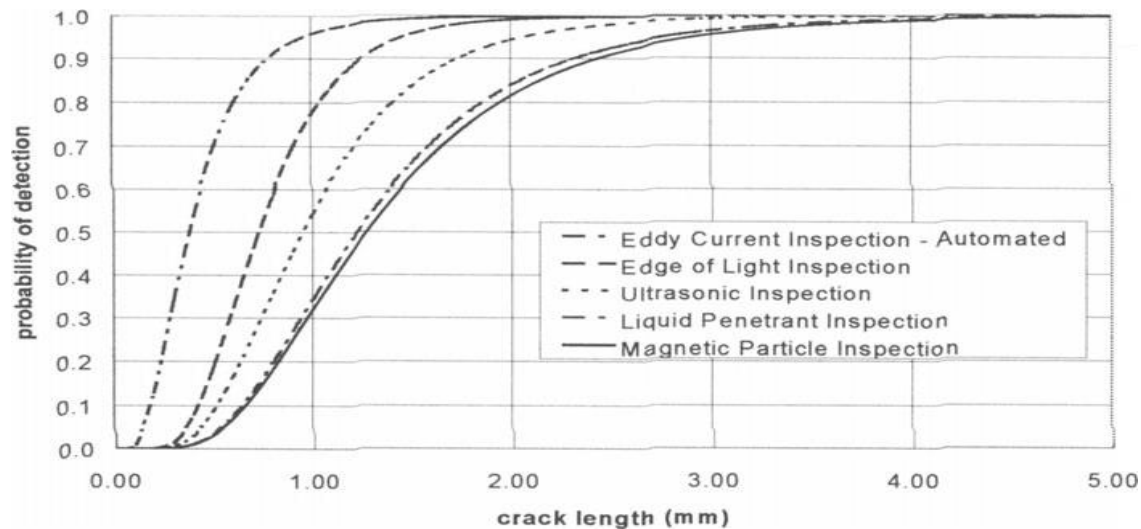


Figure 2.2: POD assessment of NDI Methods (Fahr & Forsyth, 1998)

2.4 Types of Structural Defects in aircraft components

Between 1927 and 1981, an aggregate of one thousand, four hundred and sixty six (1466) fixed-wing aircraft accidents were identified as having component fatigue fracture as a related cause, and these accidents resulted in one thousand, eight hundred and sixty one (1861) deaths. The accidents covered civil and, to a limited extent, military aircraft (Campbell & Lahey, 1983).

An aircraft structural health monitoring study was conducted by (Pfeiffer & Wevers, 2007) under the European Community's Seventh Framework Program. This was to investigate the challenges for damage detection namely; fatigue cracks in Airbus A 380 aircraft, impact damage in the tail boom of the helicopter EC 153, fatigue cracks in the helicopter tail boom of a MI-8, as well as corrosion in floor beams and fatigue damage in double repairs of an Airbus A340.

2.4.1 What causes structural failure?

A study by (Tiffany, et al., 2010) indicated the aircraft structural threats were high local stress, maintenance damages and impact due to bird strikes. The mechanisms of failure were found to be fatigue, corrosion, cracks and overload. These failures occur when an aircraft component or structure is no longer able to withstand the stresses imposed on it during operation due to many reasons including the following:

- 1) The microstructure of the material may contain voids, inclusions etc;
- 2) Service induced maintenance deficiencies;
- 3) Environmental damage such as corrosive attack of the material;
- 4) Manufacturer's defects, e.g. the presence of holes, notches, and tight fillet radii and unforeseen high local stresses resulting from design and analysis errors or test deficiencies (Findlay, & Harrison, 2002).

2.4.2 Fatigue Defects

Fatigue is a process whereby a discontinuity occurs under the influence of repeated or cyclic stresses, which are normally substantially below the nominal yield strength of the material. A crack is a sign of impending component failure that prompts an action when found.

On December 19, 2005, Chalk's Ocean Airways Flight 101 from Fort Lauderdale, Florida, United States to Bimini, Bahamas, crashed in the Government Cut Channel. National Transportation Safety Board (NTSB, 2005) accident report indicated that the probable cause of the accident was a fatigue failure in the right wing initiated by a crack in a span-wise stringer close to the wing root. This was as a result of failure of both to detect and correct deficiencies in the company's maintenance program and to identify and properly repair fatigue cracks in the right wing (NTSB, 2005).

Aloha Airlines Flight 243 (AQ 243, AAH 243) was a scheduled Aloha Airlines flight between Hilo and Honolulu in Hawaii. On April 28, 1988, a Boeing 737-297 serving the flight suffered extensive damage after an explosive decompression in flight. During investigation it was revealed that Eddy Current method had been employed in the scheduled inspection which failed to detect disbonds and fatigue damage that ultimately led to failure of the lap joint at S-10L and the separation of the fuselage upper lobe. It was further discovered that the failure mechanism was a result of multiple site disbonding defects and fatigue cracking and that quality of inspections and maintenance programs were poor (NTSB, 1989).

An accident occurred on May 25, 2002, when a Boeing B747-209B aircraft from China Airlines broke into four pieces, shortly after take-off on the flight from Taiwan Taoyuan International Airport to Hong Kong International Airport. It was found that the accident was due to metal fatigue caused by inadequate maintenance after a much earlier tail strike incident that occurred on 7 February 1980 where, part of the plane's tail scraped along the runway for several hundred feet (China Airlines Flight CI-611 Crash Report Released, 2005). The method that was used to inspect the components was mainly Eddy Current.

2.4.3 Delamination Defects

In laminated materials, repeated cyclic stresses and impact can cause layers to separate, forming a mica-like structure of separate layers, with significant loss of mechanical toughness. Delamination mode of damage is one of the key issues for laminated and bonded composite structures (Hellier, 2003). A notable case of delamination as a structural failure occurred during Flight 578 from American Airlines on 28th April, 1988 (NTSB, 1989). The Airbus A300 had a scheduled flight from John F. Kennedy International airport to Las Américas International Airport in the

Dominican Republic. Shortly after take-off, the plane's stabilizer rudder separated from the body of the aircraft. Seconds later, the jet engines were also separated from the wings and the non-controlled airplane crashed on Belle Harbour, a residential area of New York City killing all 260 people on board and 5 on the ground (NTSB, 1989). The reason of the accident was the delamination on the composite lugs that are used to attach the vertical stabilizer. The delaminations were a result of previous heavy turbulences and the poor maintenance of the aircraft did not consider the delamination a problem. It was also found that the design of the composite lugs was not strong enough to withstand the high stresses that stretch the parts above their limits (NTSB, 1989).

2.4.4 Corrosion Defects

Corrosion is the chemical degradation of metals through interaction with the environment resulting into failure of components. The forms of corrosion that exist in aircraft structures are; uniform corrosion, pitting corrosion, crevice corrosion, galvanic corrosion and stress corrosion (Findlay, & Harrison, 2002).

On 2nd October, 1971, the rear cabin pressure bulkhead of a British European Airways Flight 706 failed. The tail section depressurization caused separation of the tail planes surfaces, thus weakening and breaking off horizontal stabilizer. This led to the aircraft crashing, killing all 63 passengers and crew on impact.

It was found out that the cause of the accident was corrosion that had not been detected by the then-visual inspection techniques in the lower part of the rear pressure bulkhead underneath plating that was bonded to the structure.

2.5 Review of Studies on Evaluation of Structural Defects in Aircraft: NDT Applications

The reliability of non-destructive inspection has been a topic of concern for at least forty years. In 1968, (Packman, Pearson, Owens, & Marchese, 1968) carried out a study on the applicability of a combined fracture mechanics as a Nondestructive Inspection design procedure for aircraft structures. It was an in-depth investigation into the reliability of the four NDT methods namely: radiographic, liquid dye penetrant, magnetic particle and ultrasonic inspection, in regular use for defect detection. It was found that all the NDT methods showed high accuracies in crack location, but not crack length. It was recommended that more research effort should be directed towards

determining the sensitivity, accuracy, and reliability of all NDT methods to detect, locate, and measure all types of flaws in common aerospace materials.

An investigation on the performance of the different NDI procedures; PT, MPT, UT and EC, using ten, service-expired 7th stage compressor disks from the JS5-CAN40 of a military aircraft was carried out by Fahr and Forsyth, (1998). The detection limit of inspection techniques was established and used to calculate safe inspection interval of the Engine Compressor section. A large number of flaws were inspected by the same NDI techniques that were being used during maintenance. Each disk had 40 bolt holes and therefore there were 400 inspection sites which were adequate for POD assessment. After inspection, the existence of cracks was verified by prior opening of bolt holes and measurement of maximum crack length done. For calibration specimens, fatigue cracks were created in forty test specimens prepared from actual Compressor disks in the laboratory. Among the techniques investigated, the results showed that automated Eddy Current procedures had the highest sensitivity and reliability in locating Low Cycle Fatigue (LCF) cracks in the J85 CAN 40 engine components. In addition, the bolt holes had either a single radial crack, through cracks, corner cracks or middle cracks but in the fabricated investigated parts, most of the defects were corner cracks that were difficult to simulate and detect. It was recommended that aircraft parts with real service-induced cracks be used for realistic POD measurements, because it was difficult to make artificial cracks simulating the different shapes, sizes, locations, surface texture and combinations of different types.

A previous study by Fahr and Forsyth, (1998) recommended that aircraft parts with real service-induced cracks be used for realistic POD measurements, due to difficult in making artificial cracks simulating the different shapes, sizes, locations, surface texture.

In the early 1970s, NDT reliability was first quantified using Probability of Detection (POD) as a function of defect size in a Martin Marietta Aerospace project funded by National Aeronautics and Space Administration (NASA) to establish design allowable flaw sizes for the NASA Space Shuttle program. This project investigated the performance of a wide range of inspection techniques including ultrasonic, fluorescent penetrant, radiography, acoustic emission and eddy current. The techniques were optimized for the detection of tightly closed cracks in 2219 T-87

aluminum alloy. The design-allowable flaw sizes adopted by NASA were based on a demonstration of 95% POD with 95% statistical confidence (Harding & Hugo, 2011).

Aircraft fly and operate in harsh climatic conditions that cause structural defects from impacts of a falling tool or of hailstones and lightning. (Garnier, Pastor, Eyma, & Lorrain, 2011) evaluated the efficiency of three NDT methods in the detection of in-situ defects resulting from Barely Visible Impact Damages (BVID) or in-service damages to complex surfaces using; Ultrasonic Testing, Infrared Thermography and Speckle Shearing Interferometry(Shearography). The test specimens were manufactured in the laboratory with surface damages. The results showed that all the defects were revealed by, at least, one of the three NDT methods but only the ultrasonic method enabled the depth of a defect to be determined. It was also found out that Infrared Thermography and Shearography produced results very quickly (in about 10 s) compared to Ultrasonic Testing. Since all the three methods had their own advantages and limitations described, it appeared quite clearly that all the non-destructive methods complemented each other. Further analysis of the results obtained by Shearography was recommended in order to determine the size of the defects, and to develop the theoretical equations in thermography to evaluate their depth.

(Garnier, Pastor, Eyma, & Lorrain, 2011) carried out in situ inspection of different types of aircraft composite parts using three Non Destructive Testing methods; Ultrasonic Testing, Infrared Thermography and Shearography. The aim of the study was to evaluate the effectiveness of the three methods in the detection of in-situ defects from either Barely Visible Impact Damages (BVID) or in-service damages. Determination and measurement of defects, and comparing the results from the three methods and time taken to set up the experiment was analyzed. The defects found in the composite material, were delamination and disbonding. From the study, it was revealed that all the defects were revealed by at least one of the three methods however, Infra-red and shearography produced immediate results compared to UT.

(Kurz, Jüngert, Dugan, Dobmann, & Boller, 2013) carried out experimental POD determination from inspections of fabricated test blocks using two NDT methods; ultrasonic phased array and ultrasonic sampling phased array (SPA). The results of the study showed that SPA technique was better compared to phased array method. Further studies on experimental POD determinations were recommended.

A study was carried out to evaluate the productivity and reliability of non-destructive test (NDT) techniques for the inspection of structural welds by (Babu , Chan , & Chan , 2016). The NDT methods used were; manual ultrasonic, Phased Array Ultrasonic testing (PAUT), and Radiographic Testing to test for; lack of penetration (LP), lack of fusion (LF), crack (CR), porosity (PO) and slag inclusion (S) defects. The results of the study showed that; PAUT was more effective than manual UT by a factor of 4, in terms of; speed of test, and defect size and location detection reliability. The study recommended the application of surface non-destructive testing for structural steel and further field evaluation was recommended to be carried out in order to advance the productivity and reliability of NDT methods in the industry.

POD studies on the reliability of Eddy Current method in inspection aircraft bolt holes was conducted by (Underhil, P, Uemura, & Krause, 2018) and presented in Aeronautical Information Publication Conference Proceeding April 2018. The Bolt Hole Eddy Current (BHEC) was applied in detection of cracks from within bolt holes after fastener removal. The recommendations made included development of a measurement for minimum probe requirements, effect of condition and size ranges of the bolt hole to be inspected on the results and the inspection frequency.

In 1988, a fixed aircraft, Boeing 737-200, N73711, which was being operated by Aloha Airlines as flight number 243, while en route to Honolulu, from Hilo, Hawaii developed problems at 24,000 feet above the sea level. The airframe (cabin) skin and structure aft section of the cabin entrance door were completely separated from the airframe during the flight. According to the Aircraft Accident Report (NTSB, 1989), the probable cause of the accident was found out to be the failure of the Airline's maintenance procedure to detect the presence of significant disbonding and fatigue damage which ultimately led to failure of the joint at Frame S-10L and the separation of upper structure of the fuselage. The NSTB report revealed that general mandatory aircraft inspection was carried on lap joint S-4 only instead of inspection of all the lap joints. This led to the long term effects of disbonding, corrosion, and fatigue cracking in the lap joints. It was recommended that Eddy current inspection in accordance with AD 87-21-08 manual to be carried out in addition to visual inspection.

The AAIB Field Investigation report, 2005, a Grob trainer aircraft, powered by Lycoming AEIO-360-B1F piston engine, being flown by a Royal Air Force Qualified Flying Instructor was involved in a forced landing, after one of propeller blade detached from the hub. The aircraft had been in service for three years (AAIB, 2005). There were no fatalities. Investigation carried out revealed that one of the propeller blades detached from the aluminum alloy hub due to a high-cycle fatigue failure of the blade socket. A safety recommendation focused on review of propeller blade retaining nut maintenance procedures and frequent performance of non-destructive testing of propeller blade sockets to detect fatigue cracks by use of Eddy Current method. The causes of fatigue cracks, most of the components that were inspected during the scheduled maintenance had cracks (90%) which were caused by cyclic loading. The way forward of the investigation report recommendation of review of the maintenance procedures to take into account high frequency of inspection at the intervals of 5, 25, 50, and 100 flying hours. The action that was taken by the propeller manufacturer to issue Service Bulletin 61-10-03 SB E 15 to have OEMs sharing information with aircraft operators through issuing frequent Service Bulletins and Letters advising on new or suggested safety procedures.

Currently, Kenya is facing challenges in the integrity of concrete structures like buildings and bridges (Gatari, Kairu, Maina, & Muia, 2014). In a report presented on the assessment of the quality of reinforced concrete in columns, beams and stairs of buildings within the city of Nairobi using a Rebound Hammer and a Profometer 5+, test Samples were made from locally available materials and measurements obtained and analyzed. It was found that most of the existing buildings (16 %) had very low compressive strength and insufficient reinforcement bars. During the study, it was recommended that NDT using a Schmidt rebound hammer and the Profometer be employed to provide quick and inexpensive means of assessing the safety of new and existing structures as well as the quality of the workmanship and materials used during the construction.

Locally, Non-Destructive testing (NDT) has been applied to well rig inspection to ensure the integrity of geothermal drilling components at the Menengai Geothermal Project in Kenya. The methods employed were; visual inspection, magnetic particle inspection, penetrant testing, ultrasonic testing and electromagnetic inspection. It was found out that having an effective NDT culture would lead to the improvement of the safety standards and other key operations for the Company through cost reduction, improved equipment reliability and accident prevention

(Mulama & Ng'ang'a, 2013). It was recommended that the company invests in NDT equipment acquisition, human resource training and certification in order to cut down on the cost of hiring of expatriates and equipment.

The investigation carried out by the Aircraft Accident Investigation Department (AAID), (ROK, 2013) involved a Boeing 747-200 aircraft of registration GMKJA operated by Airlines Limited under Flight Number BGB 118 that aborted a flight at JKIA on the runway 06 of the airport. There were no reported injuries. Based on service maintenance reports, and from the visual inspection of the engine parts debris that were scattered on the runway, the probable cause of the internal engine structural failure was as a result of engine deterioration that involved compressor blade rapture or wear among other causes. The views of the investigation board are that the United Kingdom Civil Aviation Authority (UKCAA) needs review the engine condition monitoring programs of aircraft operators to ensure they reveal component deterioration and also meet pertinent requirements.

The ROK, civil aircraft accident report, 2014 on aircraft crash involved a Helicopter, Registration 5Y-HLI, Eurocopter AS 350B2, serial number 3160 that was manufactured by Eurocopter in 1998 and that was powered by a Turbomeca Arriel 1D, turbo shaft engine. The most recent inspection had been performed in December 2011 and the helicopter had flown 3992 hours. The investigation revealed that the probable cause of the accident was pilot's error contributed by an engine failure. The inspection using visual aided (boroscope) method that was conducted in accordance with Turbomeca Ariel 1 overhaul Manual X 292875002 revision 30 of October 2011 revealed erosion beyond allowable limits in the engine Diffuser Assembly with cracks in The 1st Stage Nozzle Guide Vane. They recommended increased frequency in inspection of the aircraft components supports the recommendation of this study to have small intervals between scheduled inspections to allow for early detection of defects.

Eurocopter AS 350B2 registration number 5Y-HLI crashed at Mokwo, Keiyo in Kenya on the 17th December, 2011. An investigation carried out by Aircraft Accident Investigation Department (AAID) found out that the probable cause of the accident was engine failure caused by the internal defects and were noted during the engine strip (ROK, 2014).

An aircraft registered as N733YU being operated by African Inland Mission International (AIMI) Air Services crashed at Wilson Airport, Nairobi on 26 August 1999. An investigation carried out by Aircraft Accident Investigation Department (AAID) found out that the probable cause of the accident was an engine failure (ROK, 2013).

The importance of radiographic inspection in assessing quality of welds in accordance with Article 2 and 22 of ASME V was presented by Maina et al. (2014). The problems facing Kenya's welding industry are; incomplete penetration (41 % of the samples); lack of fusion (29 % of the samples); undercuts (12 % of the samples); porosity (8 % of the samples) and cracks (2 % of the samples), (Birir, 2015). Samples were obtained from both informal and formal sectors and tested for volumetric flaws using radiography method. During the sample acquisition, visual inspection was carried out before and after welding, followed by radiographic examination. The study observed a wide variation in welding competency and proposed further studies in order to develop a comprehensive advisory report for policy makers. The retraining of the welders in the industry as a way of capacity building and improvement of safety standards were also recommended.

2.6 Summary of the Literature Review

The theory and principles of the seven (7) NDT methods; visual inspection, radiographic testing, liquid penetrant testing, magnetic particle testing, eddy current testing, ultrasonic testing and thermography have been presented. From the studies, visual testing method is limited to detecting only surface defects and is dependent the capabilities of the inspector. Radiographic method is best suited for inspection of subsurface and internal defects; liquid penetrant is applied on both ferrous and non-ferrous material while magnetic particle inspection is only used to inspect ferrous material. Eddy current is mostly used to detect corrosion related defects, ultrasonic being employed in various industries while thermography is used for inspection of delamination defects.

The evaluation of structural defects in aircraft critical components and generation of POD curves from NDT data have been discussed. The studies covered evaluation of effectiveness of the NDT methods using statistical methods to generate POD curves.

The causes of various types of structural defects include; longer inspection scheduled intervals of aircrafts, lack of monitoring mechanisms for critical aircraft components, lack of use of confirmatory methods to compliment the recommended methods, material stress, environmental conditions, failure to repair/replace defective components, wear and tear and effective NDT methods to be employed during routine inspection of aircrafts.

The other industries that employ NDT methods are geothermal to check the integrity of the equipment, construction to assess the reliability of the concrete structures and inspection of welds.

CHAPTER THREE: METHODOLOGY

3.1 Introduction

This section describes; the procedures that were used in data collection, data analysis and the instrumentation used in NDT measurements and the generation of POD curves.

The NDT measurements were done as per the technical manual for non-destructive inspection methods TM 1-1500-335-23 and the Standard Specification for agencies performing non-destructive testing specifications, E543-15, which specifies the minimum requirements for agencies performing nondestructive testing. The standard specifies written procedures for the type of work for which the agency is contracted, process control and operation procedures that contain the information necessary to control the various activities necessary for materials examination. It also specifies the personnel qualification which includes procedures for training, certification, and recertification; equipment maintenance and calibration which shall contain inventory listings; equipment operation, technical files and records.

The Quality control of MPI was done in accordance with ASTM Standard No. E1444 (ASTM, 2016) which is a Standard Practice for Magnetic Particle Inspection method.

The RT was done in accordance with ASTM Standard No. E1742-12 (ASTM, International: E1742/E1742M, 2012) which is a Standard Practice for Radiographic Inspection method.

The Quality control of UT was done in accordance with ASTM Standard No. E1324 – 11 (ASTM, International: E114, 2010) which is a Standard Practice for Ultrasonic Inspection method while the Visual Inspection was done in accordance with Advisory Circular AC-43-204 (FAA, 1997).

In summary, actual in-service aircraft parts were inspected for:

- 1) The aircraft engines and landing gears using four NDT methods.
- 2) Results of NDT measurement were recorded in a prepared data sheet.
- 3) Characterization of defects in terms of cracks, corrosion, delamination and disbonds were done following a criteria in the aircraft service manual and the ISO standards.
- 4) Generation of POD Curves using the R Software.

3.2 Description of the Landing Gear Assembly

Figure 3.1 shows the parts of the brake assembly inspected; stator plates, torque tubes and pressure plates. Figures 3.2 and 3.3 shows the schematic diagrams of the parts of the Main Landing Gear (MLG) and Nose Landing Gear (NLG); wheel hub tie bolts and drive keys inspected. Figure 3.4: shows the Helicopter Landing Gear Assembly parts that were inspected.

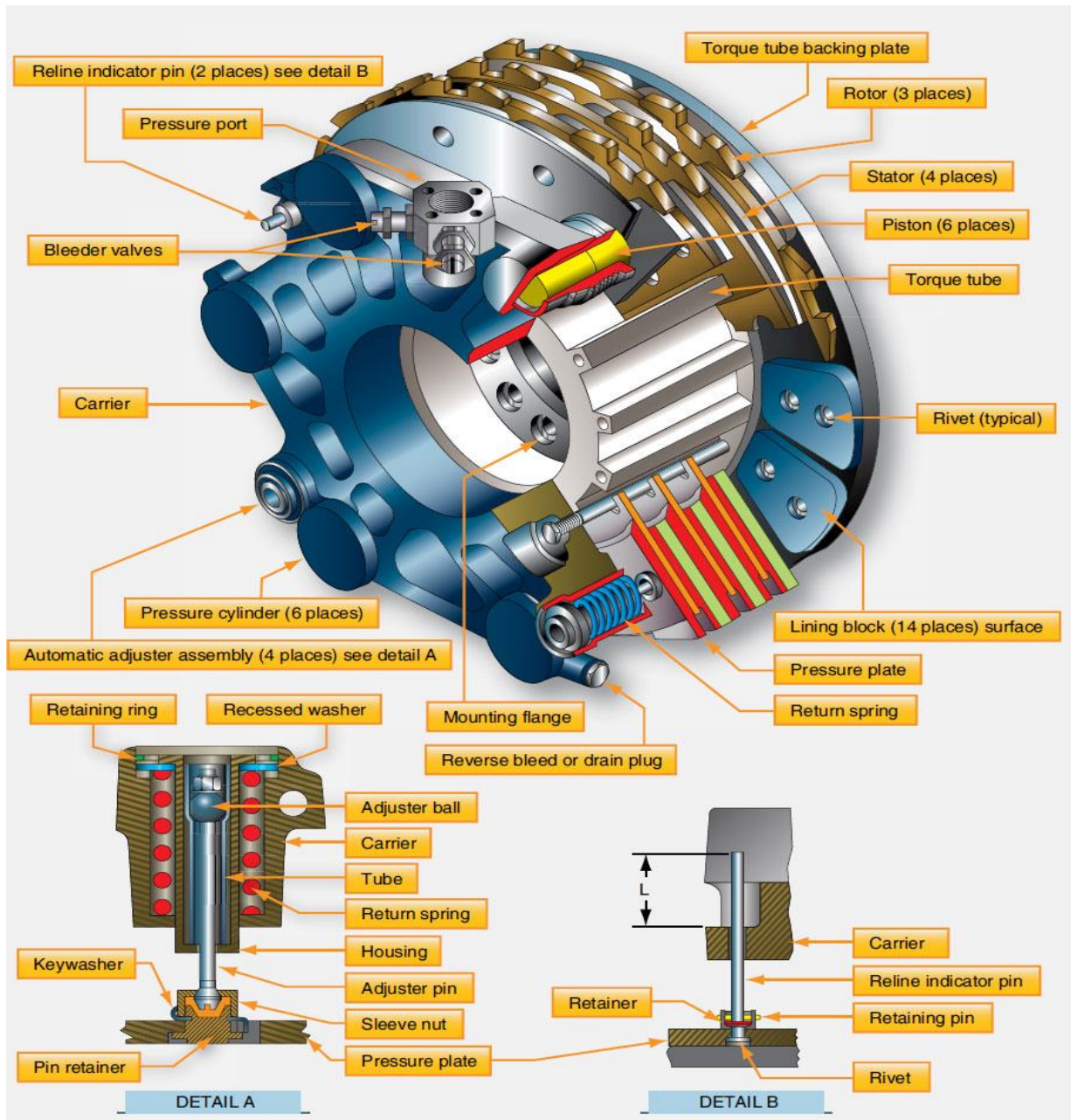


Figure 3.1: An extract from the aircraft maintenance manual of the parts of Boeing 737 Brake Assembly 3D (Boeing, 2012).

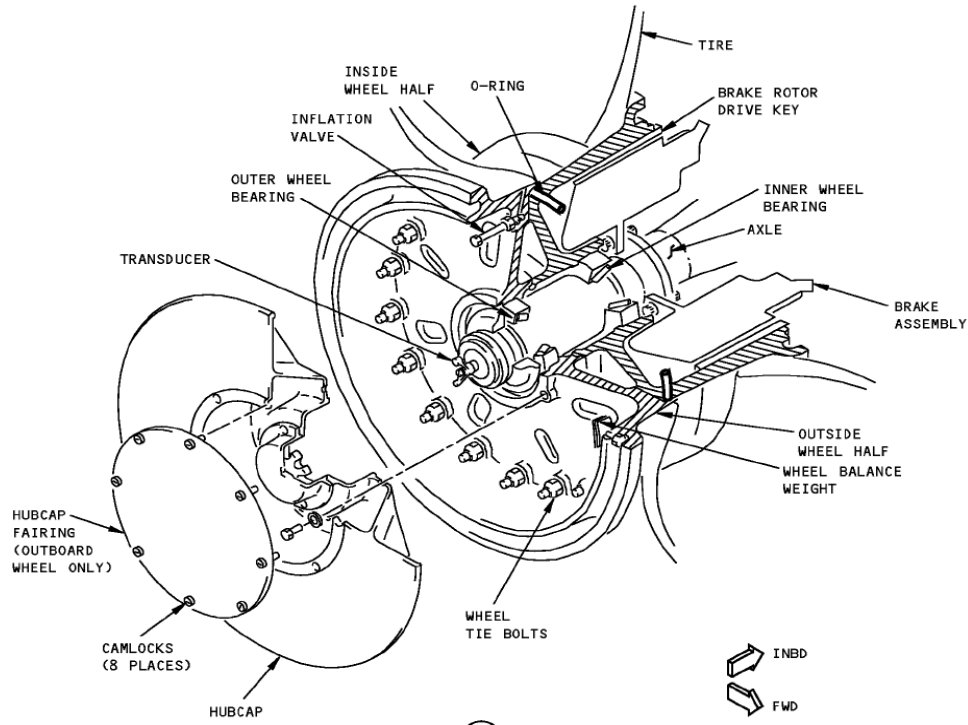


Figure 3.2: An extract from the aircraft maintenance manual of the parts of Boeing 737 Main Landing Gear Wheel Assembly (Boeing, 2012).

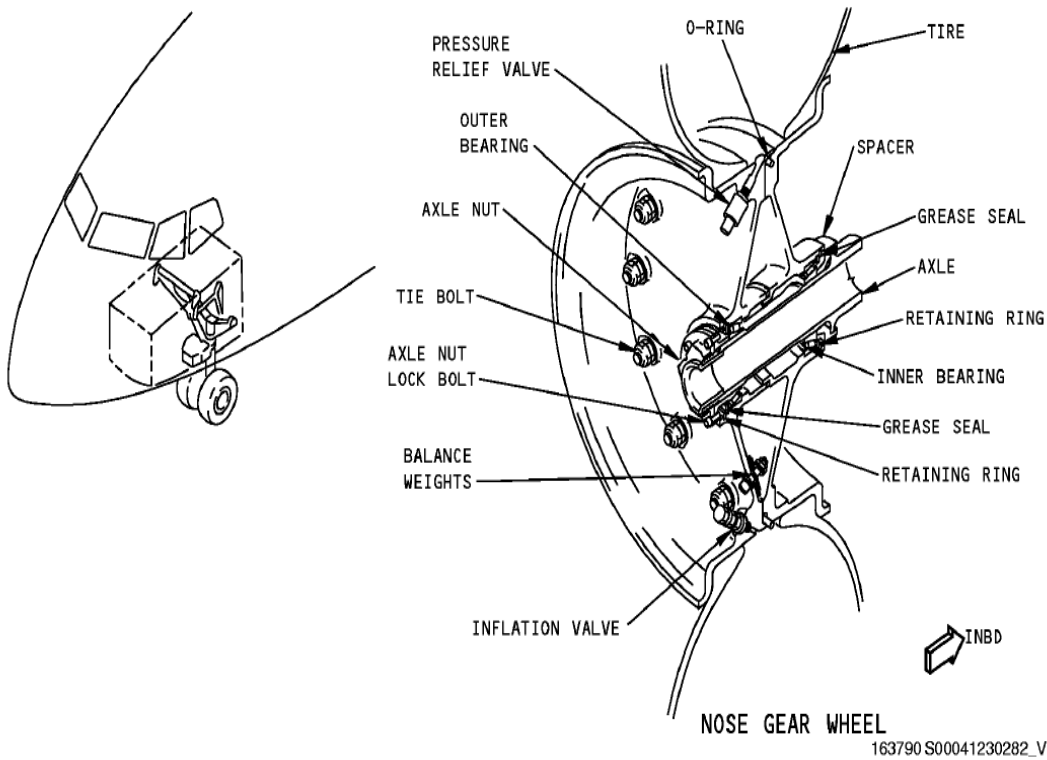


Figure 3.3: An extract from aircraft maintenance manual of the Parts of Boeing 737 Nose Landing Gear Wheel Assembly (Airlines, 2012).

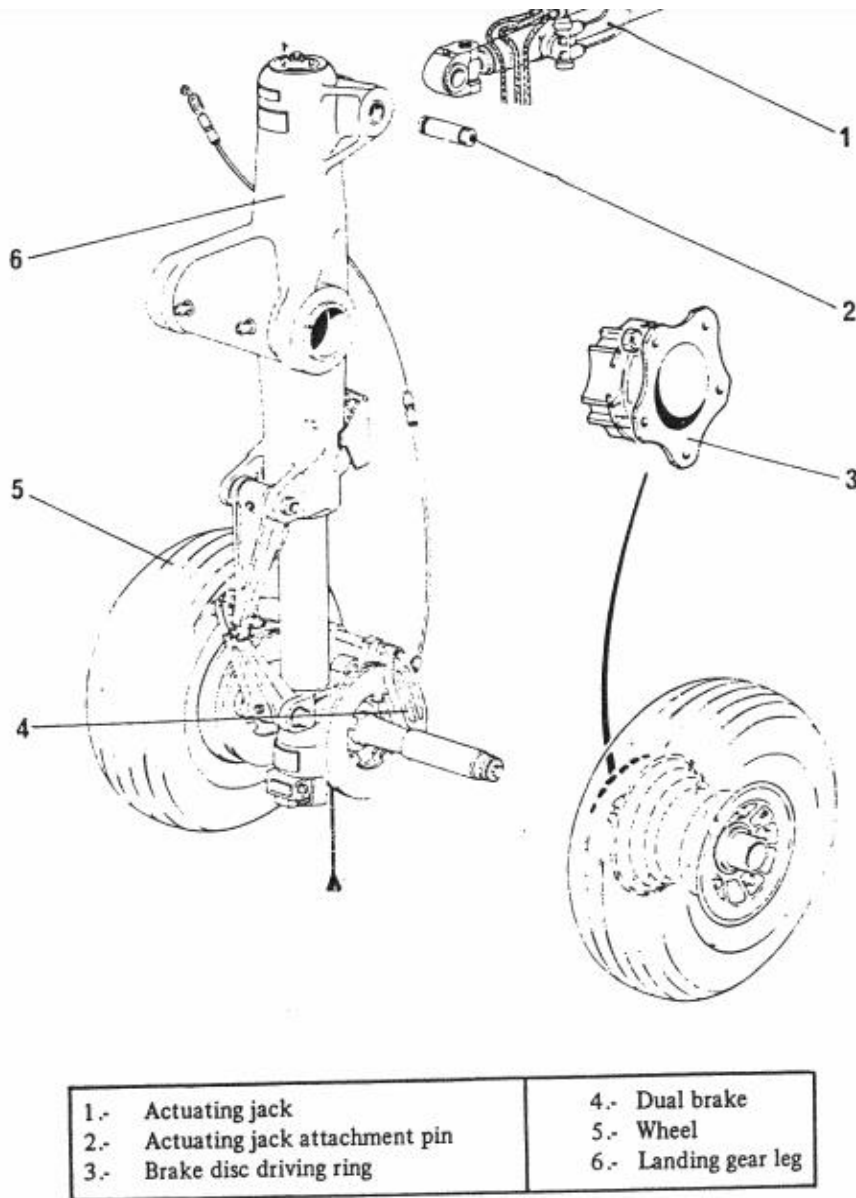


Figure 3.4: An extract of the Parts of a Typical Helicopter Landing Gear Assembly from aircraft maintenance manual (Eurocopter, 1978).

In general, the landing gear is that part of the aircraft that supports the weight of the aircraft while on the ground. It comprises of the following components; the braking system, the wheel assembly, the extension/retraction and safety devices, the air/oil shock-transferring components, gear alignment units and steering control elements. The aircraft tyres tubes are made from natural rubber compound. The parts were disassembled from the aircrafts during the servicing schedules for inspection in the laboratories, in accordance with the respective aircraft servicing and maintenance manuals requirements.

3.3 Description of Engine Assembly

Figure 3.5 shows the parts of Engine assembly inspected using NDT.

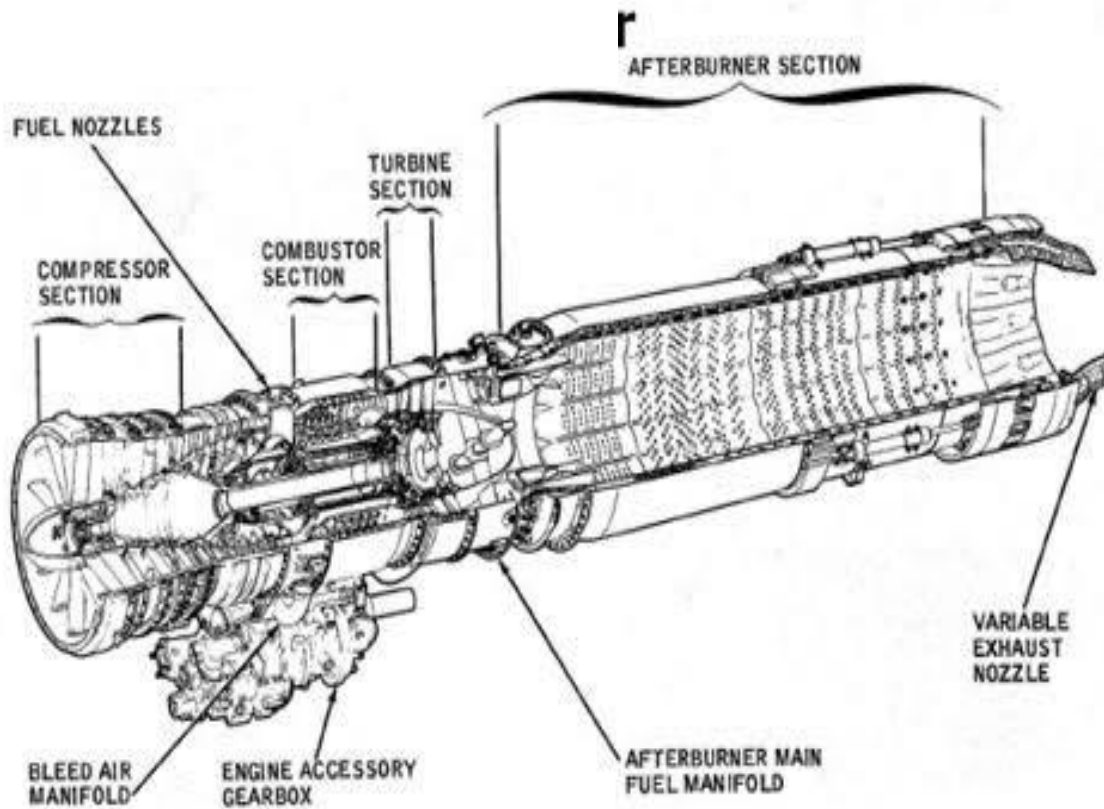


Figure 3.5: An extract from the aircraft maintenance manual of the typical Engine Assembly (Aviation, 1999).

An aircraft engine generates mechanical power for the aircraft and its major sections are the Air intake, compressor, combustion, turbine and exhaust section. The engine assemblies were inspected in situ while others were removed from the aircraft, disassembled and inspected in accordance with the aircraft maintenance manuals.

3.4 The Equipment, Instrument and Inspection Procedures

3.4.1 Stationary Magnetic Particle Inspection Unit

The Figures 3.6 and 3.7 show the magnetic particle inspection equipment: Gould-Bass GB-3509A-01 that was used in this study.



Figure 3.6: The Stationary MPI equipment: Model; GB-3509-01, Manufacturer; Gould Bass Company; Georgia, USA.

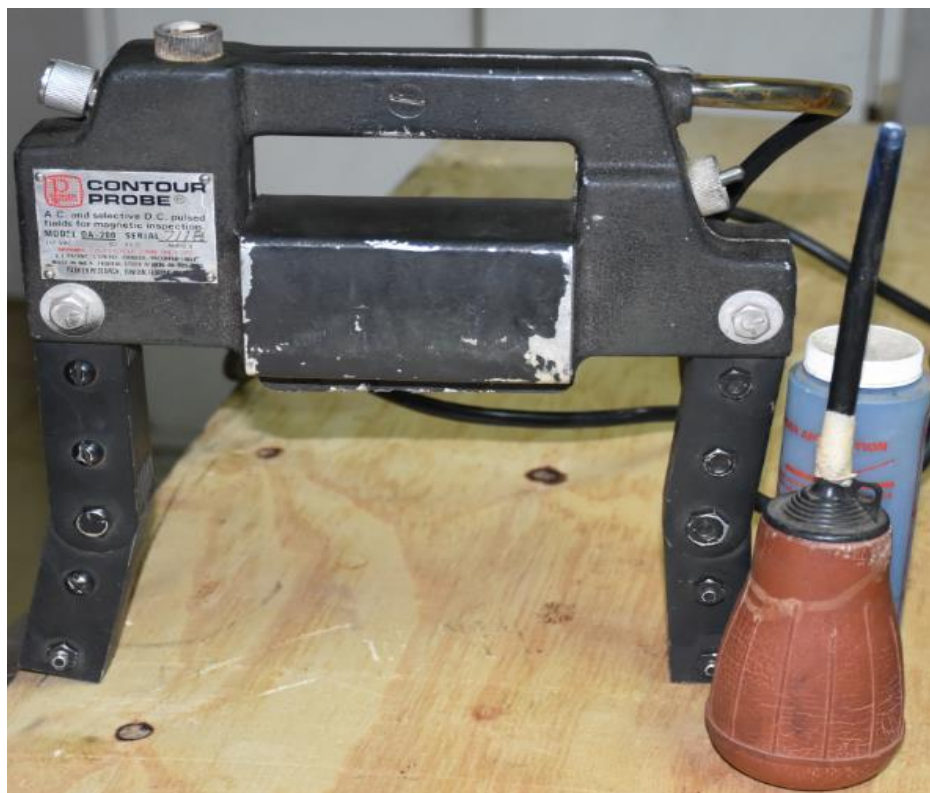


Figure 3.7: The Magnetic Yoke, Model; 200, Manufacturer; Parker Research, USA.

The Stationary magnetic particle inspection equipment used was the wet horizontal (bench) unit. The unit has head and tail stocks with electrical contact that allowed the part being inspected to be clamped. The machine has a movable coil with several turns for indirect magnetization to produce longitudinal magnetic field. It has a pump, tank and agitation and circulation system for the wet solution. It also has a nozzle for wetting the test object. The unit has current timers, amperage controls, an air or hydraulic cylinder for clamping test objects, and uses a three phase 220 or 440V AC supply.

The Magnetic Particle Testing involves magnetizing the specimen to produce magnetic lines of force, or flux, in the specimen material in accordance with ASTM E709, the standard guide for Magnetic Particle Testing, ASTM E1444, the Standard practice for Magnetic Particle Testing and respective aircraft maintenance manuals. The procedure comprises pre-cleaning, demagnetization and application of background contrast paint where applicable. This is followed by magnetization and application of magnetic particle powders or inks, Inspection of surfaces for indications of flaws, and re-magnetization by another method if necessary, recording flaws then cleaning and protecting of the material. Once the aircraft component has been magnetized, any defects are present will create a leakage field thus attracting the iron particles which produce cluster at the flux leakage fields, thus forming a visible indication. Figure 3.8 shows a typical flux leakage field from a defect.

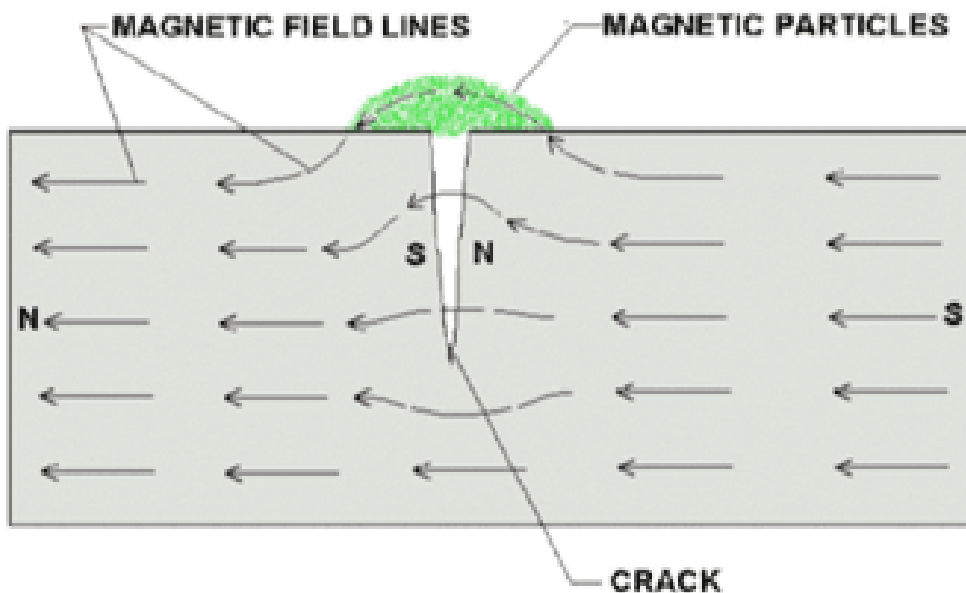


Figure 3.8: Flux Leakage from Surface and Subsurface discontinuities (Hellier, 2003).

The MPI method was used to inspect aircraft parts made of ferrous material. The magnetic yoke was used for in-situ inspection of aircraft parts, while the stationary magnetising machine (Gould Bass) was used for parts removed where varied magnetizing current was applied. The parts were magnetized in relation to the field and discontinuity orientation. The inspection of the aircraft parts for any discontinuity was also aided by the ultra-violet light (The Black Light). The defects were marked and measured clearly as seen under ultra-violet light. Demagnetization of the parts was conducted while measuring the field density using field density indicator to a value less than two gauss. The parts inspected were tagged as either serviceable or unserviceable after evaluation and post cleaning. The results from the inspection were recorded on the commercial airline record sheet for the components inspected at airline and for the components inspected at security base, the results were recorded in the NDT data form (Appendix 1 & 2).

3.4.2 Ultrasonic Inspection Machine- Phased Array

Figure 3.9 shows the UT equipment that was used in the study.



9 **Figure 3.9: The ultrasonic inspection equipment: Model-USN 60I 5W ND, Manufacturer; Krautkramer Branson, Australia.**

The UT Equipment consists of portable battery-powered ultrasonic instrument, transducers, position fixtures, reference standards, and couplant. The instrument generates ultrasonic pulse, detects and amplifies the returning echo, and displays the detected signal on a display. The positioning fixtures are used to locate the transducer at a prescribed point. The reference standards are used to calibrate the ultrasonic instrument. The couplant prevents direct contact between the part being inspected and the transducer. The couplant used was motor oil. Figure 3.9 shows the UT equipment that was used in the study.

The UT method makes use of high frequency ultra sound wave (100 KHz-10MHz) and operates on the principle of echo. The sound waves are sent into the material being inspected and are reflected back by defects in the material. The reflected waves reveal information about the defect.

The Pulse-Echo method was used during the inspection of the aircraft parts using a single transducer. The selection of the transducer was based on defect size, resolution and material requirements. The surface to be inspected was cleaned and couplant applied to achieve the most consistent signal. The standardization of the system by use of the reference blocks was conducted and probes selected in order to achieve at least a discontinuity to parent material ratio of 3:1 signal to noise response from the reference standard. The instrument adjustment of the controls was done in order to minimize the spread of front surface signals while maximizing the signal-to-noise ratio and maintaining the response required from the reference discontinuity. The data from the inspection were recorded the commercial airline record sheet for the components inspected at the airline and for the components inspected within the security department, the results were recorded in the NDT data form (Appendix 1). The instrument was calibrated in accordance with the calibration manual (See a copy of the calibration certificate - Appendix 3).

3.4.3 Visual Inspection by Magnifying glass

Figure 3.10 shows the magnifying glass that was used for visual inspection of the aircraft parts.



Figure 3.10: The magnifying glass, Model; X10 Magnifier, Manufacturer; E-Tay Industrial Company Ltd, Taiwan.

Magnifying glass is a convex lens that produces magnified images during inspection of materials. The lens has power X10 to X20 which is used to inspect accessible and disassembled parts from the aircraft engine. The magnification of the magnifying glass depends on the holding position and the distance between the inspector's eye and the aircraft part being inspected. The highest magnifying power is obtained when the lens is put closer to the eye. The aircraft surfaces to be inspected were cleaned in order to reveal or open the defects to be easily seen by magnifying glass. Those that had lubricants and oils like the driver and driven gears were cleaned using vapour degreaser. The surfaces that had paints were cleaned by sand, vapour or ice blasting method, using the specified methods in accordance with NDT manual requirements.

The inspection using an X10 to X20 power magnifying glass on the aircraft parts that were easy to access was carried out, either under sufficient lighting natural light or under light provided by 150 Watt torch. The critical areas were inspected for defects; volume of material loss, wear of the moving parts, such as the splines and gears, corrosion and burns caused by excess engine temperatures in hot section of the engine. Scanning through the magnifying glass was done systematically to ensure complete coverage. The presence of any defects was marked with a permanent marker. Corrosion areas were marked with a permanent marker. Cracked splines and gears were also marked. Turbine nozzles were inspected with aid of magnifying glass for cracks. The defect areas were marked, length and depth determined and recorded in NDT data sheet (Appendix 1).

3.4.4 Everest XLG3 Videoprobe Borescope

Figure 3.11 and 3.12 show the borescope type that was used in this study, for visual inspection.

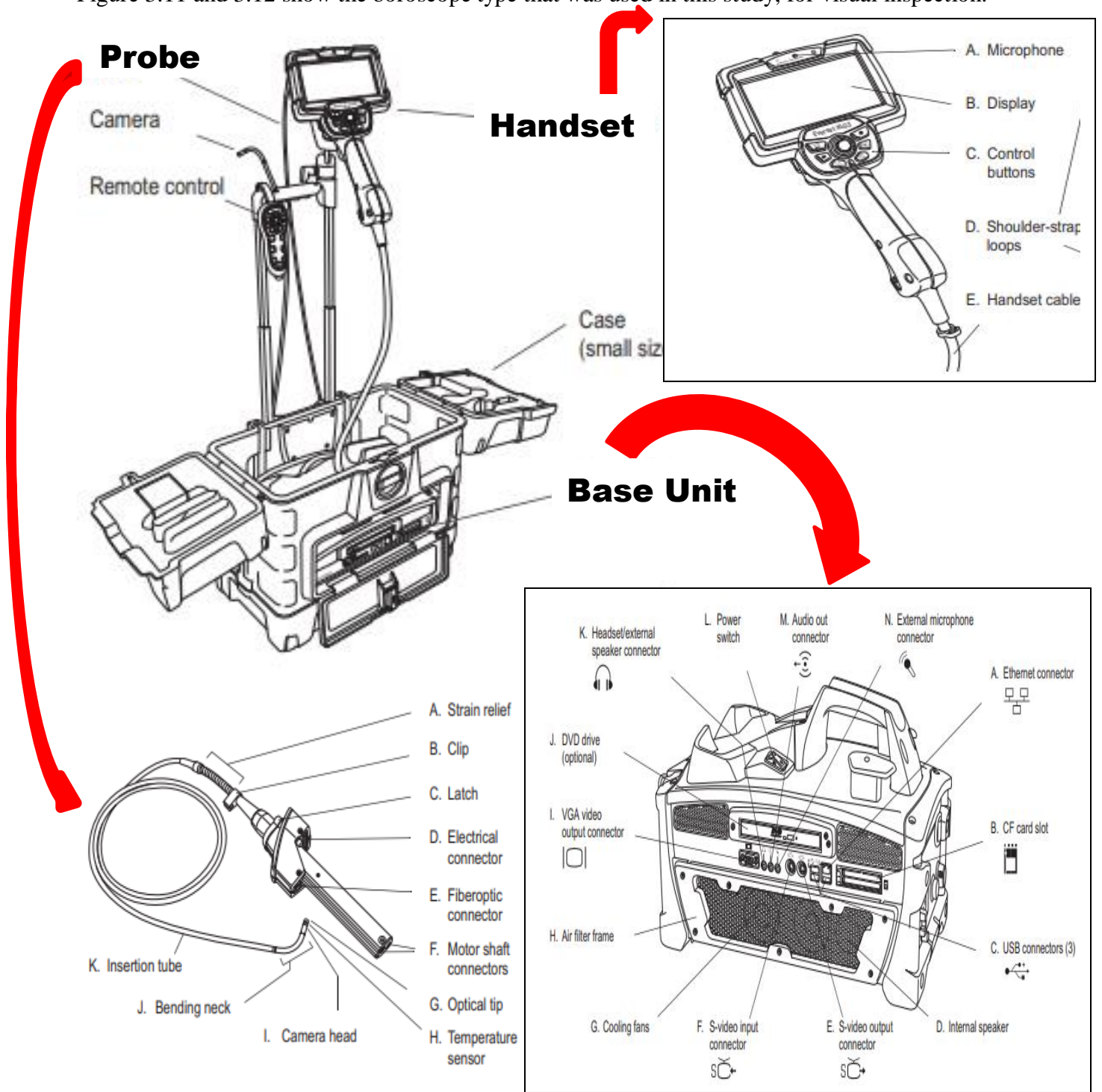


Figure 3.11: Parts of Everest Borescope, Model; XIG3 Videoprobe, Manufacturer; General Electric Company, USA (Extract from Equipment Operating Manual).



Figure 3.12: Photo of Everest Borescope, Model; XLG3 Videoprobe, Manufacturer; General Electric Company, USA (Extract from Equipment Operating Manual).

The borescope is an optical device used for visual inspection of inaccessible aircraft parts. It has an optical system that consists of an eyepiece connected by rigid or flexible tube fitted to a video camera. It has quick change probes of different dimensions, hand set with LCD displays, base unit with system CPU and software.

In principle, the sample that was inspected was illuminated by a light which made it possible to capture a video or still pictures of the hidden places. The captured image was then processed by the computer and displayed through an LCD monitor.

The inspection of aircraft internal parts of the engine were done by use of the scanning probe which was inserted through the borescope guide tube to get access to the compressor, combustion and turbine sections of the aircraft engine. The probe was inserted until a good view of the surface to be inspected was achieved. For the turbine section, the turbine blades and guide vanes, the blade tips, leading edge and trailing edges were inspected for any damage. The results from this study were recorded in the NDT data form (Appendix 1).

3.4.5 Radiographic Inspection Machine

The Figures 3.13 and 3.14 respectively shows the X-Ray tube and control unit used this study.



Figure 3.13: Radiography-X-Ray machine (X-Ray Control Unit), Model; Film Type, Manufacturer; Gilardoni, Italy.



Figure 3.14: Radiography- X-Ray control unit; Model; 583, Manufacturer; Gilardoni, Country, Italy.

The X-ray machine was of Model SMART HP 300 that used in conjunction with a control unit model 583. The X-Ray machine has the tube, cathode and anode. The X-Ray tube had a focal spot size of 3 mm in diameter and operated in the voltage range of 50 kV to 300 kV. It operates at a constant current of 3 mA, which has a power rating of 900 W. It is air cooled and weighs 33 Kg.

In principle, radiographic inspection of internal and surface defects in aircraft parts uses the concept of penetration and differential absorption of the X-rays in matter. The radiation that passes through the part being inspected produces a radiographic image which is recorded on a film. Thicker parts of the material will absorb less radiation thus producing lighter images while parts with defects were highly exposed allowing more radiation to pass through, thus producing darker places on the film.

The radiographic inspection was conducted inside the designated aircraft Hangar only accessible to qualified and certified NDT personnel. The part of the aircraft to be inspected was positioned at an appropriate place within the hangar and restricted for access with Warning Signs. The aircraft test specimens were radiographed following the laid down procedures in the Instruction manuals. The personnel were monitored for radiation exposure. The radiographs were assessed for quality and evaluated for defects. The results of the inspections were recorded.

3.4.6 Other Facilities and Accessories

The size of the bunker that housed the X-ray unit was approximately 15 m by 20 m with thick concrete walls of thickness of 0.6 m while the door was made of steel material. This was to ensure maximum protection of personnel and the public against radiation exposure. Next to the Bunker was the control room; where the X-Ray control system was housed and there was a dark room for radiograph processing.

3.5 Inspection Methods Used in identification of Aircraft structural Defects

Tables 3.1 and 3.2 summarize the landing gear and engine components that were inspected.

Table 3.1: Landing Gear Defects and Inspection Methods

Landing Gear Components	Landing Gear Part	Type of defect	NDT Method
1) Brakes	a. Stator Plates	Cracks	Visual and MPI
	b. Torque tubes	Cracks	Visual and MPI
	c. Pressure Plates	Cracks	Visual and MPI
2) Wheels	a. Wheel Hubs Tie Bolts	Cracks	Visual and MPI
	b. Wheel Hub Drive keys(MLG)	Cracks	Visual and MPI
	c. Wheel Hub Drive keys(NLG)	Cracks	Visual and UT
3) Landing gear assembly	Landing Gear Struts	Cracks	Radiographic Inspection

Table 3.2: Engine Defects and Inspection Methods

Engine Components	Type of defect inspected	NDT Method
1) Compressor	Cracks Corrosion Delamination Disbond	Visual Inspection & MPI
2) Combustion	Cracks Corrosion Delamination Disbond	Visual Inspection & MPI
3) Turbine	Cracks Corrosion Delamination Disbond	Visual Inspection & MPI
4) Others	Corrosion	Visual Inspection

3.6 Data collection: NDT Inspections of aircraft components

NDT inspection was done during the maintenance periods, when most aircraft operators were performing scheduled and non-scheduled maintenance. This ensured that most aircraft parts of interest for this study were available for this inspection exercise.

In this study, one hundred and one (101) aircraft parts from in-service aircraft due for both scheduled and non-scheduled maintenance were considered. The landing gear parts that were fifty eight (58) and the engine parts were forty three (43). These samples were taken to NDT laboratories and subjected to Ultrasonic, Radiographic, Magnetic Particle Inspection and Visual Testing methods.

The NDT personnel that assisted in the inspections and NDT measurements were qualified and certified in accordance with the internationally recognized NDT personnel certification/qualifications Practice and Standards, as ANSI/ASNT-CP-189, SNT-TC-1A and NAS410. In addition, the personnel were also qualified in general aircraft inspection (Appendix 4).

The sample preparation and inspections were done in accordance with technical procedures in the aircraft respective inspection/maintenance manuals. Prior to inspection, samples were labelled for easier identification as follows; LGP codes for landing gear parts and EP codes for engine parts.

Characterization of the structural defects was done at the following facilities: Laboratories at the Institute of Nuclear Science, University of Nairobi, a commercial airline in JKIA and in the security department.

All measurements were recorded in a prepared Non Destructive Inspection data record sheet for further analyses. This included the following particulars:

- 1) Types of components for inspection and the description of the defect/reason for inspection;
- 2) Methods of inspection and description of the equipment used, equipment setup, reagents used, operating conditions and parameters.
- 3) Inspection procedures used; sketches/diagrams and photos of the parts for inspection in accordance with the applying standards/ component maintenance manual. (*See the attachment of the data record sheets-as Appendices 1 and 2*).

3.7 Statistical Data Analysis

The concept of Probability of Detection (POD) is used in various industry sectors to establish the capability of an inspection to detect flaws. This is generally expressed as a POD curve, which relates the likelihood of detection to a characteristic parameter of the flaw, usually its size.

Estimation of the POD typically relies on a large numbers of realistic defect specimens, followed by practical trials of the inspection procedure. These can be costly and time consuming activities. The sample sizes used are determined based on the cost, time, or convenience of collecting the data, and the need for it to offer sufficient statistical power (Li, Samuels, Zhao, & Shyr, 2017). In this study, one hundred and one (101) components were inspected during scheduled and nonscheduled maintenance for NDI examinations using four (4) NDT methods to determine defects for acceptance/rejection characterization criteria. The defect sizes were determined from structural measurements and the number of defects for the various defect sizes determined. The data that was obtained was analyzed using the R software to generate POD curves. The percentages and probability of detection was determined. As a central tendency statistic, the mean for number of defects in selected components was calculated. The distribution of defects detected was determined for each procedure used to enable POD assessment.

The Probability of Detection, POD (a) indicated that the probability of detection is a function of a parameter, usually a size. The relationship between the POD (a) and size is indicated as a POD curve. For each of the POD curves, a specific test method was used that had the name of the data set, the salient defect sizes, a_{50} , the size having 50% POD, a_{90} , the size having 90% POD and a_{95} , the size having 95% POD estimate. The equation of POD model based on the $\log(a)$ is shown below:

$$s = POD(a) = \Phi\left(\frac{\log(a) - \mu}{\sigma}\right) \dots\dots\dots \text{Eqn 3.1}$$

Where

s is Probability of Detection, POD(a)

a is the size of the defect

Φ is an absolute sign to make the value positive

μ is the mean of the defect sizes

σ is the standard deviation

The data is normally distributed (*pnorm*) in that s is plotted against a where from equation (1);

$$s = \text{pnorm}(a, \text{mean} = \mu, \text{sd} = \sigma) \dots\dots\dots \text{Eqn 3.2}$$

The value of the mean and hence standard deviation determines the type of the curve that will be plotted.

The Excel program and R Version MH 1823 POD Software were used to analyze data to enable to produce POD curves. All POD curves had similar characteristics. The POD of a specific defect size was plotted against the defect size a . The results were presented in a typical POD curve.

3.8 Criteria for Acceptance

The criterion used for acceptance of the indication of a defect was based on the ASNT and MIL-STD-271 standards and aircraft maintenance manuals specifications and requirements. The different types of defects were identified using NDT Methods. They were characterized for the sizing, position and orientation in accordance with the aircraft type servicing manuals.

CHAPTER FOUR: RESULTS AND DISCUSSIONS

4.1 Introduction

The discussion on data from the four NDT methods is presented and includes the identification of defects, characterization of the defects and assessment of the effectiveness of the NDT methods used in routine aircraft inspections.

4.2 Quality Assurance Tests

The NDT personnel that assisted in the inspections and NDT measurements were qualified and certified in accordance with the internationally recognized NDT personnel certification/qualifications Practice and Standards, as ANSI/ASNT-CP-189, SNT-TC-1A and MIL-STD-410. In addition, the personnel were also qualified in general aircraft inspection, in level I, II and III (Appendix 4). Appendix 3 shows the certificate of UT Equipment Model USN 60L 5W ND; Serial Number 19A01JNS, that was calibrated and certified by General Electric (GE) Company, US on 5th February, 2019.

4.3 Results of NDT Measurements and Defect Evaluations

4.3.1 Structural Defects Distributions in Aircraft Components

Figure 4.1 shows a summary of distribution of cracks defects in the aircraft brake assembly derived data in the Appendices 5, 6 and 7.

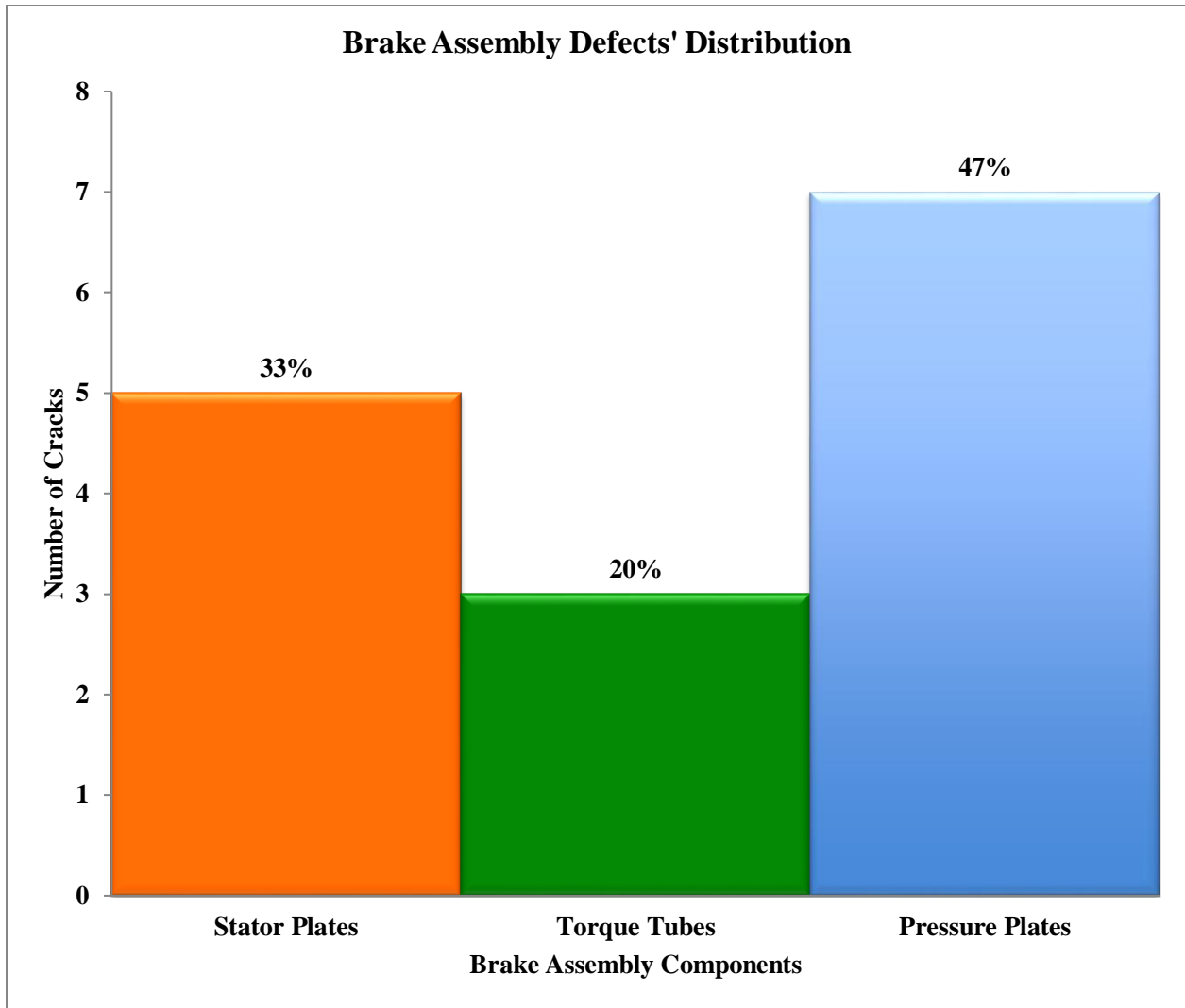


Figure 4.1: Distribution of Cracks in Brake Assembly Components.

The aircraft components were inspected using MPI method in accordance with aircraft technical manuals. Overall, the brake assembly components inspected, had fifteen (15) crack defects varying between 1.9 mm - 14.8 mm, of which, the Stator Plates had 33%, Torque Tube 20% while Pressure Plates had 47% of brake assembly defects. The high occurrence of cracks in the pressure plates is attributed to the nature of operation of the aircraft braking system during landing phase.

Figure 4.2 shows the summary of distribution of cracks in the aircraft wheel assembly derived from Appendices 8, 9 and 10.

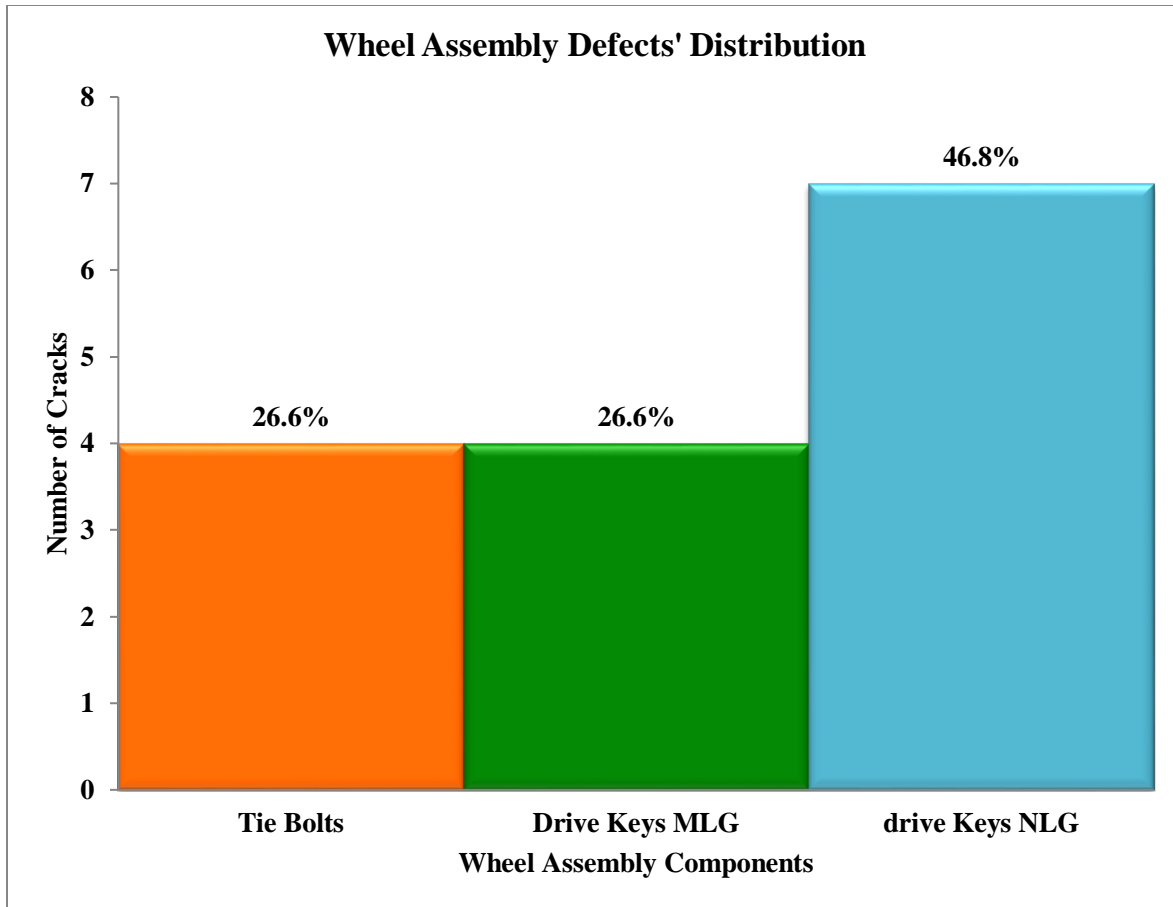


Figure 4.2: Distribution of Cracks in Wheel Assembly Components.

The aircraft components were inspected using MPI, UT and RT methods in accordance with aircraft technical manuals. Overall, there were fifteen crack defects, 2.5 mm - 10 mm (55.6%) of the wheel assembly components, most of which were concentrated in the Nose Landing Gear drive keys, approximately 47%. The high occurrence of cracks in the drive keys in the wheel assembly components were attributed to the proximity of these parts to the aircraft braking system.

In general, 50% of all the components inspected for brake and wheel assemblies had crack defects (1.9 mm-14.8 mm). However, those found within 3.18 – 6.0 mm permissible limits were repaired and those found > 6.0 mm, were replaced. The specification limits for the tie bolts and drive keys requires that, no crack defects are allowed.

The radiographic inspection of the aircraft landing gears found no defects during the unscheduled maintenance and the aircraft was cleared for flying (Appendix 11). The service life of the inspected aircraft was more than thirty (30) years.

Figure 4.3 shows the summary of distribution of crack defects and Figure 4.4 shows the summary of distribution of defects in the aircraft engine assembly, results extracted from data sheet in Appendices 12- 16. The components were inspected using two (2) NDT methods; Visual and MPI methods in accordance with respective, aircraft technical manuals.

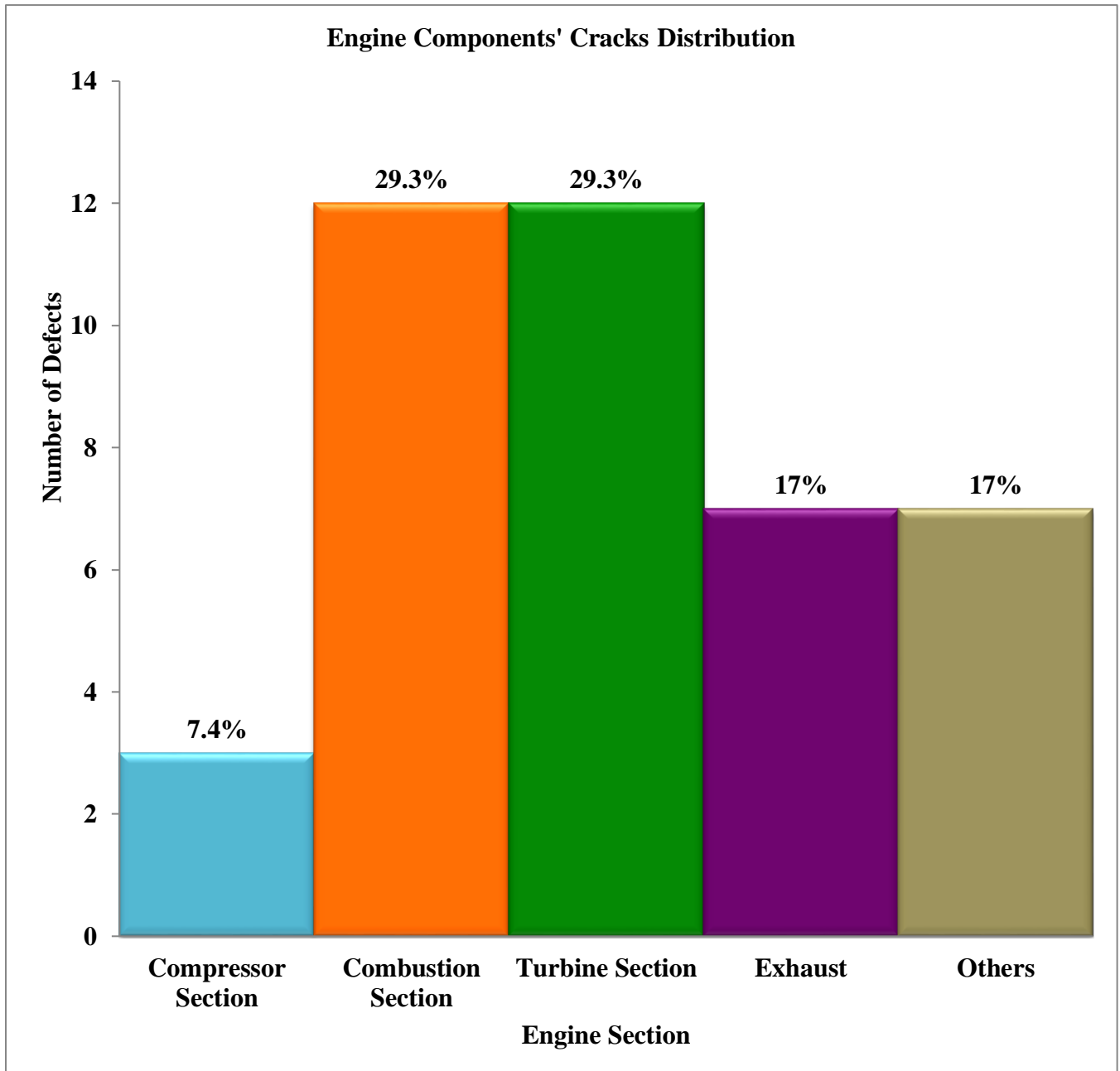


Figure 4.3: Distribution of Cracks in Engine Assembly Components.

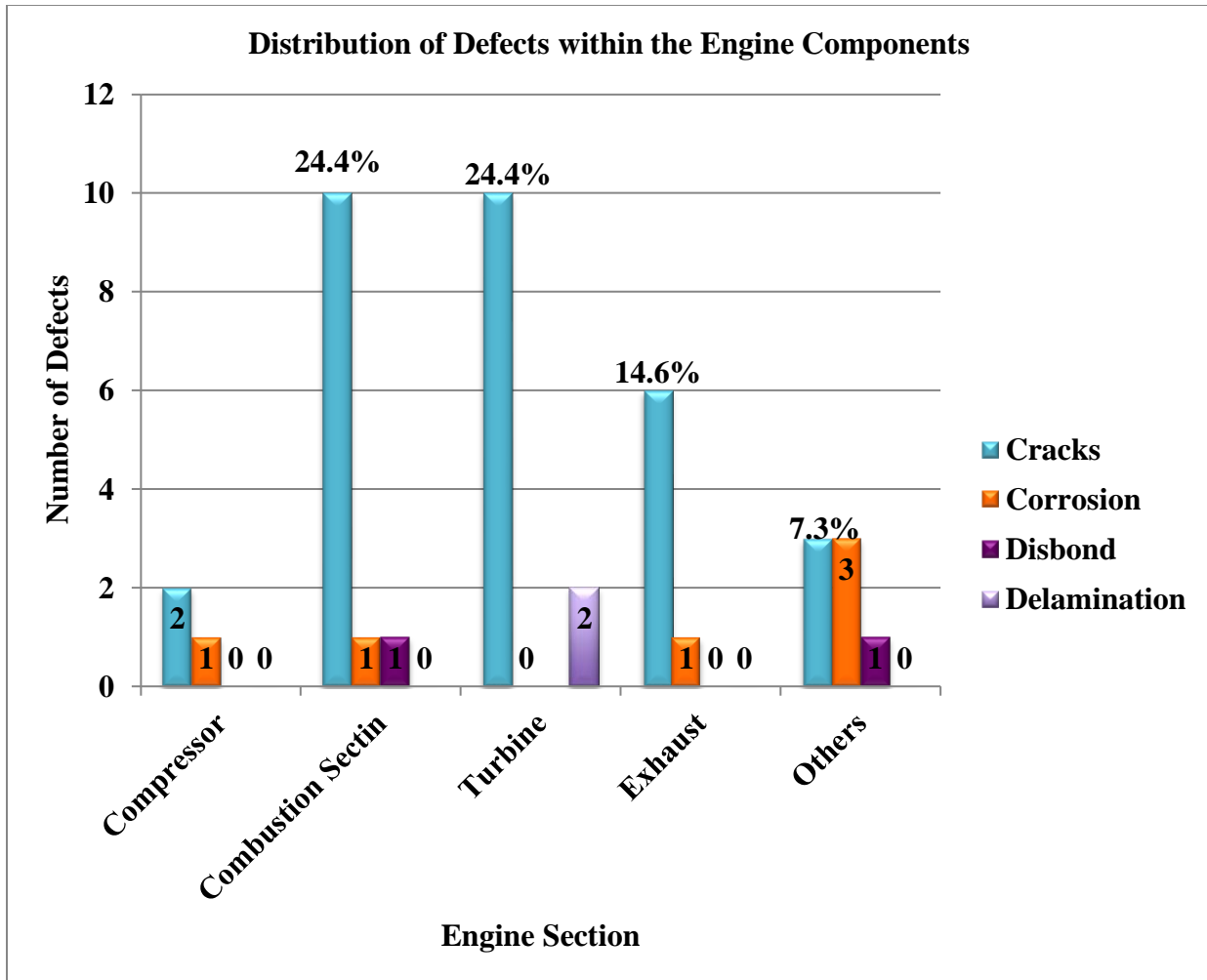


Figure 4.4: Distribution of Defects in Engine Assembly Components

Crack defects were found in all the engine components; highest, in combustion chamber at 24.4%, turbine section at 24.4%, followed by the exhaust section at 14.6%. Other engines components had less than 10% of other defects; corrosion, disbond and delamination. In general, the cracks defects varied between 1.00 mm - 220 mm, for corrosion between 5 mm - 40 mm, disbond between 1.8 mm - 3.00 mm and delamination between 0.5 mm - 1.00 mm. However, there were no defects found in the helicopter landing gear (Appendix 17).

The results of the forty three (43) engine components that were inspected, in this study; indicate that, forty one engine components (95.4 %) had defects in varying proportions; compressor section (7.4% - Fig. 4.3) and vary from 8 mm – 40 mm (Appendices 18, 19, 20, 21, 22, 23 and 24). The specification limits requires no defect whatsoever. The combustion section had 29.3% defects, ranging from 1.8 mm – 10mm in the inner and outer shell and the louvers but the

allowable limits are 1.6 mm – 4.2 mm, according to the criteria for evaluation in the maintenance manual (Appendices 25, 26 and 27).

The turbine section had 29.3% defects. Specifically, the Engine Free and Power Turbine blades, leading and trailing edges had crack defect size of 3.9 mm and 6.1 mm respectively. The stage 2 turbine nozzles had axial cracks ranging from 0.5 mm to 4.0 mm. The allowable limit for axial cracks is 4.2 mm while radial cracks are not allowed, according to the requirements limits. For the aircraft, PTO driven Bevel gear shaft, no defect was found. (Appendices 28, 29, 30, 31, 32, 33, 34, 35 and 36).

The exhaust and other engine components had 17% each of defects range from 3.0 mm - 220.0 mm (Fig. 4.3), (Appendices 37, 38, 39, 40, 41, 42, 43, 44, 45 and 46). For the exhaust section, the allowable limits are from 12.7 mm to 25.4 mm, whilst, no crack is allowed in the oil sump according to the maintenance manual requirements, and in case of any leakage, the sump flanges seals should be replaced. The highest crack defect size of upto 220 mm was detected in the aircraft after burner assembly in exhaust section and the component was immediately repaired using TIG welding (Appendix 42).

In the diffuser casing, there were no defects, but the defect size allowed is 25.4 mm in the boring sector (Appendix 46). The high temperatures in the combustion chamber and turbine section, contribute to occurrence of defects in general.

4.4 The Characterization of Aircraft Components Structural Defects

4.4.1 Fatigue Cracks

Figures 4.5 and 4.6 show typical cracks which were characterized as either longitudinal or transverse cracks in the Engine Exhaust using Visual Inspection (Borosopic). Other methods used for cracks detection include; UT and MPI.

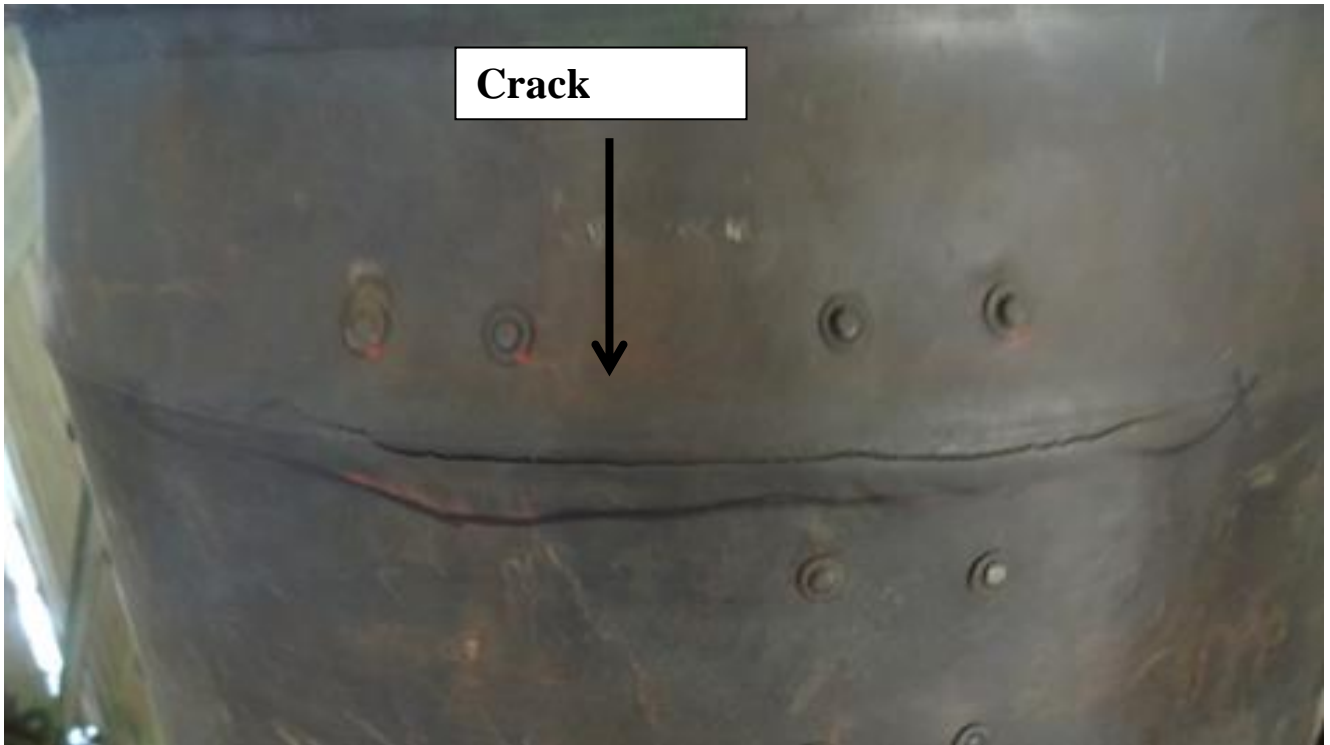


Figure 4.5: Boroscopic Image of Longitudinal Crack defect in the Engine Exhaust Section.



Figure 4.6: Boroscopic Image showing Transverse Crack defect in the Engine Exhaust Section.

4.4.2 Corrosion Defects

Figures 4.7 and 4.8 show typical corrosion defects in the aircraft engine component, as observed by visual inspection. In general, an aircraft component experiences corrosion depending on its service conditions, operation and maintenance. Corrosion is the degradation of metals through interaction with the environment and was caused by the moisture from humid environment.

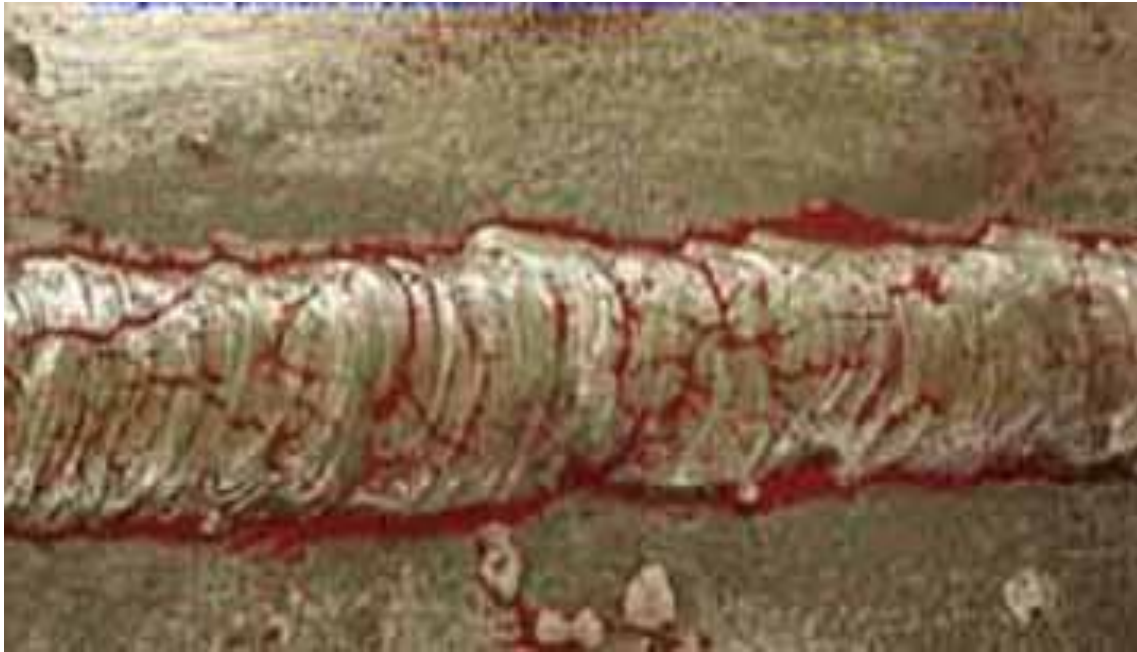


Figure 4.7: Corrosion defect in the aircraft Engine Compressor Section

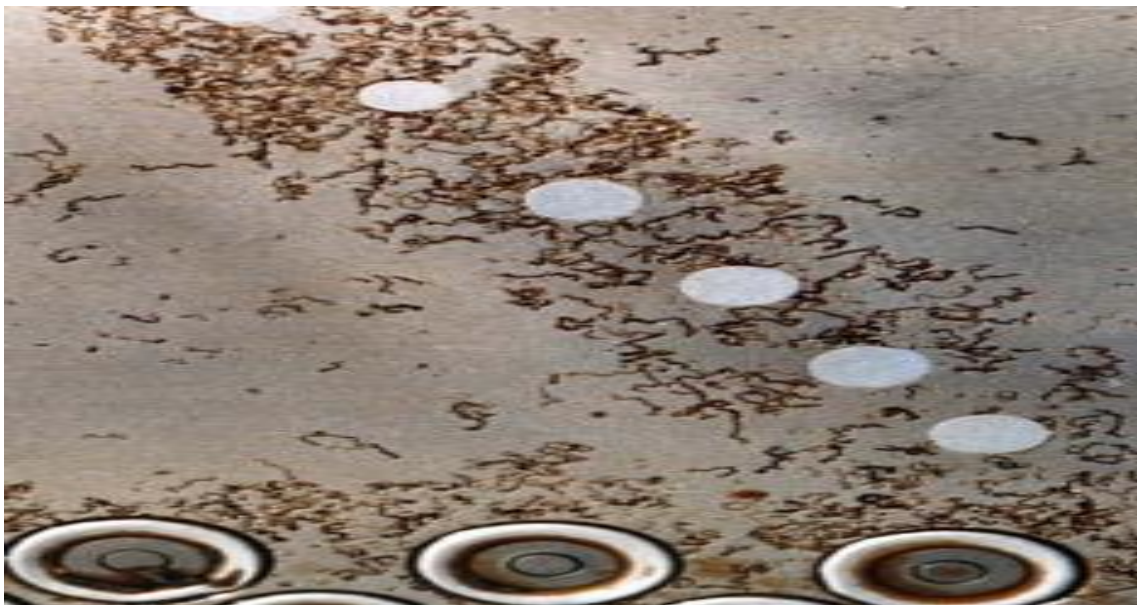


Figure 4.8: Filiform Corrosion under paint coating on the other parts of the Engine

4.4.3 Delamination Defects

Figure 4.9 shows a typical delamination defect in engine cowling of the aircraft that were detected by visual inspection method.

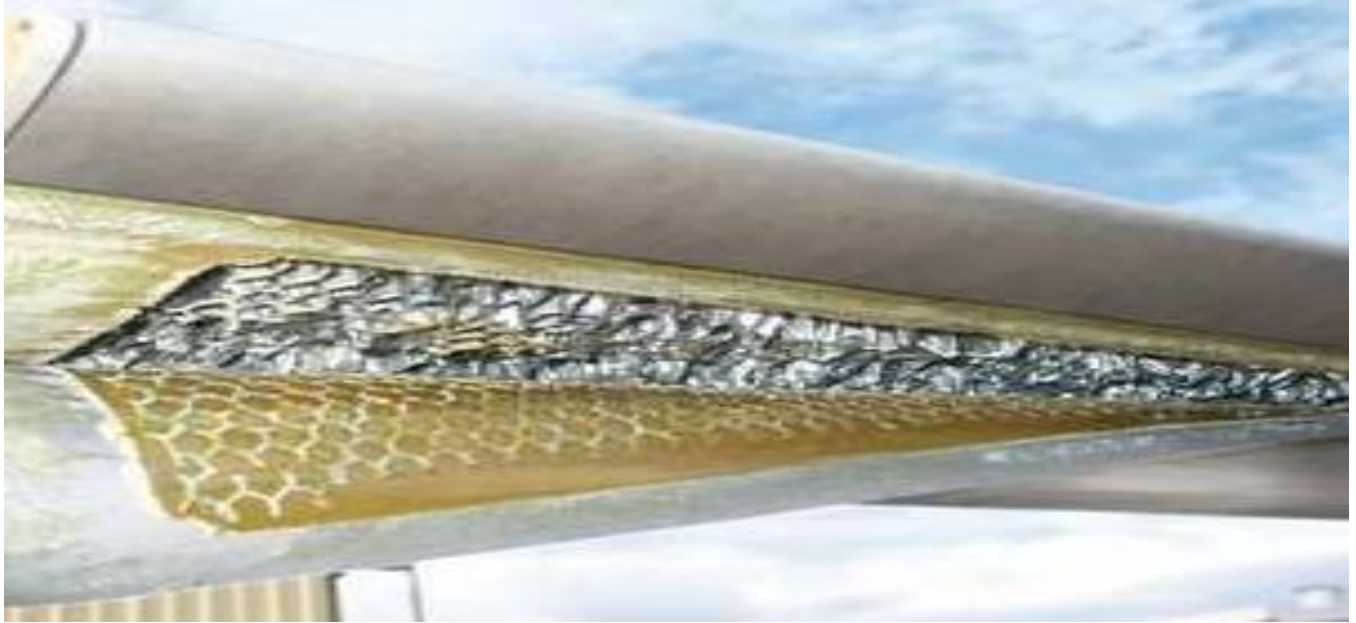


Figure 4.9: Delamination defect in the other aircraft Engine parts

4.4.4 Disbonds

Figure 4.10 shows a typical disbond defect in the engine assembly of the aircraft in the combustion chamber and other engine sections, disbond defects were detected by visual inspection method.



Figure 4.10: A disbond defect in the other Engine Sections.

Figure 4.11 shows the overall prevalence of defects in the aircraft samples that were examined using four NDT methods in this study.

Of the one hundred and one (101) aircraft parts examined in this study, the following defects; cracks (60%), corrosion (6%), delamination (2%), disbond defects (2%) were found. Twenty nine samples (30%) had no defects.

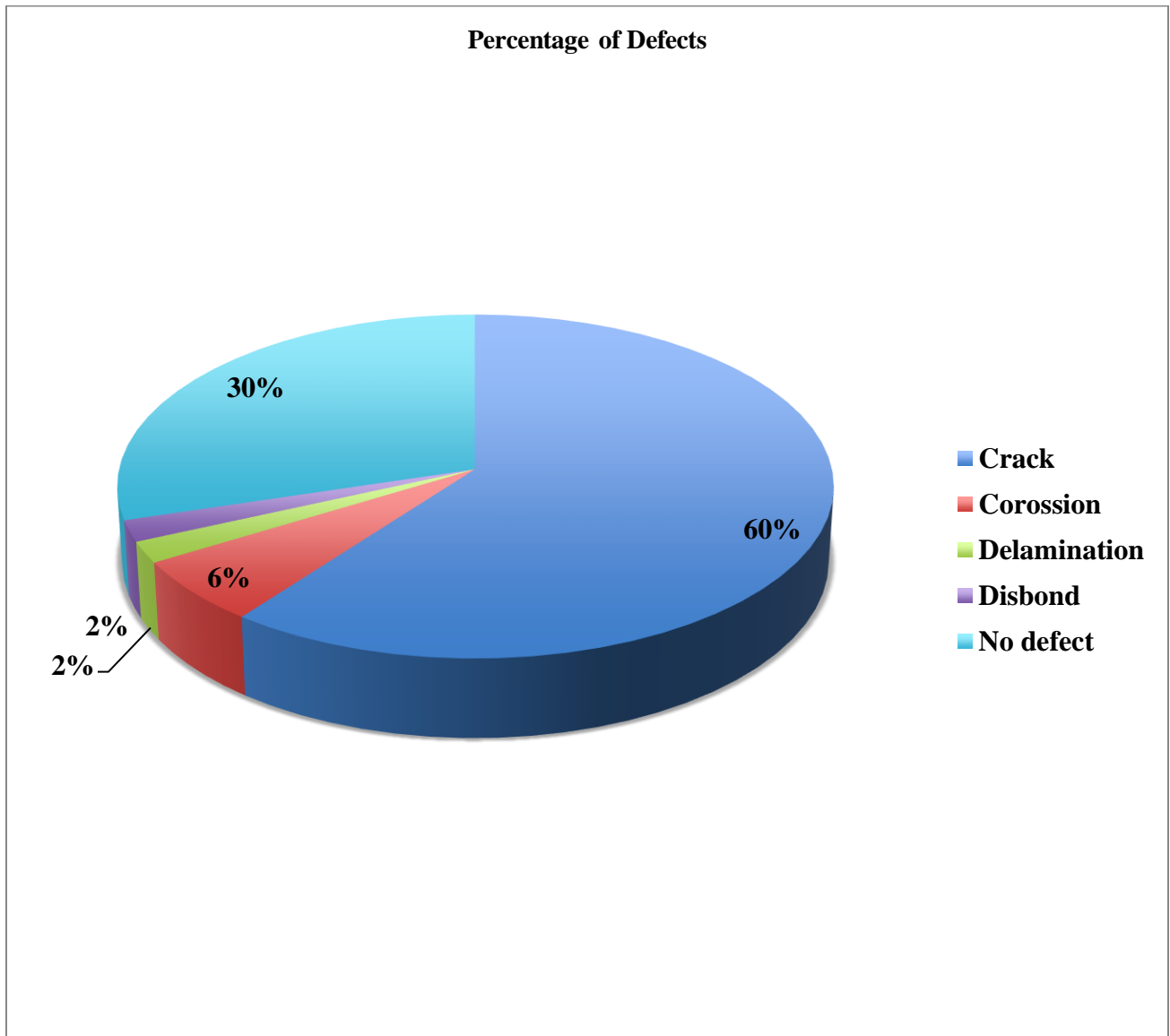


Figure 4.11: Prevalence of Defects in aircraft samples.

Figure 4.12 shows the frequency of use of the four NDT methods.

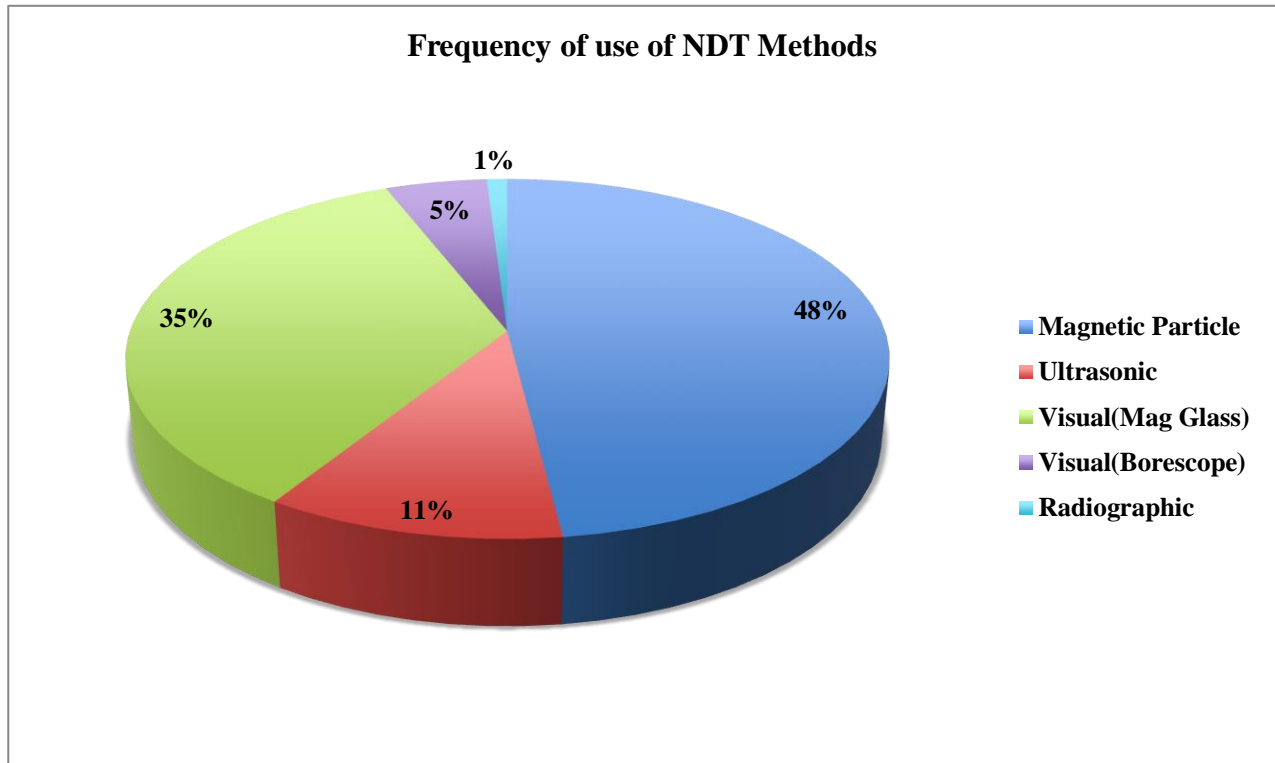


Figure 4.12: A Summary of Frequency of use of NDT Methods

The most frequently used method in aircraft inspection in this study was MPI (48%), followed by visual inspection using magnifying glass (35%).

4.5 Statistical analysis of the NDT Data

One of the key features that determine suitability for application of an NDT method is the minimum defect size, a_{90} , which can be reliably detected by a technique, relative to the sizes of defects that might be structurally significant.

Studies of NDT effectiveness is usually focused on avoiding catastrophic failure and demonstrating that the requirements set out in airworthiness standards are achieved.

Two defect sizes are frequently extracted from POD information: a_{90} is the defect size at which the estimated POD, reaches 0.9 and $a_{90/95}$ is the defect size at which the lower 95% confidence limit POD curve reaches 90%. This information assists with the evaluation of limitations for

standard NDT methods. In this context, “limitations” refers to the sizes and types of defects that will be reliably detected by an NDT procedure.

Figures 4.13 - 4.16 show the POD curves that were generated using the data from the inspections of one hundred and one (101) in-service aircraft samples using the four (4) NDT methods (See appendices 12 - 16).

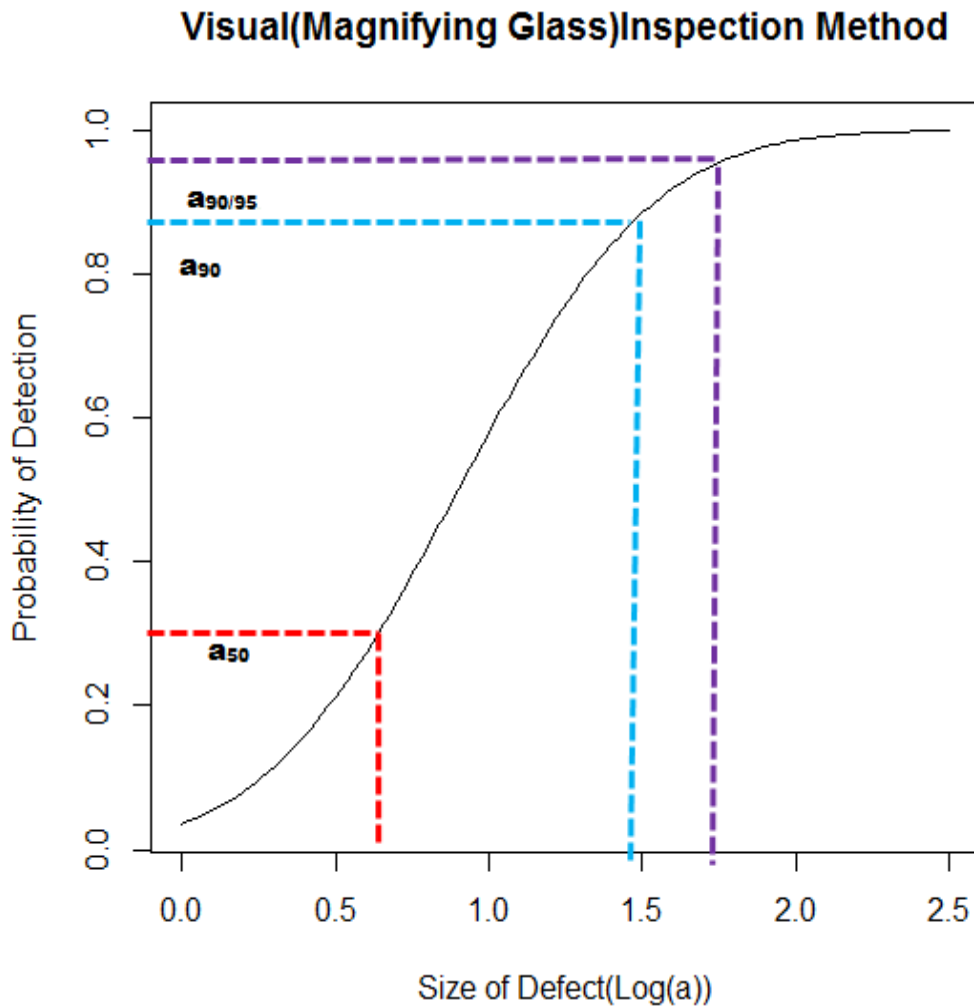


Figure 4.13: POD Curve for Visual (Magnifying Glass).

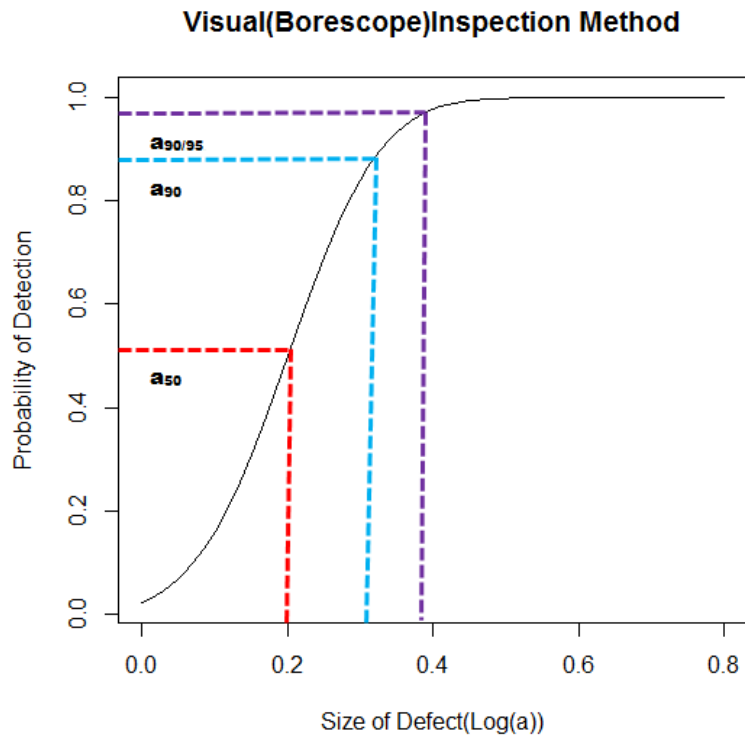


Figure 4.14: POD Curve for Visual (Borosopic) Inspection.

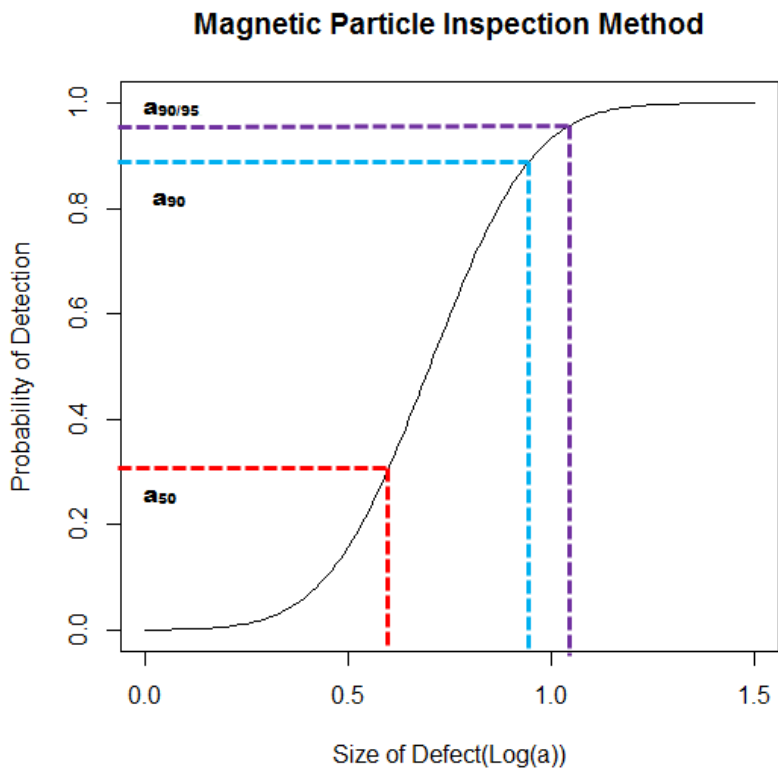


Figure 4.15: POD Curve for Magnetic Particle Inspection Method.

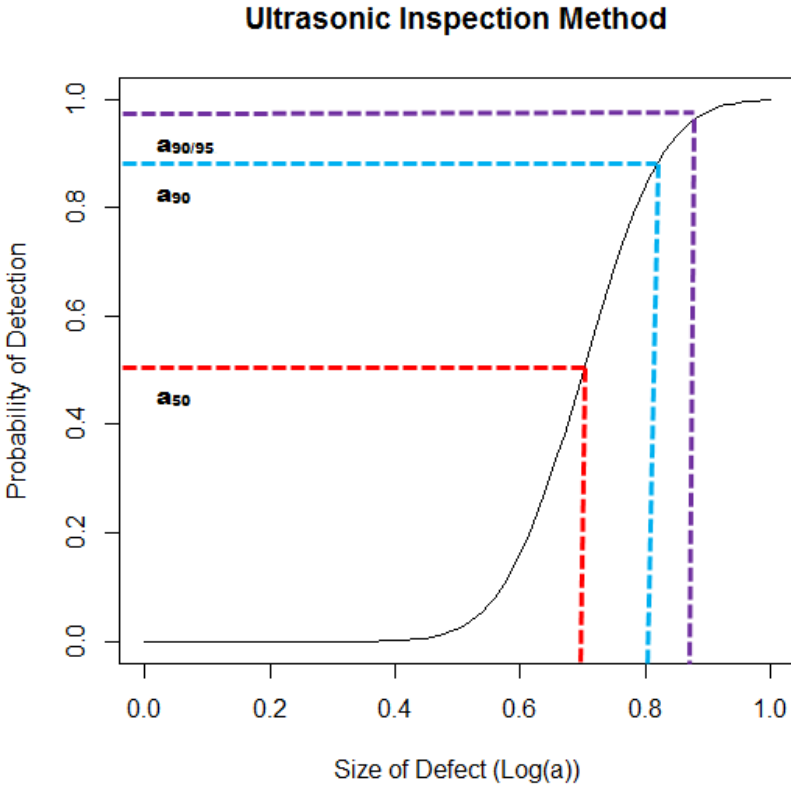


Figure 4.16: POD Curve for Ultrasonic Inspection Method.

The results of the PODs plot for the four NDT methods are summarized as follows:

Table 4.1: Actual Defect Sizes from the POD Curves

NDT Method	a ₅₀	a ₉₀	a _{90/95}
Visual (Mag Glass)	4.0 mm	28.2 mm	56.2 mm
Visual (Boroscope)	1.6 mm	2.2 mm	2.5 mm
MPI	4.0 mm	8.0 mm	12.6 mm
Ultrasonic	5.0 mm	6.3 mm	7.1 mm

Boroscope was sensitive to small size defects (> 2.5 mm) at the 95% confidence. This method offers immediate results without further analysis. It is fast and requires less time in sample preparation.

Visual inspection by magnifying glass is generally sensitive to larger size defects, but requires additional method for confirmation of results. It is less expensive, is portable and easy to use equipment with minimum training. The effectiveness in detection using visual inspection (boroscopic) was considered better than MPI and UT.

MPI method is appropriate in defect detection of both surface and subsurface defects of the aircraft landing gear and engine parts of ferrous materials, $a_{90/95} = 12.6$ mm (Fig. 4.15). However, demagnetization of inspected parts is required after the inspection. The method requires average skill to do the inspection and offers immediate results.

The application of UT method was appropriate for use to detect size defects ($a_{90/95} = 7.1$ mm) (Figure 4.16). The UT Machine is portable and has the capability to detect surface and subsurface defects. The results are obtained immediately, however little part preparation is necessary prior to measurements. A wide range of aircraft wheel hub drive keys were inspected using UT and 63.6% were found defective with cracks indications. The limitation with this method was that, the sample surface had to be accessible to the probe, and is sensitive to interference from the rough surfaces and prone to sound beam-defect orientation. It also required high degree of skill to set up.

4.6 The probable causes of the defects in the aircraft parts and the corrective actions

Fatigue crack is a severe defect in aircraft component, which is not allowed by ISO 19-100 standard. In the aircraft samples inspected, cracks could have resulted from exposure to loadings during the flights. In practice, Aircraft components are sometimes subjected to either Static or Dynamic Cyclic loadings. Dynamic loadings are more conspicuous, since the conditions are unpredictable during flying. During different flight phases, each component of the aircraft responds dynamically to the forces. In addition, the aircraft structure exhibits more concentrated response in the extreme conditions such as bird strikes or wind gusts. Cyclic loading on the other hand, results in material fatigue leading to structural failure in the aircraft. For this reason, the aircraft or component service lives are designated and defined by flight hours and these components should be inspected and changed after a certain number of flying hours for the material not to attain fatigue limits. The findings of this study show that 60% of the defects were cracks.

The existence of corrosion and corrosive environments can lead to reduced structural fatigue performance through either component damage acting as precursor to cracking or corrosive environments, which often causes acceleration in crack growth. In material/environment systems found in aircraft components, hydrogen embrittlement is the main cause of acceleration to corrosion (Li, Samuels, Zhao, & Shyr, 2017). This understanding of the fundamental nature of the initiation of fatigue from corrosion damage will help in developing strategies for alleviating

corrosion induced fatigue cracking in aircraft components. The occurrence of corrosion damage by an equivalent initial defect proved to be a dominant way and should be included into conventional fatigue analyses. This will lead to the proper understanding of the relationship between fatigue loading and associated environmental conditions and its significance on fatigue crack growth. In this study, it was revealed that 6% of the Engine samples inspected had corrosion related defects.

From the Engine cowlings and panels that were inspected, 2% each were found to have a variety of damage with the basic ones being delaminations and disbond. The causes of these defects were found to be attributed to poor material layup conditions and damages while in operation. The main parts that were affected were in the core, where material failure manifested itself in the form of cracks or buckles when the parts were exposed to excessive loads. In addition, the bond between the face sheet and the core was found to be vulnerable to damage, instigating a skin-to-core disbond. Most of the aircraft parts that had damage impact, contained delaminations and skin-to-core disbonds. There was no much variance between the delamination and the disbond defects. In the panels, it was realized that any assortment of cracking allowed corrosive fluid to leak into the core of the sandwiched panel. The result resembles a cascading effect, in which one defect was found to lead to another. This finding only supported the need to regularly carry out repairs.

CHAPTER FIVE: CONCLUSION AND RECOMMENDATIONS

5.1 Introduction

This chapter presents the conclusions and recommendations of this study.

5.2 Conclusion

The serviceability of engine and landing gear parts was evaluated using NDT methods as a basis for developing policies for a continuous improvement of the maintenance standards in the aviation industry.

The results showed that 50% of all the components inspected for brake and wheel assemblies had crack defects. The cracks defects in the engine components were highest, in combustion chamber at 24.4% and the turbine section at 24.4% followed by the exhaust section at 14.6%. Other engines components had less than 10% of other defects; corrosion, disbond and delamination.

The study assessed the effectiveness and reliability of the four (4) NDT methods for use in routine engine and landing gear inspection. Visual inspection (Borosopic) was found to be sensitive to small defect sizes (>2.5 mm). The use of nondestructive testing techniques enabled the inspectors to evaluate the integrity of structures and the properties of components non-intrusively and institute corrective measures; repair or reject. Specifically, this study identified the various structural defects in the aircraft engines and landing gear parts using ultrasonic inspection, radiography, visual testing and magnetic particle inspection methods and characterization of the defects.

The result from this study will contribute to effective use of NDT inspection techniques in the Kenya aviation industry. The challenges in the aviation industry are accidents caused by structural defects and extension of inspection intervals due to budget constraints.

This study confirmed the importance of NDT application as a necessary tool in industrial services/products inspection in aviation industry and in support for Kenya towards realization of its long-term strategic plan towards attaining Vision 2030 objectives.

5.3 Recommendations

Most of the aircraft components inspected, after service life extensions, had developed corrosion defects due to various reasons; budgetary constraints, operational need, long lead times of spare parts. Increasing the frequency of scheduled and nonscheduled inspection, to small intervals of flying hours, is highly recommended to improve the quality of inspections and maintenance programs, more so, for aircrafts operating in tropical climatic areas.

Further research is required to improve maintenance of corrosion related defects, upon approval by OEMs. The most urgent areas of concern, are the effective modelling of corrosion development, growth and the characterization and to predict strength and fatigue in aircraft inspections.

Further studies on experimental POD determinations are recommended towards determining the highest sensitivity, accuracy, and reliability of all NDT methods in locating Low Cycle Fatigue (LCF) cracks and all other types of flaws in common aerospace materials.

It was also observed during this study, that most of the specialists, were trained and certified, but required recertification. It is therefore recommended that NDT Specialists should undergo refresher training after proper *ab-nitio* training. This periodic recertification will ensure standardized and quality inspection work.

REFERENCES

- AAIB. (2005). *Field Investigation report, Royal Air Force, Grob G115E Tutor, G-BYXJ*. Southwest of Salisbury: Wiltshire.
- Airline, B. C. (2012, December 01). *Boeing Commercial Airline*. Retrieved 2018, from Boeing_737-300_400_500_Aircraft_Maintenance_ManualCommercial Airline: <https://www.academia.edu/8278925>
- Airlines, B. C. (2012). *Boeing 737-300/400/500/800 Aircraft Maintenance Manual Chapter 32-42-00*. Boeing Commercial Airlines.
- Ansley, G., Bakanas, S., Castronuovo, M., & Grant, T. (1992). Current Nondestructive Inspection Methods for Aging Aircraft. *Galaxy Scientific Corp Mays Landing NJ*, 2-29.
- ASTM. (2010). International: E114. In *Standard Practice for Ultrasonic Pulse-Echo Straight-Beam Contact Testing*.
- ASTM. (2012). International: E1742/E1742M. In *Standard Practice for Radiographic Examination*.
- ASTM. (2016). ASTM International: E1444/E1444M. In *Standard Practice for Magnetic Particle Testing*.
- Aviation, G. E. (1999). *J85-GE-21/21A/21B Aircraft Maintenance Manual IPC Chapter 73-00-05, figure 7/73-00-05-117*. General Electric Aviation Engines.
- Babu , S. J., Chan , A., & Chan , W. T. (2016). Productivity & Reliability Study of Non Destructive testing techniques for Inspection of structural welds in Construction industry. *19th World Conference on Non-Destructive Testing 2016*. Munich: German.
- Birir, J. K. (2015). *Investigation of welding quality in the Kenyan informal sector (“Juakali-sector”)*. Nairobi: Doctoral dissertation, University of Nairobi.
- Boeing. (2012). *Boeing 737-300/400/500/800 Aircraft Maintenance Manual Chapter 32-41-00*. Boeing 737 500 Commercial Airlines.

- Burke, S. K., & Ditchburn, R. J. (2013). *Review of Literature on Probability of Detection for Magnetic Particle Nondestructive Testing*. Australia: Defense Science And Technology Organization Victoria; Maritime Platforms Div.
- Campbell, G. S., & Lahey, R. (1983). A survey of serious aircraft accidents involving fatigue fracture. *1*.
- China Airlines Flight CI-611 Crash Report Released. (2005). *International Aviation Safety Organisation*. China: International Aviation Safety Organisation.
- Da Silva, R. R., & de Padua, G. X. (2012). Nondestructive inspection reliability: state of the art. pp. 4-6.
- Eurocopter. (1978). *Puma SA 330*. Retrieved May 8, 2019, from Airbus helicopters website: <https://www.airbus.com/us/en/helicopters/technical-publications.html>
- FAA. (1997). *Advisory Circular for Visual Inspection for Aircraft*. AFS-350.
- Fahr, A., & Forsyth, D. S. (1998). POD Assessment Using Real Aircraft Engine Components. *In Review of Progress in Quantitative Nondestructive Evaluation (pp. 2005-2012)*.
- Findlay, , S. J., & Harrison, N. D. (2002). Why aircraft fail. *Materials today*, 5(11), 18-25.
- Garnier, C., Pastor, M. L., Eyma, F., & Lorrain, B. (2011). The detection of aeronautical defects in situ on composite structures using Non Destructive Testing. *Composite structures*, 93(5), 1328-1336.
- GASP. (2013). *State Safety Programme (SSP) framework*. Canada: ICAO, Montréal .
- Gatari, M. J., Kairu, W. M., Maina, D. M., & Muia, M. (2014). Quality of Reinforced Concrete used on Selected Building in Nairobi, Kenya. . *11th European Conference on Non-Destructive Testing*. Czech Republic.: Prague.
- Hagemaiier, D. (1990). Nondestructive inspection of aging aircraft structure. *Materials Evaluation*, 48(12), 1499–1512.
- Harding, C. A., & Hugo, G. R. (2011). Review of Literature on Probability of Detection for Liquid Penetrant Nondestructive Testing. *Maritime Platforms Div(DSTO-TR-2623)*, pp. 7-9.

- Hellier, C. J. (2003). *Handbook of non destructive evaluation*. McGraw Hill publishers.
- IAEA. (2003). *External Events Excluding Earthquakes in the Design of Nuclear Power Plants*, IAEA. Vienna: IAEA Safety Standards Series No. NS-G-1.5.
- Ibarra-Castanedo, C., Susa, M., Klein, M., Grenier, M., Piau, J. M., Larby, W., et al. (2008). Infrared thermography: Principle and Applications to Aircraft Materials. *Proceedings from International Symposium on NDT in Aerospace*, (pp. 1-2). Germany.
- Jolly, M. R., Prabhakar, A., Sturzu, B., Hollstein, K., Singh, R., Thomas, S., et al. (2015). Review of Non-destructive Testing (NDT) Techniques and their Applicability to Thick Walled Composites. *Procedia CIRP*, 38, 129-136.
- Kurz, J. H., Jüngert, A., Dugan, S., Dobmann, G., & Boller, C. (2013). Reliability considerations of NDT by probability of detection (POD) determination using ultrasound phased array. *Engineering Failure Analysis*, 35, 609-617.
- Li, C. I., Samuels, D. C., Zhao, Y. Y., & Shyr, Y. (2017). Power and sample size calculations for high-throughput sequencing-based experiments. *Briefings in bioinformatics*, 19(6), 1247-1255.
- Maldague, X. P. (2002). Introduction to NDT by Active Infrared Thermography . *Materials Evaluation*, 60(9), 1060-1073.
- Mariera, A. N. (2013). *Review of Aviation Accidents in Kenya*. Nairobi: University of Nairobi.
- Mulama, D., & Ng'ang'a, A. (2013). Non-destructive testing applied to rig inspection (A Case Study of Menengai Geothermal Project) Geothermal Development Company (K) Ltd. Nairobi, Kenya. *GRC Transactions.*, 37, pp. 93-96.
- NDT Resource Centre Online, Nondestructive Testing in the Aerospace Industry*, [http://www.ndt-ed.org/AboutNDT/Selected Applications/ Aircraft Inspection/Aircraft%20 Inspection.htm](http://www.ndt-ed.org/AboutNDT/Selected%20Applications/Aircraft%20Inspection/Aircraft%20Inspection.htm). (n.d.).
- NTSB. (1989). *Aircraft Accident Report: NTSB/AAR-07/04, PB2007-910405*. . Washington D.C.: United States of America Government.

- NTSB. (2005). *Aircraft Accident Report: NTSB/AAR-07/04, PB2007-910405*. United States of America Government., Washington D.C.
- Packman, P. F., Pearson, H. S., Owens, J. S., & Marchese, G. B. (1968). *The Applicability of a Fracture Mechanics-Nondestructive Testing Design Criterion*. Lockheed-Georgia CO Marietta Materials Sciences Research Lab.
- Pfeiffer, H., & Wevers, M. (2007). Aircraft integrated structural health assessment—Structural health monitoring and its implementation within the European project AISHA. *In EU project meeting on aircraft integrated structural health assessment (AISHA)*. 26. Belgium: Leuven.
- Pitropakis, I. (2015). *Dedicated Solutions for Structural Health Monitoring of Aircraft Components*.
- ROK. (2012). *Kenya Airways boosts its fleet for regional expansion*. Nairobi: Ministry of Transport and Infrastructure.
- ROK. (2013). *Civil Aircraft Accident Report: CAV/ACC /8/99,2013*. Nairobi: Ministry of Transport and Infrastructure.
- ROK. (2014). *Air Accident Investigation Report: Helicopter AS350B2 Registration 5Y-HLI,2012*. Nairobi: Ministry of Transport and Infrastructure.
- Tiffany, C. F., Gallagher, J. P., Babish, I. V., & Charles, A. (2010). Threats to Aircraft Structural Safety Including a Compendium of Selected Structural Accidents/Incidents (No. ASC-TR-2010-5002). pp. 1-24.
- Underhil, P. R., Uemura, C., & Krause, T. W. (2018). Probability of detection for bolt hole eddy current in extracted from service aircraft wing structures.
- USAF, A. o. (2014). Non Destructive Inspection Methods, Technical Manual Technical Manual, T.O 33B-1-1 NAVAIR 01-1A-16, TM 1-1500-335-23. *T.O 33B-1-1 NAVAIR 01-1A-16, TM 1-1500-335-23*,. USA.

APPENDICES

Appendix 1: Non Destructive Inspection Data Form

NON-DESTRUCTIVE INSPECTION DATA				
1.control number	2. base and organization			3.MDS
4.NOMENCLATURE			5. PART OR ASSEMBLY NO.	
6. TECHNICAL ORDER NO.	PAGE NO.	FIGURE NO.	INDEX NO.	DATE OF ISSUE
7. NEXT HIGHER ASSEMBLY (noun or part No.)		8. MFR SERIAL NO. (if applicable)	9. INITIATOR NAME & PHONE NO.	
10.DESCRPTION OF DEFFECT/CONDITION OR REASON FOR INSPECTION				
11.PART INSTALLED REMOVED		12.PART PREPARATION (Disassembly, cleaning and materials)		
RADIOGRAPHIC INSPECTION TECHNIQUE				
13.EQUIPMENT AND MATERIAL USED		14. TECHNIQUES		
MANUFACTURES NAME:	MODEL	FFD TUBE TO AIMING POINT		
FILM USED	NO. OF SHEETS	KILOVOLTS	MILLIAMPERES	TIME EXPOSURE
TYPE	SIZE	DENSITY	AREA OF INTEREST	
SCREENS (0) YES (0) NO		HAND PROCESS (0)AUTOMATIC		
PENETRANT INSPECTION TECHNIQUE				

PENETRAANT MATERIAL USED					
TYPE	GROUP			PENETRANT	
EMULSIFIER	DEVELOPER			CLEANER	
16. METHOD OF APPLICATION.	17. DWELL TIMES				
(0)DIP (0)BRUSH	PENETRANT	TEMP.	EMULSIFIER	DEVELOPER	WASH RINSE TIME
(0)SPRAY					
MAGNETIC PARTICLE INSPECTION TECHNIQUE					
18. EQUIPMENT AND MATERIALS					
MANUFACTURER NAME	MODEL	NSN		WET FLUORESCENT	
DRY POWDER	VISIBLE DYE	COLOUR		HOW APPLIED	
19. INSPECTION METHOD					
Continuous b. residual c. longitudinal d. AC e. DC f. circular					
AMPS OR AMP TURNS					
EDDY CURRENT INSPECTION TECHNIQUE					
20. EQUIPMENT USED					
MANUFACTURE NAME:	MODEL	NSN		TYPE MATERIAL	
PROBE	DRAWING /SKETCH OF SHOE/HOLDER YES (0) NO	DIAMETER			
IF MORE SPACE IS NEEDED USE BLANK SHEET OF PAPER					
SEE REVERSE FOR ULTRASONIC INSPECTION TECHNIQUE					
ULTRASONIC INSPECTION TECHNIQUE					
21. EQUIPMENT AND MATERIAL USED				TYPE MATERIAL TESTED	
MANUFACTURER NAME	MODEL	NSN			
TRANSDUSER (crystal material/frequency/angle/size)					

TEST BLOCK	SHOE/WEDGE	COUPLANT	
22. INITIAL EQUIPMENT SETTINGS (all settings on machine including those that will be later adjusted)			
INSPECTION PROCEDURE (step by step description of inspection set up)			
24. SKETCH /PHOTO OF PART (show critical areas, location/orientation of defect etc.)			
25. POST INSPECTION PROCEDURES (demagnetize, post clean etc)			
IF MORE SPACE IS NEEDED USE BLANK SHEET OF PAPER			

Appendix 2: A typical record of MPI data of a commercial airline

RECEIVED UNITS SHOP RECORD											
UNIT	PART NUMBER	SERIAL NO	EX A/C		DATE		DEFECT	REGISTER NUMBER	DATE COMPLETED	AUTHORITY STAMP	REMARKS
			TYPE	REG	REMOVED	RCVD					
Tie Bolts	MS 21260-05039	N/S	E190	N/A	20/10	21/10	u.p.i	NO1/367/14	25/10	[Stamp]	Inspected
Tie Bolts	2612924	N/S	B737	N/A	16/10	21/10	u.p.i	NO1/366/14	25/10	[Stamp]	Inspected
Tie Bolts	2612924	N/S	B737	N/A	23/10	24/10	u.p.i	NO1/365/14	25/10	[Stamp]	Inspected
Tie Bolts	MS 21260-06026	N/S	E190	N/A	21/10	23/10	u.p.i	NO1/372/14	25/10	[Stamp]	Inspected
Tie Bolts	MS 21260-06026	N/S	E190	N/A	23/10	24/10	u.p.i	NO1/371/14	25/10	[Stamp]	Inspected
Tie Bolts	MS 21260-09034	N/S	E190	N/A	23/10	24/10	u.p.i	NO1/370/14	25/10	[Stamp]	Inspected
Tie Bolts	2612924	N/S	B737	N/A	15/10	24/10	u.p.i	NO1/373/14	25/10	[Stamp]	Inspected
Tie Bolts	2613109	N/S	B737	N/A	14/10	24/10	u.p.i	NO1/374/14	25/10	[Stamp]	Inspected
Drive Keys	90002335-1	N/S	E190	N/A	20/10	24/10	u.p.i	NO1/375/14	25/10	[Stamp]	Inspected
Drive Keys	90002335-1	N/S	E190	N/A	24/10	24/10	u.p.i	NO1/376/14	25/10	[Stamp]	Inspected
Drive Keys	90002335-1	N/S	E190	N/A	24/10	24/10	u.p.i	NO1/377/14	25/10	[Stamp]	Inspected
Tie bolt	2613109	N/S	737	N/A	26/10	26/10	M.P.I	NO1/378/14	27/10	[Stamp]	Inspected
Tie bolt	2613109	N/S	737	-	24/10	26/10	M.P.I	NO1/379/14	27/10	[Stamp]	Inspected
Tie bolt	2613109	N/S	737	-	24/10	26/10	M.P.I	NO1/380/14	27/10	[Stamp]	Inspected
Tie bolt	2612924	N/S	737	-	24/10	26/10	M.P.I	NO1/381/14	27/10	[Stamp]	Inspected
Tie bolt	MS 21260-06026	N/S	E190	-	24/10	26/10	M.P.I	NO1/382/14	27/10	[Stamp]	Inspected
Tie bolt	MS 21260-09034	N/S	E190	-	24/10	26/10	M.P.I	NO1/383/14	27/10	[Stamp]	Inspected
Tie bolt	MS 21260-09034	N/S	E190	-	24/10	26/10	M.P.I	NO1/384/14	27/10	[Stamp]	Inspected
Tie bolt	MS 21260-09034	N/S	E190	-	24/10	26/10	M.P.I	NO1/385/14	27/10	[Stamp]	Inspected
Tie bolt	MS 21260-09034	N/S	E190	-	24/10	26/10	M.P.I	NO1/386/14	27/10	[Stamp]	Inspected
Tie bolt	MS 21260-09034	N/S	E190	-	24/10	26/10	M.P.I	NO1/387/14	27/10	[Stamp]	Inspected
Tie bolt	MS 21260-09034	N/S	E190	-	24/10	26/10	M.P.I	NO1/388/14	27/10	[Stamp]	Inspected
Tie bolt	MS 21260-09034	N/S	E190	-	24/10	26/10	M.P.I	NO1/389/14	27/10	[Stamp]	Inspected
Tie bolt	MS 21260-09034	N/S	E190	-	24/10	26/10	M.P.I	NO1/390/14	27/10	[Stamp]	Inspected
Drive Keys	90002335-1	N/S	E190	-	24/10	26/10	M.P.I	NO1/391/14	27/10	[Stamp]	Inspected
Drive Keys	90002335-1	N/S	E190	-	24/10	26/10	M.P.I	NO1/392/14	27/10	[Stamp]	Inspected
Drive Keys	90002335-1	N/S	E190	-	24/10	26/10	M.P.I	NO1/393/14	27/10	[Stamp]	Inspected
Drive Keys	90002335-1	N/S	E190	-	24/10	26/10	M.P.I	NO1/394/14	27/10	[Stamp]	Inspected
Tie bolts	2613109	N/S	737	-	24/10	26/10	M.P.I	NO1/395/14	27/10	[Stamp]	Inspected
Tie bolts	MS 21260-09034	N/S	Revised	-	01-11-18	01-11-19	u.p.i	NO1/397/14	01-11-19	[Stamp]	Inspected
Tie bolts	MS 21260-09034	N/S	Revised	-	01-11-18	01-11-19	u.p.i	NO1/398/14	01-11-19	[Stamp]	Inspected

Appendix 3: Copy of UT Equipment Model; USD-15S Calibration Certificate

RETURN TO TECH RECORDS WHEN PART IS REPLACED


FORM NUMBER KA73C
141FCM288D4

DETAILS OF PART REMOVED

SERVICEABLE / UNSERVICEABLE*

SERVICEABLE

STAY WITH PART



Certificate of Calibration/Conformity Statement

This Certificate shall not be reproduced, except in full, without written approval of GE Inspection Technologies

Model#: USN 60L SW ND **Serial#:** 19A01JN5


Procedure Used: QCP-1350 **Calibration Date:** 05-FEB-2019

We certify that the product mentioned above was subjected to a quality inspection and testing procedure, and meets our test specifications for this product. In view of the measures taken by us for the product quality assurance, we assure you of the conformity with the product data specified in the operating documentation. All measuring tools used for testing are calibrated and traceable to national or international standards. Our quality management system is certified according to DIN EN ISO 9001.

The following Test Equipment was used to CALIBRATE/CERTIFY YOUR Instrument

Serial#	Manufacturer	Model#	Cal Date	Cal Due
17031CET	GE	CA-111A	03-05-2018	03-05-2019
20088	GE	IW-TESTBLOCK	24-10-2018	24-10-2019
628T	GE	STEEL TEST BLOCKS	22-05-2018	22-05-2019
MY40018887	AGILENT	POWERSUPPLY	12-11-2018	12-11-2019
100178	ROHDE&SCHWARZ	ATTENUATOR	05-12-2018	03-12-2019
40019872	AGILENT	WAVE GENERATOR	12-11-2018	12-11-2019
7799013	FLUKE	MULTI-METER	12-11-2018	12-11-2019
C010774	TEXTRONIX	SCOPE	12-11-2018	12-11-2019

Certified by: J. McDonnell



GE Sensing EMEA, Sensing House, Shannon Free Zone East, Shannon, Co. Clare, Ireland
 For Customer Service, call 1-866-243-2638
 www.gesensing.com
 201-247-858_SNN Rev. 2

Page 1 of 1

CDG/021-247-858_SNN/000/00

Appendix 4: Personnel Qualifications Certificates

The Hashemite kingdom of Jordan
Jordan Aeronautical-systems Company (JAC)
Amman –Marka Airport



Certificate of Recognition
This certificate of Recognition is issued to:
[Redacted Name]

place of Birth: Kenya
has successfully completed the following course
NDT /Radiography Inspection Theoretical and Practical

Dates:
7 Mar.-27 Mar.2016
Duration: 21 Days
Issued Date 14 April 2016

Instructor Name [Redacted] 

Training Manager [Redacted] 

Jordan Aeronautical Systems Company
P.O.Box 341362
Amman 11134 - Jordan
Training Department

The Hashemite kingdom of Jordan
Jordan Aeronautical-systems Company (JAC)
Amman –Marka Airport



Certificate of Recognition
This certificate of Recognition is issued to:
[Redacted Name]

place of Birth: Kenya
has successfully completed the following course
NDT /Magnetic Inspection Theoretical and Practical

Dates:
22 Feb.-6 Mar.2016
Duration: 14 Days
Issued Date 14 April 2016

Instructor Name
Mohammad F. Shishani 

Training Manager [Redacted] 

Jordan Aeronautical Systems Company
P.O.Box 341362
Amman 11134 - Jordan
Training Department

The Hashemite kingdom of Jordan
Jordan Aeronautical-systems Company (JAC)
Amman –Marka Airport



Certificate of Recognition
This certificate of Recognition is issued to:
[Redacted Name]

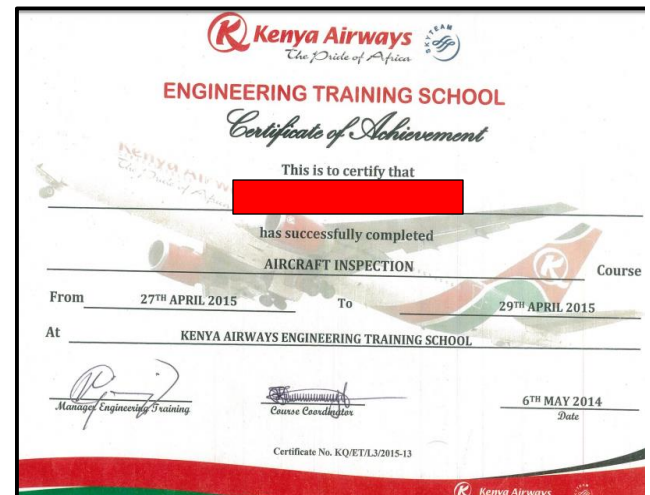
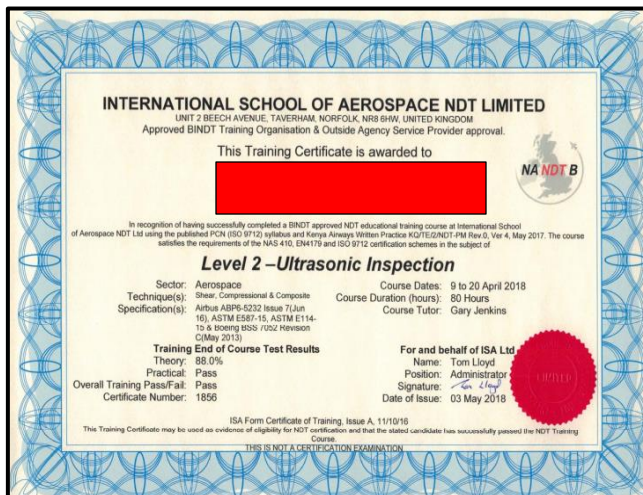
place of Birth: Kenya
has successfully completed the following course
NDT /Ultrasonic Inspection Theoretical and Practical

Dates:
28 Mar.-14 Apr.2016
Duration: 18 Days
Issued Date 14 April 2016

Instructor Name [Redacted] 

Training Manager [Redacted] 

Jordan Aeronautical Systems Company
P.O.Box 341362
Amman 11134 - Jordan
Training Department



Appendix 5 : Landing Gear Defects and Record Sheet for Stator Plates
(Permissible limits: 3.18-6.00 mm)

Code No	Comp P/No	Date Inspected	Type of defect	Size (mm)	NDT method	Defect Found (Y/N)	Aircraft Type	Reference Document
LPG1	2612875	15/12/2017	Cracks	13.5	MPI	Y	B737-800	32-40-15Rev8
LGP2	2614056	14/5/2017	Cracks	6.4	MPI	Y	B737-300	32-40-08Rev 15
LGP3	2614056	21/8/2018	Cracks	0	MPI	N	B737-300	32-40-08Rev 15
LGP4	2612875	29/8/2018	Cracks	6	MPI	Y	B737-800	32-40-15Rev8
LGP5	2614056	16/10/2018	Cracks	8.5	MPI	Y	B737-300	32-40-08Rev 15
LGP6	2612875	22/11/2018	Cracks	0	MPI	N	B737-800	32-40-15Rev8
LGP7	2614056	3/12/208	Cracks	0	MPI	N	B737-300	32-40-08Rev 15
LGP8	2614056	4/2/19	Cracks	0	MPI	N	B737-300	32-40-08Rev 15
LGP9	2614056	18/2/2019	Cracks	2.5	MPI	Y	B737-300	32-40-08Rev 15

Appendix 6: Landing Gear Defects and Record Sheet for Torque Tubes
(Permissible limits: 3.18-6.00 mm)

Code No	Comp P/No	Comp S/No	Date Inspected	Type of defect	Size (mm)	NDT method	Defect Found (Y/N)	Aircraft Type	Reference Document
LGP10	90002347	1658	24/12/2017	Cracks	3.6	MPI	Y	E190	32-49-30Rev8
LGP11	A37076	AC 149	4/8/18	Cracks/Corrosion	0	MPI	N	B737-800	32-49-80Rev8
LGP12	A36076	AC152	15/8/2018	Cracks	0	MPI	N	B737-800	32-49-80Rev8
LGP13	90002347	1291	26/8/2018	Cracks	8	MPI	Y	E190	32-49-30Rev8
LGP14	2608978	X5509	11/10/18	Cracks	0	MPI	N	B737-300	32-40-15Rev8
LGP15	2608978	X11498	12/12/18	Cracks	0	MPI	N	B737-300	32-40-15Rev8
LGP16	2608978	-	11/1/19	Cracks	0	MPI	N	B737-300	32-40-15Rev8
LGP17	2612553	-	22/2/2019	Cracks	12	MPI	Y	B737-800	32-40-15Rev15
LGP18	90002347	1297	8/7/19	Cracks/Corrosion	0	MPI	N	E190	32-49-30Rev8

Appendix 7: Landing Gear Defects and Record Sheet for Pressure Plates
(Permissible limits: 3.00-6.00 mm)

Code No	Comp P/No	Date Inspected	Type of Defect	Size (mm)	NDT method Used	Defect Found (Y/N)	Aircraft Type	Reference Document
LGP19	2612725	18/10//17	Cracks	14.8	MPI	Y	B737-300	32-40-15Rev8
LGP20	2612527	12/5/17	Cracks	5.6	MPI	Y	B737-300	32-40-15Rev8
LGP21	2612725	23/12/17	Cracks	8.5	MPI	Y	B737-800	32-40-15Rev15
LGP22	2606703	30/12/17	Cracks	1.9	MPI	Y	B737-300	32-40-15Rev8
LGP23	2606703	8/8//18	Cracks	4.0	MPI	y	B737-300	32-40-15Rev8
LGP24	2606703	22/9/18	Cracks	4.0	MPI	Y	B737-300	32-40-15Rev8
LGP25	2612725	30/10/18	Cracks	0.0	MPI	N	B737-800	32-40-15Rev15
LGP26	2606703	26/11/18	Cracks	0.0	MPI	N	B737-300	32-40-15Rev8
LGP27	2612725	28/11/18	Cracks	0.0	MPI	N	B737-800	32-40-15Rev15
LGP28	2612725	4/2/19	Cracks	0.0	MPI	N	B737-800	32-40-15Rev15
LGP29	2606703	8/2/19	Cracks	0.0	MPI	N	B737-300	32-40-15Rev8
LGP30	2606703	4/3/19	Cracks	0.0	MPI	N	B737-300	32-40-15Rev8
LGP31	2612725	10/3/19	Cracks	3.5	MPI	Y	B737-800	32-40-15Rev15

Appendix 8: Landing Gear Defects and Record Sheet for Wheel Hub Tie Bolts
(Permissible limits: No Cracks allowed)

Code No	Comp P/No	Date Inspected	Type of defect	Size (mm)	NDT method Used	Defect Found (Y/N)	Aircraft Type	Reference Document
LGP32	2612540	27/8/2018	Cracks	10.0	MPI	Y	B737-300M/W	32-40-09Rev16
LGP33	2612924	23/8/2018	Cracks	10.5	MPI	Y	B737-800N/W	32-40-10Rev9
LGP34	MS21250-09038	4/9/2018	Cracks	0.0	MPI	N	ERJ190M/W	32-49-28Rev5
LGP35	2601004	13/8/2018	Cracks	3.0	MPI	Y	B737-300N/W	32-40-10Rev9
LGP36	2612540	17/9/2018	Cracks	0.0	MPI	N	B737-300M/W	32-40-09Rev16
LGP37	MS21250	4/10/2018	Cracks	0.0	MPI	N	ERJ190N/W	32-49-16Rev5
LGP38	2313109	22/12/2018	Cracks	2.5	MPI	Y	B737-800M/W	32-40-14Rev10
LGP39	MS21250-09038	8/1/2019	Cracks	0.0	MPI	N	ERJ190M/W	32-49-28Rev5

Appendix 9: Landing Gear Defects and Record Sheet for Wheel Hub Drive Keys using MPI method

(Permissible limits: No cracks allowed)

Code No	Comp P/No	Date Inspected	Type of defect	Size (mm)	NDT method Used	Defect Found (Y/N)	Aircraft Type	Reference Document
LGP40	90002335-1	15/8/2018	cracks	0.0	MPI	N	E190	SPM 32-46-35Rev6
LGP41	9002335-1	22/8/2018	Cracks	3.0	MPI	Y	E190	SPM 32-46-35Rev6
LGP42	2606683	29/9/2018	Cracks	4.0	MPI	Y	B737-300	32-40-15Rev8
LGP43	90001323	9/10/2018	Cracks	0.0	MPI	N	E170	32-49-80Rev8
LGP44	2612925	20/11/2018	Cracks	3.5	MPI	Y	B737-800	32-40-15Rev15
LGP45	90002335-1	21/2/2019	Cracks	0.0	MPI	N	E190	SPM 32-46-35Rev6
LGP46	2612529	2/3/2019	Cracks	4.2	MPI	Y	B737-800	32-40-15Rev15

Appendix 10: Landing Gear Defects and Record Sheet for Wheel Hub Drive Keys using UT method (Permissible limits: No cracks allowed)

Code No	Wheel S. No	Inner/ Outer	Date Inspected	Type of defect	Size (mm)	NDT method Used	Defect Found (Y/N)	Aircraft Type	Ref Document (15 Rev15)
LGP47	B-10113	Outer	8/2/18	Cracks	4.0	UT	Y	B737-800	32-40-15 Rev15
LGP48	B-11608	Outer	17/12/18	Cracks	0.0	UT	N	B737-800	32-40-15 Rev15
LGP49	B-10221	Outer	18/5/18	Cracks	3.1	UT	Y	B737-800	32-40-15 Rev15
LGP50	B-13072	Outer	06/09/17	Cracks	0.0	UT	N	B737-800	32-40-15 Rev15
LGP51	B-11611	Outer	22/01/18	Cracks	3.2	UT	Y	B737-800	32-40-15 Rev15
LGP52	B-13350	Outer	31/12/18	Cracks	0.0	UT	N	B737-800	32-40-15 Rev15
LGP53	B-2236	Outer	17/01/18	Cracks	4.5	UT	Y	B737-800	32-40-15 Rev15
LGP54	B-9754	Outer	04/07/17	Cracks	10.0	UT	Y	B737-800	32-40-15 Rev15
LGP55	B-9844	Outer	17/02/19	Cracks	0.0	UT	N	B737-800	32-40-15 Rev15
LGP56	B-9966	Outer	01/05/18	Cracks	3.9	UT	Y	B737-800	32-40-15 Rev15
LGP57	B-18784	Outer	16/09/17	Cracks	4.7	UT	Y	B737-800	32-40-15 Rev15

**Appendix 11: Landing Gear Defects and Record Sheet for Landing Gear
(Permissible limits: No defects allowed)**

Code	Insp Date	Defect	Size (mm)	Method	Defect Found (Y/N)	Technical Order
LGP58	27/8/2018	Cracks	0.00	RT	N	2J-J85-9 & 2J-1-13

**Appendix 12: Compressor Section Defects and Record Sheet
(Permissible limits: No defects allowed)**

Code	Comp P/No	Date Inspected	Type of defect	Size (mm)	NDT method Used	Defect Found (Y/N)	Technical Order
EP1	000J85-091101	25/07/2018	Cracks	35.0	Visual	Y	2J-J85
EP2	000J85-183901	25/07/2018	Corrosion	40.0	Visual	Y	2J-J85
EP3	000J85-484900	18/04/2019	Cracks	0.0	MPI	N	2J-J85-9
EP4	000J85-091101	10/07/2018	Cracks	8.0	MPI	Y	2J-J85-9 & 2J-1-13

**Appendix 13: Combustion Section Defects and Record Sheet
(Permissible limits: 1.60-4.20 mm)**

Code	Comp P/No	Date Inspected	Type of defect	Size (mm)	NDT method Used	Defect Found (Y/N)	Technical Order
EP5	6013T43G09	14/03/2019	Disbond	1.8	Visual	Y	2J-J85-9
EP6	6013T43G09	14/03/2019	Cracks	4.0	Visual	Y	2J-J85-9
EP7	6013T43G09	14/03/2019	Cracks	4.6	Visual	Y	2J-J85-9
EP8	6013T43G09	14/03/2019	Cracks	4.9	Visual	Y	2J-J85-9
EP9	6013T43G09	14/03/2019	Cracks	5.2	Visual	Y	2J-J85-9
EP10	6013T43G09	14/03/2019	Cracks	5.5	Visual	Y	2J-J85-9
EP11	6013T43G09	14/03/2019	Cracks	6.4	Visual	Y	2J-J85-9
EP12	6013T43G09	14/03/2019	Cracks	7.0	Visual	Y	2J-J85-9
EP13	6013T43G09	14/03/2019	Cracks	7.4	Visual	Y	2J-J85-9
EP14	6013T43G09	14/03/2019	Cracks	8.1	Visual	Y	2J-J85-9
EP15	6013T43G09	14/03/2019	Cracks	9.0	Visual	Y	2J-J85-9
EP16	6013T43G09	14/03/2019	Corrosion	10.0	Visual	Y	2J-J85-9

Appendix 14: Turbine Section Defects and Record Sheet

(Permissible limits: No defects allowed on EP 17, EP 18, EP27, EP 26, EP27 & EP28, for EP 19-EP25 4.20 mm allowed)

Code	Comp P/No	Date Inspected	Type of defect	Size (mm)	NDT method Used	Defect Found (Y/N)	Technical Order
EP17	T53-L-703	24/09/2018	Cracks	1.0	Visual	Y	2J-J85-9 & 2J-1-13
EP18	T53-L-703	24/09/2018	Cracks	3.5	Visual	Y	2J-J85-9 & 2J-1-13
EP19	000J85-092702	18/04/2019	Delamination	0.5	Visual	Y	2J-J85-9 & 2J-1-13
EP20	000J85-092702	18/04/2019	Delamination	1.0	Visual	Y	2J-J85-9 & 2J-1-13
EP21	000J85-092702	18/04/2019	Cracks	2.0	Visual	Y	2J-J85-9 & 2J-1-13
EP22	000J85-092702	18/04/2019	Cracks	2.5	Visual	Y	2J-J85-9 & 2J-1-13
EP23	000J85-092702	18/04/2019	Cracks	3.5	Visual	Y	2J-J85-9 & 2J-1-13
EP24	000J85-092702	18/04/2019	Cracks	4.0	Visual	Y	2J-J85-9 & 2J-1-13
EP25	002972655	18/04/2019	Cracks	3.9	Visual	Y	PT6MM VOL 1
EP26	0279005070	03/06/2018	Cracks	3.9	Visual	Y	2J-J85-9 & 2J-1-13
EP27	0227905070	03/06/2018	Cracks	6.1	Visual	Y	2J-J85-9 & 2J-1-13
EP28	000J85-003903	10/01/2019	Cracks	8.0	MPI	Y	2J-J85-9

Appendix 15: Exhaust Section Defects and Record Sheet

(Permissible limits: 12.70-25.4 mm for EP29-EP34)

Code	Comp P/No	Date Inspected	Type of defect	Size (mm)	NDT method Used	Defect Found (Y/N)	Technical Order
EP29	000J85-183901	10/02/2019	Cracks	8.0	Visual	Y	2J-J85-9 & 2J-1-13
EP30	000J85-183901	10/02/2019	Cracks	10.0	Visual	Y	2J-J85-9 & 2J-1-13
EP31	000J85-183901	10/02/2019	Cracks	13.0	Visual	Y	2J-J85-9 & 2J-1-13
EP32	000J85-183901	10/02/2019	Cracks	15.0	Visual	Y	2J-J85-9 & 2J-1-13
EP33	000J85-183901	10/02/2019	Corrosion	18.0	Visual	Y	2J-J85-9 & 2J-1-13
EP34	000J85-183901	10/02/2019	Cracks	20.0	Visual	Y	2J-J85-9 & 2J-1-13
EP35	6011T25G17	09/07/2018	Cracks	220	Visual	Y	2J-J85-9 & 2J-1-13

Appendix 16: Other Sections Defects and Record Sheet

(Permissible limits: No crack allowed for EP36-EP42 & 25.40 mm for EP43)

Code	Comp P/No	Date Inspected	Type of defect	Size (mm)	NDT method Used	Defect Found (Y/N)	Technical Order
EP36	000J85-183901	15/11/2018	Corrosion	22.0	Visual	Y	2J-J85-9 & 2J-1-13
EP37	000J85-183901	15/11/2018	Corrosion	25.0	Visual	Y	2J-J85-9 & 2J-1-13
EP38	000J85-183901	15/11/2018	Corrosion	5.0	Visual	Y	60294-7
EP39	000J85-183901	15/11/2018	Cracks	6.0	Visual	Y	60294-7
EP40	000J85-183901	15/11/2018	Disbond	3.0	Visual	Y	60294-7
EP41	000J85-183901	15/11/2018	Cracks	8.0	Visual	Y	60294-7
EP42	000J85-183901	15/11/2018	Cracks	25.0	Visual	Y	60294-7
EP43	000J85-183901	26/03/2019	Cracks	0.0	Visual	N	2J-J85-9 & 2J-1-13

Appendix 17: Radiographic Inspection of Landing Gear Parts

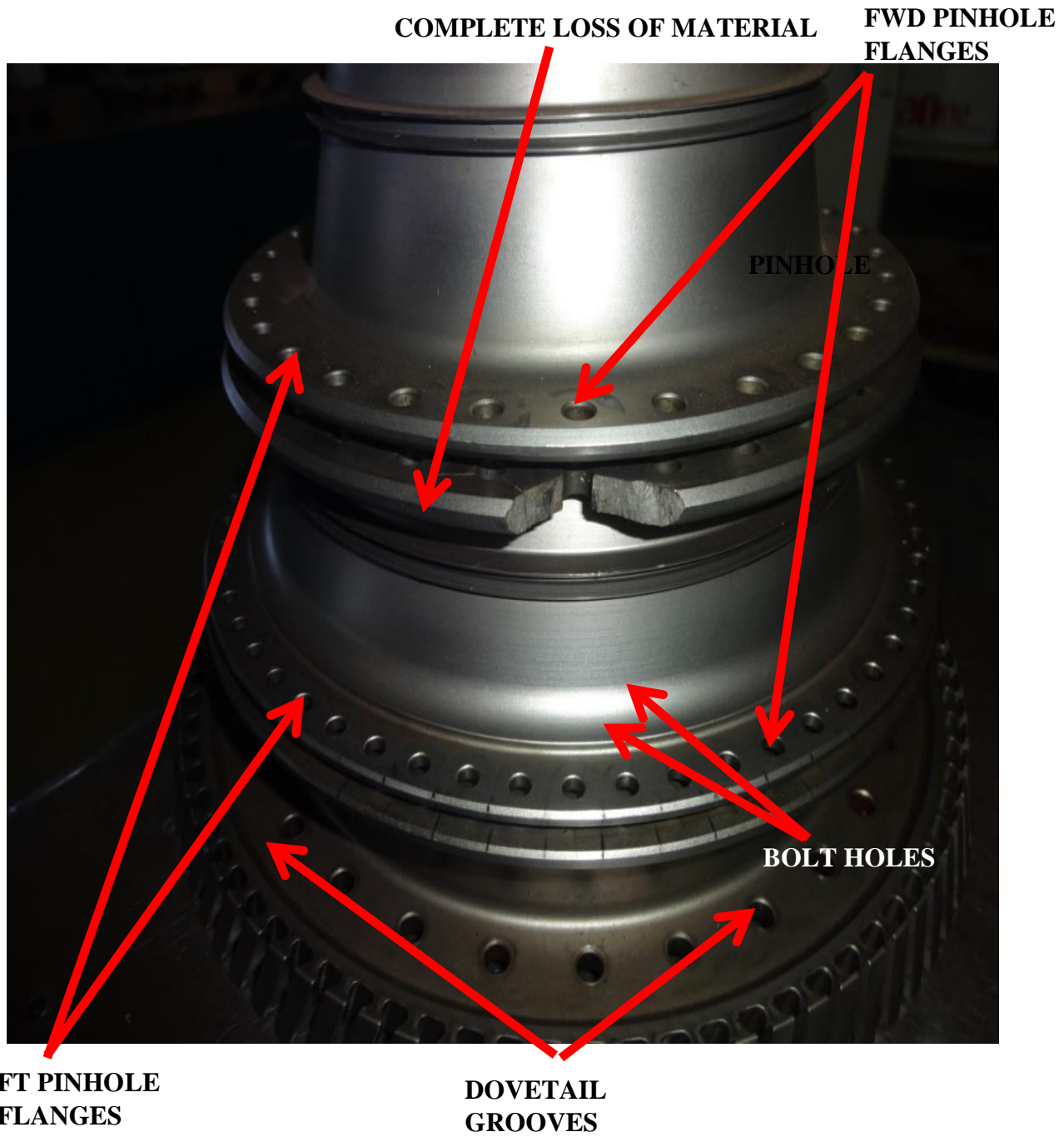
NON-DESTRUCTIVE INSPECTION DATA						30
1. control number		15/19 [REDACTED]			3. MDS	
4. NOMENCLATURE				5. PART OR ASSEMBLY NO.		
- Right and left hand main landing gear strut - Left and Right hand Main landing gear Support				61097		
6. TECHNICAL ORDER NO.	PAGE NO.	FIGURE NO.	INDEX NO.	DATE OF ISSUE		
MIA	MIA	MIA		8/15/2019		
7. NEXT HIGHER ASSEMBLY (noun or part No.)		8. MFR SERIAL NO. (if applicable)		9. INITIATOR NAME & PHONE NO.		
MAIN LANDING GEAR						
10. DESCRIPTION OF DEFECT/CONDITION OR REASON FOR INSPECTION						
- Heavy landing of the Puma helicopter that resulted to the port main landing gear to be damaged to beyond and extended the damage to the airframe.						
11. PART			12. PART PREPARATION (Disassembly, cleaning and materials)			
- landing support installed - main landing gear removed			- Jack the aircraft and remove the main landing gear - Remove access panels to landing gear support for the film placement and X-ray shooting points - cleaning is mandatory.			
RADIOGRAPHIC INSPECTION TECHNIQUE						
13. EQUIPMENT AND MATERIAL USED			14. TECHNIQUES			
MANUFACTURER NAME:	MODEL	FFD TUBE TO AIMING POINT				
gilardoni	Film type	.1000mm / 1mr				
FILM USED	NO. OF SHEETS	KILOVOLTS	MILLIAMPERES	TIME EXPOSURE		
D4	5 sheets	140KV	4	6min		
TYPE	SIZE	DENSITY	AREA OF INTEREST			
D4	- 17 x 14 inches - 17 x 10 inches	2.5				
SCREENS		HAND PROCESS		AUTOMATIC		
<input checked="" type="checkbox"/> YES () NO		<input checked="" type="checkbox"/>		<input type="checkbox"/>		
INSPECTION PROCEDURE (step by step description of inspection set up)						
<ul style="list-style-type: none"> - Cord on the area to be used for X-ray - do a setup of the xray machine, x-ray generator and Control unit to the Power supply - Set the generator control unit to power of 140kv, 4ma and exposure time of 6min delay time of .60 seconds. - prepare the film to be used in a dark room and put in film cassette - section of the landing gear to be filmed to be between the film and x-ray source considering the FFD of .1000mm. - Make trial shots as you develop the films to right density of 2.5 - Now you can make the x-ray for the rest of the parts using the set parameters. - Develop the films in well prepared room that has the developer and fixer. 						
24. SKETCH /PHOTO OF PART (show critical areas, location/orientation of defect etc.)						
<ul style="list-style-type: none"> - on the main landing gear support more emphasis on the stiff of the bolt nuts and cracks around the area. - All section of the landing gear should be free from any kind of damage. - wheel axial and its attachment. <p>Films are Provided for views.</p>						
25. EVALUATION						
- Results after developing the film show that the main landing gear and main landing gear support had no damage thus serviceable.						

N.D.I. SECTION
STAR...

Appendix 18: Visual (Magnifying Glass) Inspection of Engine Compressor Rotor Spool

NON-DESTRUCTIVE INSPECTION DATA				
1. control number 10/18 [REDACTED]		3. MDS		
4. NOMENCLATURE COMPRESSOR ROTOR SPOOL			5. PART OR ASSEMBLY NO. 0000J85-091101	
6. TECHNICAL ORDER NO. T.O. 25-J85-9	PAGE NO. 4-32	FIGURE NO. 4-22	INDEX NO.	DATE OF ISSUE 25/7/2018
7. NEXT HIGHER ASSEMBLY (noun or part No.) COMPRESSOR SECTION		8. MFR SERIAL NO. (if applicable)	9. INITIATOR NAME & PHONE NO.	
10. DESCRIPTION OF DEFECT/CONDITION OR REASON FOR INSPECTION - ENGINE COMPRESSOR SURGE.				
11. PART - REMOVED		12. PART PREPARATION (Disassembly, cleaning and materials) - Open the compressor casing to access the compressors - Remove the compressor vanes and stator in order to remain with the rotor.		
VISUAL (MAGNIFYING GLASS) INSPECTION				
20. EQUIPMENT USED Magnifying glass.				
MANUFACTURE NAME: M/A		MODEL M/A	NSN M/A	
PROBE M/A	GUIDE TUBE USED () YES <input checked="" type="checkbox"/> NO		DIAMETER (mm) 35.0 400mm	TYPE MATERIAL 150-watt standard spot light X10 magnifying glass
INSPECTION PROCEDURE (step by step description of inspection set up) - Remove the compressor vanes and stator in order to access the spool. - Clean the spool and inspect under white light with aid of the X10 magnifying glass.				
N.D.I-SECTION STATUS: Inspector SIGN: [REDACTED] DATE: 25/7/2018				
24. SKETCH /PHOTO OF PART (show critical areas, location/orientation of defect etc.) a) Pin hole. b) bolt holes. c) Pin hole flanges. SEE APPENDIX 12.				
25. EVALUATION - The compressor spool was broken and lost part of the material on aft pin hole. - The loss to material ranging from 20mm in depth and 40mm in length.				
25. POST INSPECTION PROCEDURES. - Compressor rotor to be replaced with a new serviceable rotor.				

Appendix 19: Photo of Compressor Spool

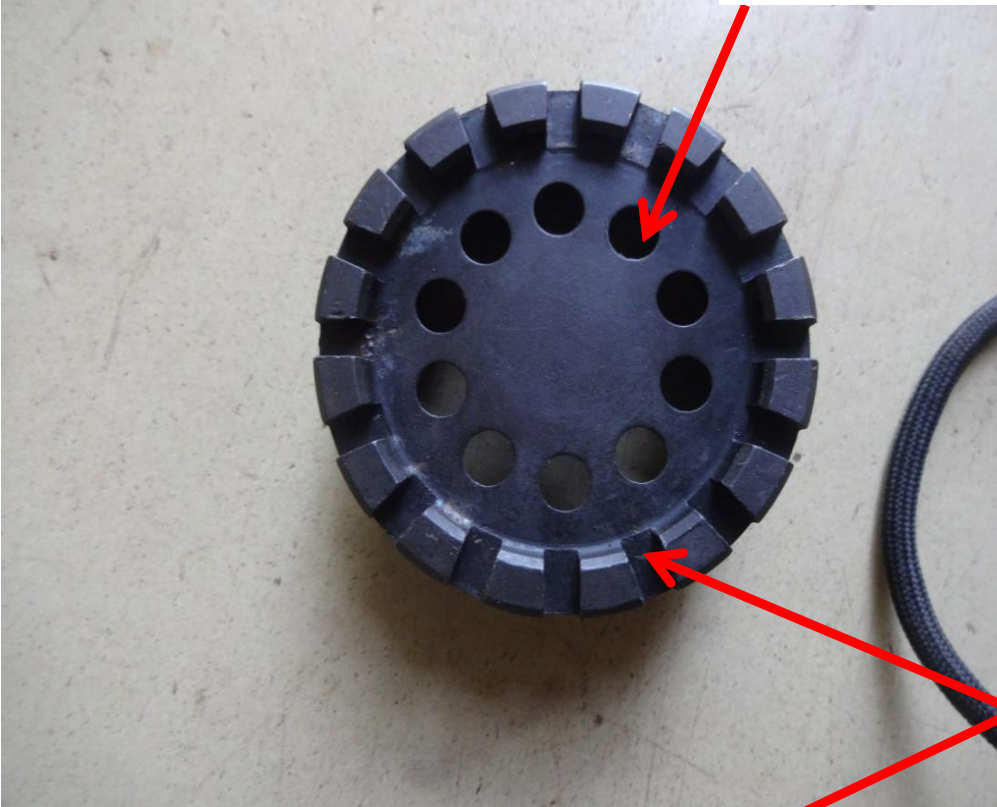


Appendix 20: MPI Data for Bearing Lock Nut

NON-DESTRUCTIVE INSPECTION DATA					18
1. CONTROL NUMBER 13/18		[REDACTED]		3. MDS	
4. NOMENCLATURE BEARING LOCK NUT			5. PART OR ASSEMBLY NO. 000J85-484900		
6. TECHNICAL ORDER NO. T.O 2J-785-9	PAGE NO. 2-3	FIGURE NO. 2-3	INDEX NO.	DATE OF ISSUE 18/3/2018	
7. NEXT HIGHER ASSEMBLY (noun or part No.)		8. MFR SERIAL NO. (if applicable)		9. INITIATOR NAME & PHONE NO.	
10. DESCRIPTION OF DEFECT/CONDITION OR REASON FOR INSPECTION - removed for inspection due to engine vibrations					
11. PART Removed			12. PART PREPARATION (Disassembly, cleaning and materials) - Loosen the nut and remove - Clean the bearing nut by vapour blasting		
MAGNETIC PARTICLE INSPECTION TECHNIQUE					
18. EQUIPMENT AND MATERIALS					
MANUFACTURER NAME Gib Gould Bass		MODEL GB-3509A-01	NSN 6635-01366-6791	WET FLUORESCENT YES	
DRY POWDER MIA		VISIBLE DYE MIA	COLOUR GREEN	HOW APPLIED Flowing or Pouring	
19. INSPECTION METHOD (MAGNETIZING METHODS)					
<input checked="" type="checkbox"/> a. Continuous <input type="checkbox"/> b. residual <input checked="" type="checkbox"/> c. longitudinal <input type="checkbox"/> d. AC <input checked="" type="checkbox"/> e. DC <input checked="" type="checkbox"/> f. circular					
AMPS OR AMP TURNS - 4500 amps for circular and 8000 amps turns for longitudinal					
INSPECTION PROCEDURE (step by step description of inspection set up) - Magnetize the bearing lock nut circularly - Flow or Pour fluorescent magnetic suspension and inspect for defects originating from the nut slots. - Magnetize the bearing lock nut longitudinally and inspect the cracks along the threads. - Interpretation of the indication the demagnetize the lock nut to residual magnetism not to exceed 2 gauss.					
24. SKETCH /PHOTO OF PART (show critical areas, location/orientation of defect etc.) a) Along the threads b) From the wrench slots Appendix 19 and 20				N.D.I-SECTION STATUS... Inspector SIGN... [REDACTED] DATE 18/3/2018	
25. EVALUATION NO CRACKS (0.0mm) were found from wrench slots and along threads					
26. POST INSPECTION PROCEDURE (DEMAGNETIZATION, POST CLEAN) - Demagnetize the bearing lock nut to residual magnetism not to exceed 2 gauss using gauss indicator					

Appendix 21: Photos of Defects on The Bearing Locknut (Around the holes)

AROUND THE HOLES



LOCK NUT SLOTS

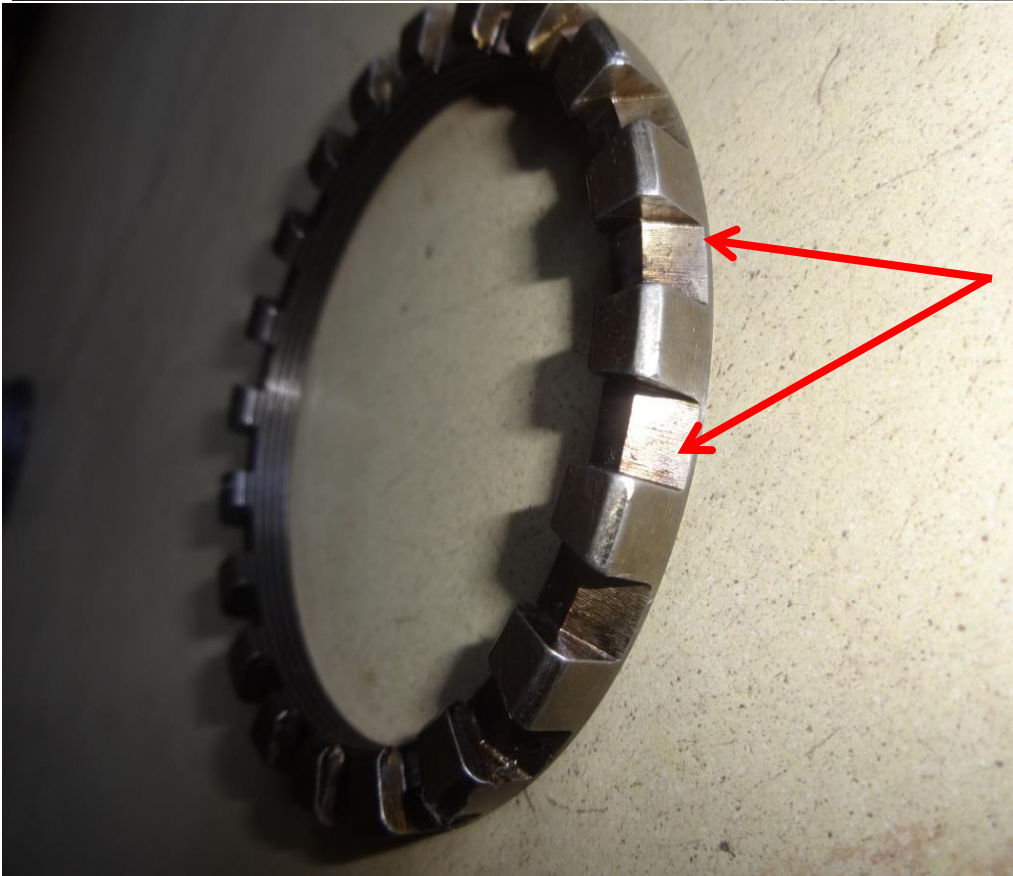


ALONG THE THREADS

Appendix 22: Photos of Defects on The Bearing Locknut (Along the nut threads)



**ALONG THE NUT
THREADS**



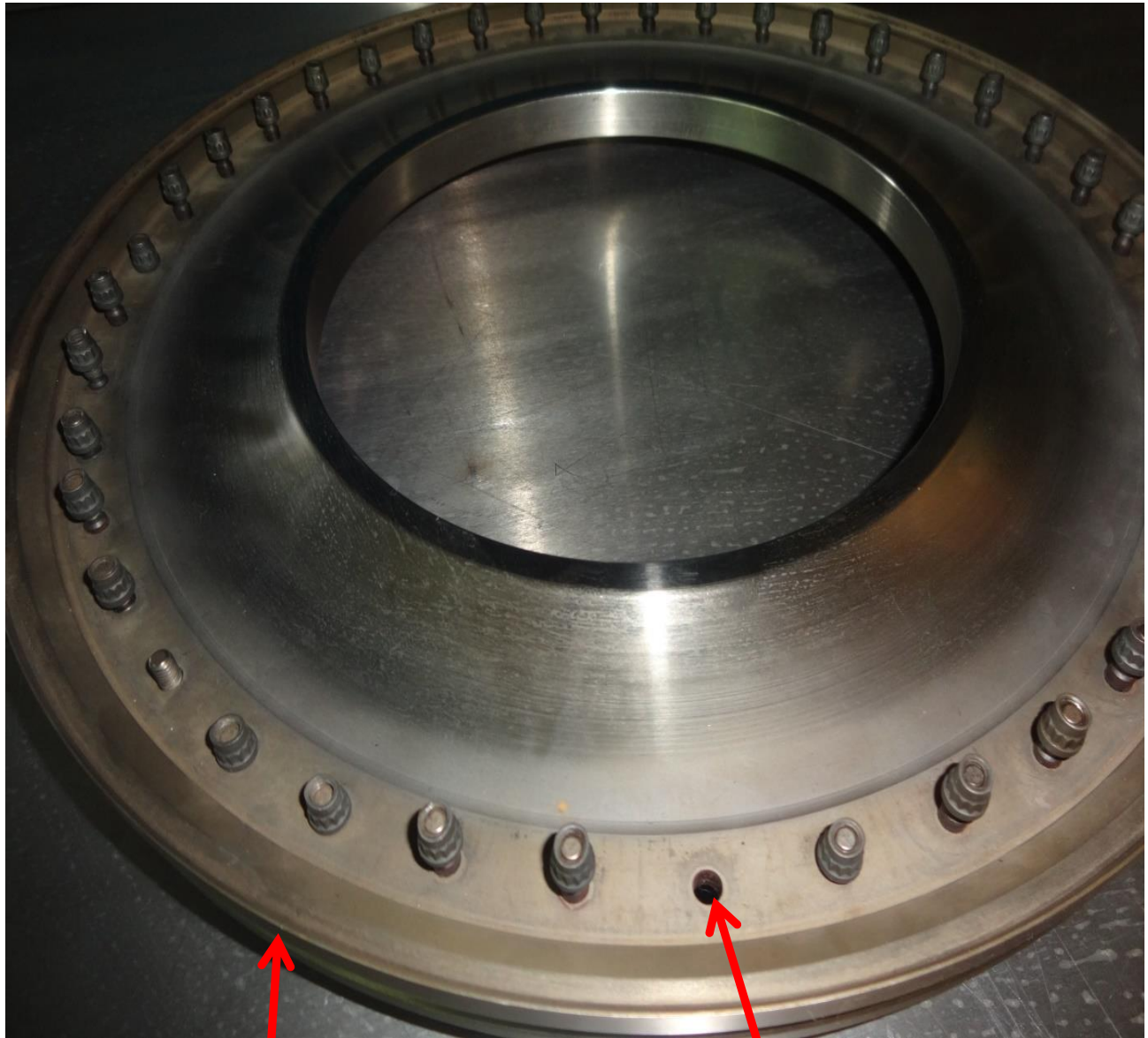
**POINTS FOR
CRACKS**

Appendix 23: MPI of Engine Compressor Rotor Spacer Disc

NON-DESTRUCTIVE INSPECTION DATA						23
1. CONTROL NUMBER 40/18					3. MDS	
4. NOMENCLATURE Compressor rotor spacers disk				5. PART OR ASSEMBLY NO.		
6. TECHNICAL ORDER NO. 2JJB5-9		PAGE NO. 4-29-31	FIGURE NO. 4-21	INDEX NO.	DATE OF ISSUE 16/07/2018	
7. NEXT HIGHER ASSEMBLY (noun or part No.) Compressor section			8. MFR SERIAL NO. (if applicable)		9. INITIATOR NAME & PHONE NO.	
10. DESCRIPTION OF DEFECT/CONDITION OR REASON FOR INSPECTION - Compressor Surge.						
11. PART - Removed			12. PART PREPARATION (Disassembly, cleaning and materials) - Disassemble of the disk from the engine - Loosen the bolts nuts and remove to access the holes			
MAGNETIC PARTICLE INSPECTION TECHNIQUE						
18. EQUIPMENT AND MATERIALS						
MANUFACTURER NAME GB Gould Boss		MODEL GB-3509A-01	NSN 6635-01 366-6791		WET FLUORESCENT YES	
DRY POWDER N/A		VISIBLE DYE N/A	COLOUR yellow green		HOW APPLIED Wet continuous	
19. INSPECTION METHOD (MAGNETIZING METHODS)						
<input checked="" type="checkbox"/> a. Continuous <input type="checkbox"/> b. residual <input checked="" type="checkbox"/> c. longitudinal <input type="checkbox"/> d. AC <input type="checkbox"/> e. DC <input checked="" type="checkbox"/> f. circular						
AMPS OR AMP TURNS - 3000 amps for circular magnetization and 16000 amps longitudinal						
INSPECTION PROCEDURE (step by step description of inspection set up) - Clean the Compressor rotor spacer - Circular Magnetize the part with 3000 amps and inspect the cracks - longitudinally magnetize with 16000 amps and inspect. - Demagnetize the Compressor rotor spacer and check for magnetism by field indicator.						
24. SKETCH /PHOTO OF PART (show critical areas, location/orientation of defect etc.) - cracks from belt holes. - cracks from edges of the compressor rotor spacer. - No cracks allowed on the compressor disk. APPENDIX 24						
25. EVALUATION - crack of 8.0mm on longitudinal magnetization. - No cracks from belt holes.						
26. POST INSPECTION PROCEDURE (DEMAGNETIZATION, POST CLEAN) - Demagnetize the part to magnetism less than 2 gauss.						

N.D.I. SECTION
 STATUS... Inspector
 CIRC. 1/1/1 1.

Appendix 24: Photos of Engine Compressor Section



COMPRESSOR DISK EDGE

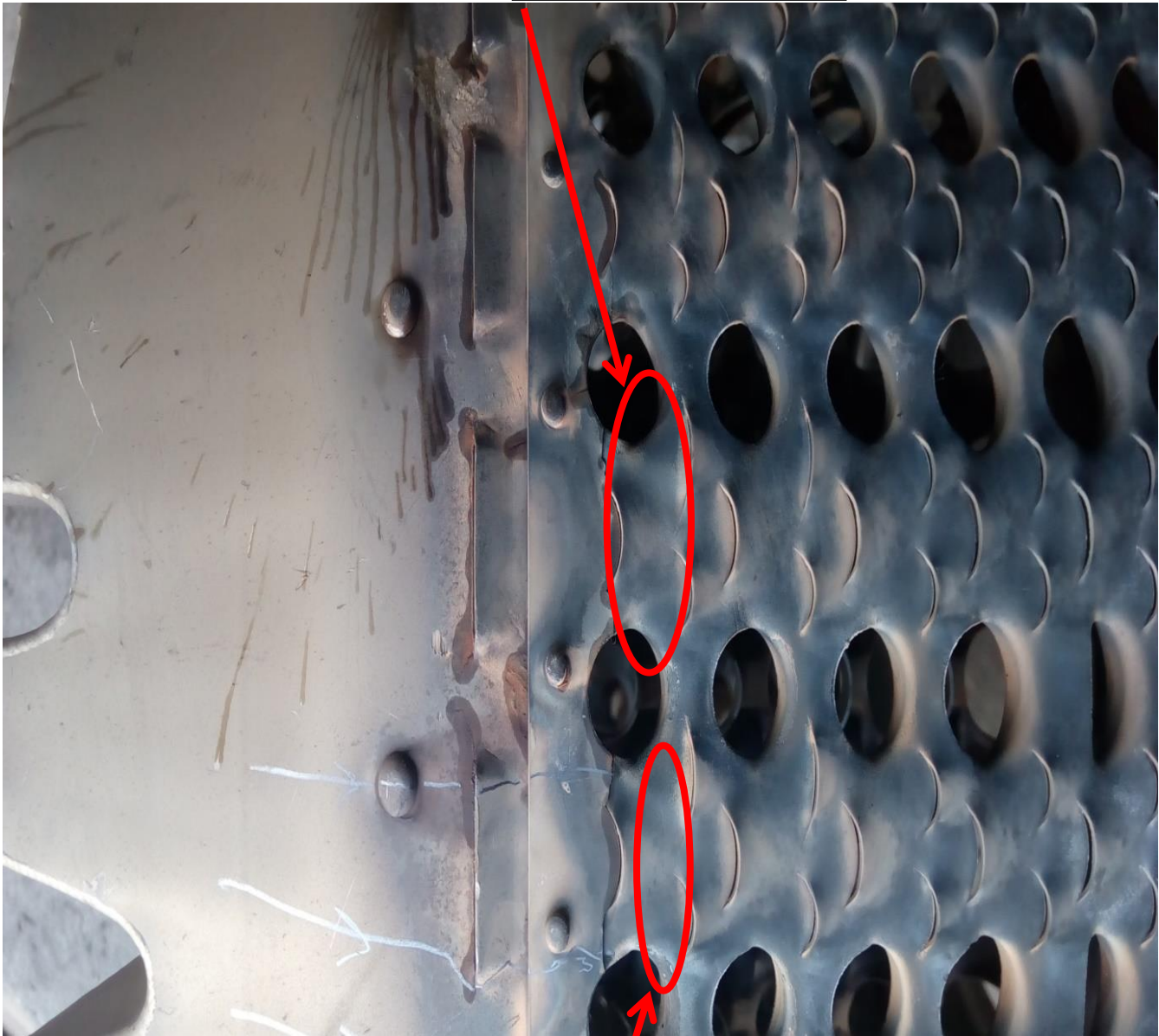
BOLT HOLES

Appendix 25: Visual (Magnifying Glass) Inspection of Combustion Section

NON-DESTRUCTIVE INSPECTION DATA					
1. control number 17/19					3. MDS
4. NOMENCLATURE COMBUSTION LINNER.			5. PART OR ASSEMBLY NO. 6013T43G09		
6. TECHNICAL ORDER NO. 2I-J85-9	PAGE NO.	FIGURE NO.	INDEX NO.	DATE OF ISSUE 14/3/2019	
7. NEXT HIGHER ASSEMBLY (noun or part No.) Combustion Chamber		8. MFR SERIAL NO. (if applicable)		9. INITIATOR NAME & PHONE NO.	
10. DESCRIPTION OF DEFFECT/CONDITION OR REASON FOR INSPECTION - Hot section inspection after variation in T5 or temperature oscillation.					
11. PART - Removed			12. PART PREPARATION (Disassembly, cleaning and materials) - Disassemble the engine and remove the chamber - Remove the combustion liner and clean in the combustor to remove carbon.		
VISUAL (MAGNIFYING GLASS) INSPECTION					
20. EQUIPMENT USED					
MANUFACTURE NAME: MIA		MODEL MIA	NSN MIA		
PROBE MIA	GUIDE TUBE USED () YES <input checked="" type="checkbox"/> NO		DIAMETER (mm) 1.2, 4.0, 4.6, 4.9 5.2, 5.5, 6.4, 7.0 7.4, 8.1, 9.0, 10.5	TYPE MATERIAL 150-watt standard spot light X10 Magnifying glass	
INSPECTION PROCEDURE (step by step description of inspection set up) - Clean the combustion liner by ice blasting or chemical cleaning in the combustor. - Visually inspect for cracks on both inner and outer liner by aid of a magnifying glass.					
24. SKETCH /PHOTO OF PART (show critical areas, location/orientation of defect etc.) a) cracks from or along the welds b) cracks originating from the outer liner baffles Appendix 26 & 27					
25 EVALUATION a) cracks were found originating from the baffles and inner welds b) excessive burnout of the combustion liner. c) cracks length from 1.8mm to 10.00mm.					
25. POST INSPECTION PROCEDURES. - No repair on the combustion liner thus considered as scrap N.D.I-SECTION STATUS: Inspector SIGN: [Signature]					

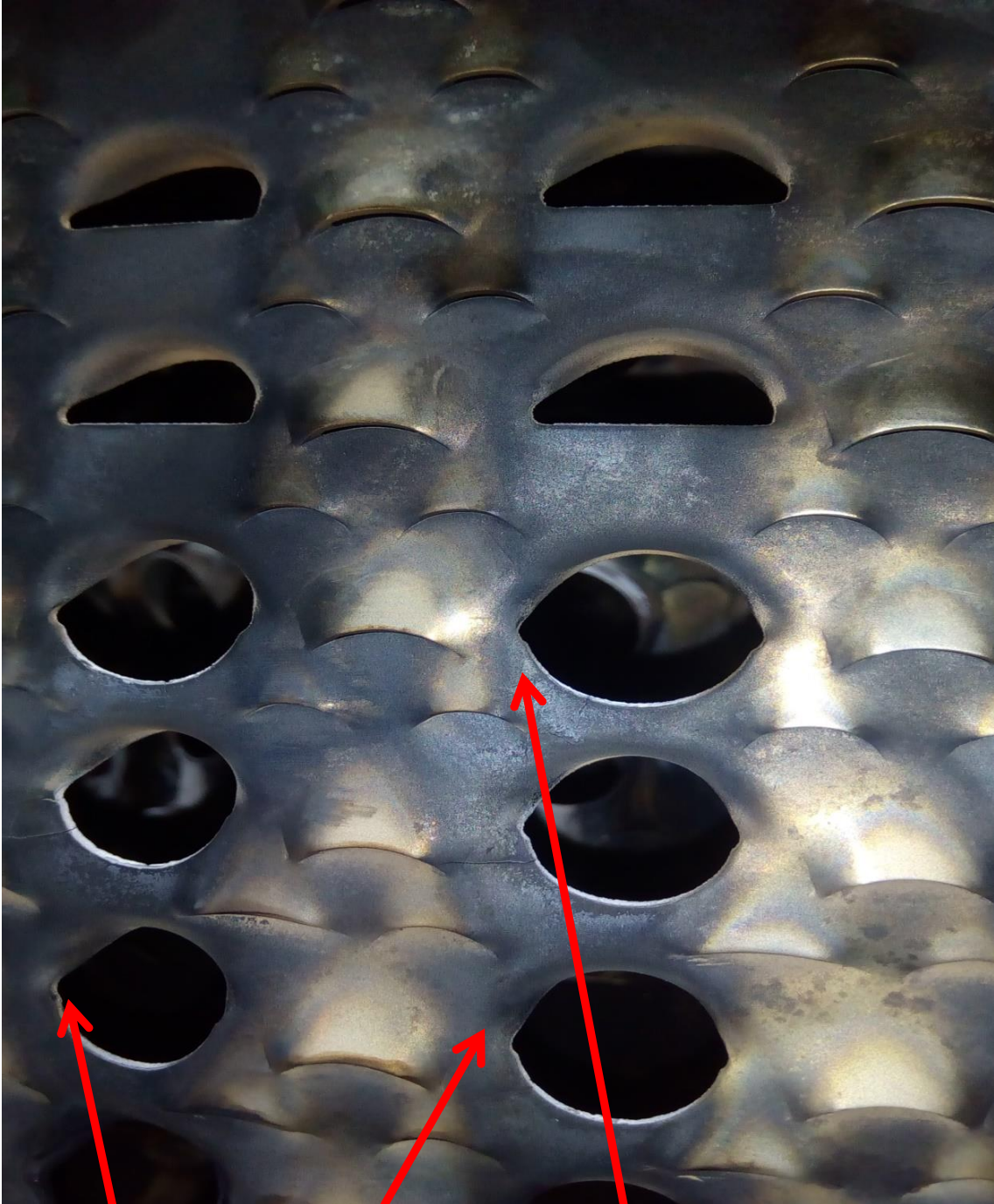
Appendix 26: Photos of Combustion Liner showing cracks

CRACKED AREAS



CRACKS FROM THE BAFFLES

Appendix 27: Photos of Defects on the Combustion Liner



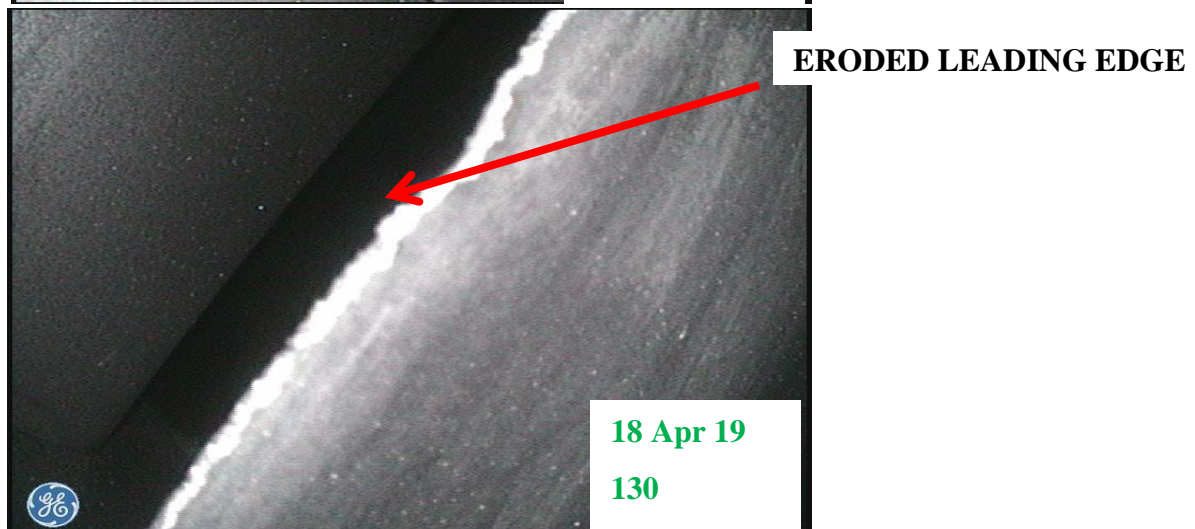
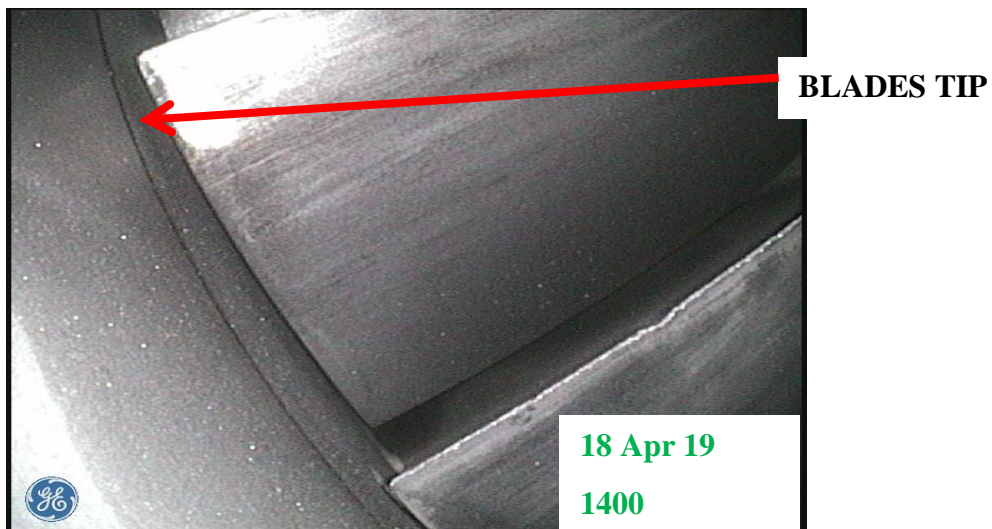
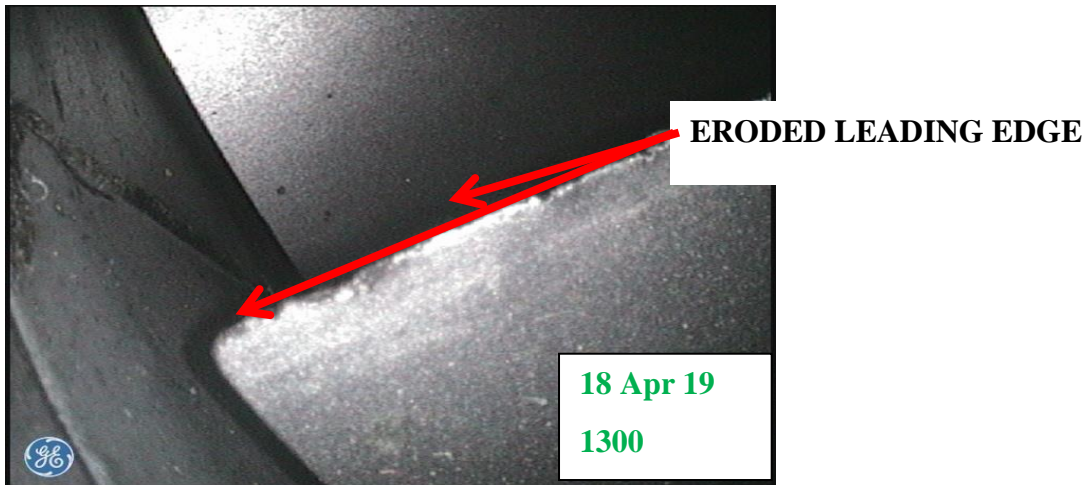
CRACKS ON COMBUSTION LINER AND BURNED OUT

Appendix 28: Visual (Borosopic) Inspection of Engine Turbine Section

13				
NON-DESTRUCTIVE INSPECTION DATA				
1. CONTROL NUMBER 20/18			3. MDS	
4. NOMENCLATURE ENGINE TURBINE SECTION			5. PART OR ASSEMBLY NO. TS3-L-703	
6. TECHNICAL ORDER NO. TM 55-2840-229-23-1	PAGE NO.	FIGURE NO.	INDEX NO.	DATE OF ISSUE 24/9/2018
7. NEXT HIGHER ASSEMBLY (noun or part NO) ENGINE		8. MFR SERIAL NO. (if applicable) M		9. INITIATOR NAME & PHONE NO.
10. DESCRIPTION OF DEFECT/CONDITION OR REASON FOR INSPECTION - scheduled bore scope inspection at 150 flying hours				
11. PART - installed		12. PART PREPARATION (Disassembly, cleaning and materials) - unsecure and remove the blank to get access port to the turbine section		
VISUAL (BORESCOPE) INSPECTION				
20. EQUIPMENT USED Bore scope				
MANUFACTURE NAME: GF Inspection Technologies		MODEL Everest XLG3	NSN N/A	
PROBE XLG3 video probe	GUIDE TUBE USED (0) YES <input type="checkbox"/> NO <input checked="" type="checkbox"/>		DIAMETER 1.0mm 3.5mm 3.9mm	TYPE MATERIAL titanium
INSPECTION PROCEDURE (step by step description of inspection set up) - unsecure and remove the blank to access port to turbine section - Carefully slide in the probe cable until you see the turbine blades on the bore scope LCD screen - shoot the pictures as you rotate the compressor section for complete coverage of the turbines - save all the pictures and stereos on the internal memory of the scope for future reference.				
24 SKETCH/PHOTO OF PART (show critical areas, location/orientation of defects) a) cracks on the turbine blades leading and trailing edges b) cracks on the roots and broken blade tips c) Carbon and other dirt substances in these hot section. d) Hot section burn out.				
25. EVALUATION - After inspection it was found that, the power turbines blades were eroded on the leading edges towards the blade tips rendering the engine to undergo Manufacturers Maintenance. - The depth of erosion being 1mm to 3.9mm which exceeds the limit of 0.5mm.				
26. POST INSPECTION PROCEDURE - Remove the optical cable from the port - secure the blank to close the access port.				

N.D. SECTION
STATUS... INSPECTOR
... [Signature] ...

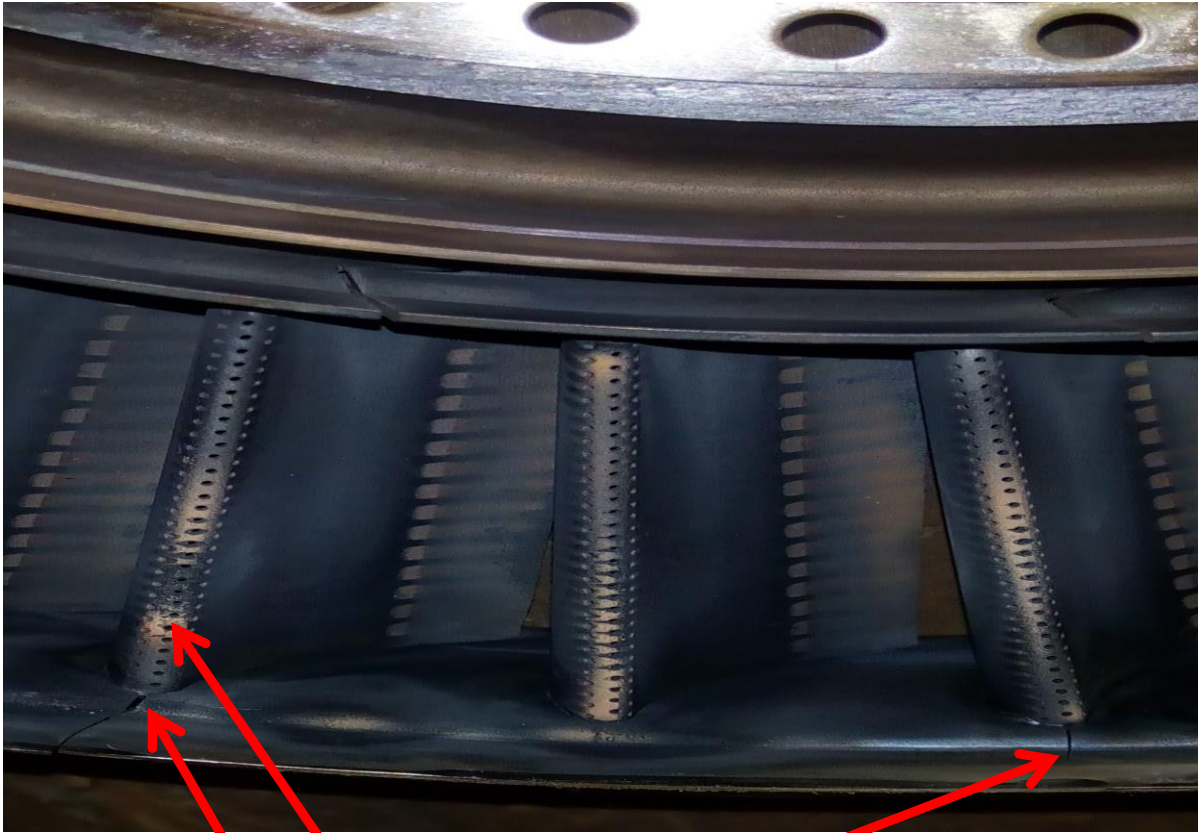
Appendix 29: Photos of Aircraft Engine Power Turbine



Appendix 30: Visual (Magnifying Glass) Inspection of Engine Turbine Section

NON-DESTRUCTIVE INSPECTION DATA					
1. control number 21/19			3. MDS		
4. NOMENCLATURE NOZZLE STAGE 2 TURBINE			5. PART OR ASSEMBLY NO. 000185-092702		
6. TECHNICAL ORDER NO. 25-J85-98 2J-1-13	PAGE NO. 8-8	FIGURE NO. 8-5	INDEX NO.	DATE OF ISSUE 13/4/2019	
7. NEXT HIGHER ASSEMBLY (noun or part No.) TURBINE SECTION		8. MFR SERIAL NO. (if applicable)		9. INITIATOR NAME & PHONE NO.	
10. DESCRIPTION OF DEFFECT/CONDITION OR REASON FOR INSPECTION - Turbine section burnout or Excessive T5 temperatures					
11. PART - removed			12. PART PREPARATION (Disassembly, cleaning and materials) - Engine disassembly - Carbon removal by vapour blasting - cleaning I. AW T.O 2J-1-13 PROCESS 6		
VISUAL (MAGNIFYING GLASS) INSPECTION					
20. EQUIPMENT USED Magnifying glass					
MANUFACTURE NAME: N/A		MODEL N/A	NSN N/A		
PROBE N/A	GUIDE TUBE USED (0) YES <input checked="" type="checkbox"/> NO		DIAMETER 0.5, 1.0, 2.0, 2.5 3.5 and 4.0	TYPE MATERIAL 150-watt standard spot light. X10 magnifying glass	
INSPECTION PROCEDURE (step by step description of inspection set up) - Clean the stage 2 turbine nozzle to remove carbon deposits - Inspect for cracks dents and Corrosion in white light through X10 magnifying glass.					
24. SKETCH /PHOTO OF PART (show critical areas, location/orientation of defect etc.) a) Partition leading and trailing edges. b) Partition Concave surface inner band forward edge. c) outer flange forward lip. APPENDIX 16 and 17					
25 EVALUATION - cracks on trailing edge length 0.5mm to 4mm not repairable - cracks from the front side of 40mm - Stage burn out due to high T5 temperatures.					
25. POST INSPECTION PROCEDURES. - Inspect the part by fluorescent penetrant after TIG welding repair for the stage that is repairable. N.D.I-SECTION STATUS: Inspector SIGN: [Signature]					

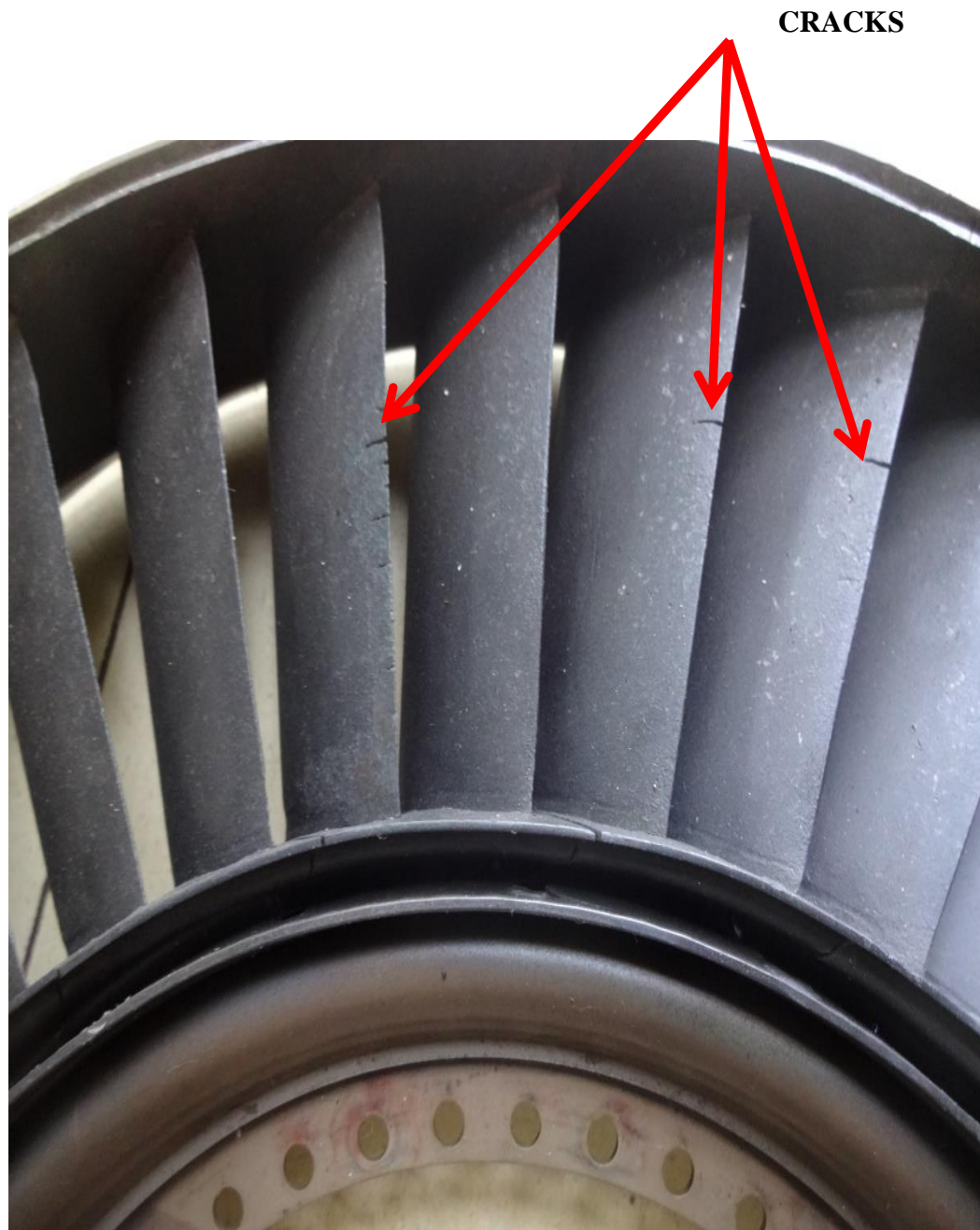
Appendix 31: Photos of Defects on Stage Two Nozzle



CRACKS AND BURNOUT VIEWED FROM FRONT AND SIDE



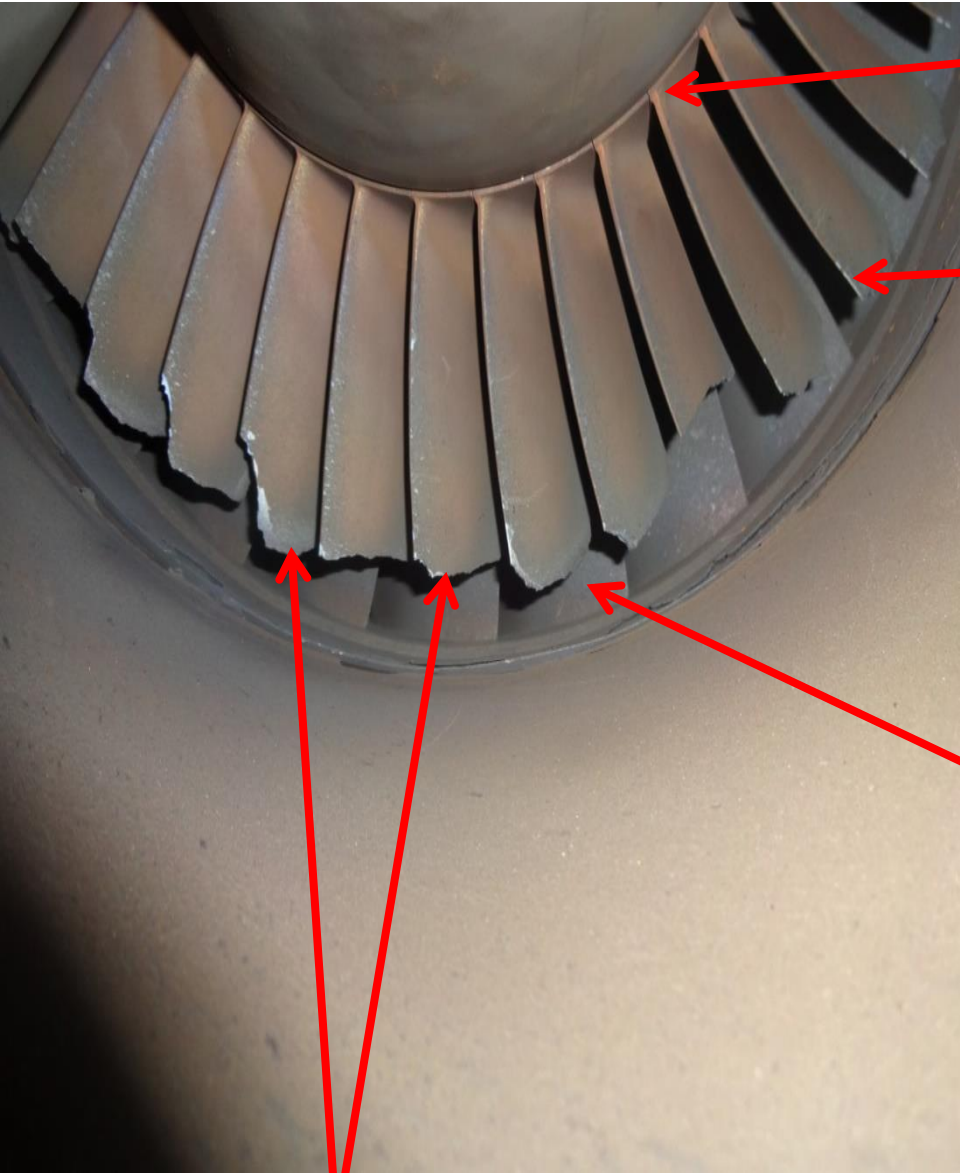
Appendix 32: Photos of Cracks on Stage 2 Stator Blades



Appendix 33: Visual (Boroscopic) Inspection of Engine Turbine Section

NON-DESTRUCTIVE INSPECTION DATA				
1. CONTROL NUMBER 3418			3. MDS	
4. NOMENCLATURE			5. PART OR ASSEMBLY NO. 0279005070	
6. TECHNICAL ORDER NO. TURMOVC MM	PAGE NO.	FIGURE NO.	INDEX NO.	DATE OF ISSUE 03/06/2018
7. NEXT HIGHER ASSEMBLY (noun or part NO) ENGINE HOT SECTION		8. MFR SERIAL NO. (if applicable) 1440	9. INITIATOR NAME & PHONE NO.	
10. DESCRIPTION OF DEFECT/CONDITION OR REASON FOR INSPECTION Engine take off Power Loss.				
11. PART Installed		12. PART PREPARATION (Disassembly, cleaning and materials) - Remove the Ignition Plug to access the turbine section.		
VISUAL (BORESCOPE) INSPECTION				
20. EQUIPMENT USED Everest XG23 Video Probe.				
MANUFACTURE NAME: General electrics	MODEL XG23	NSN MIA.		
PROBE Video probe	GUIDE TUBE USED (0) YES <input checked="" type="checkbox"/> NO	DIAMETER 3.9mm & 6.1mm	TYPE MATERIAL Titanium Construction	
23. INSPECTION PROCEDURE (step by step description of inspection set up) - Power the borescope Machine with the right probe fixed - Remove the ignition plug to get access to the turbine section - Inspect both power turbine and free turbines for defects. N.D.I-SECTION STATUS: Inspected SIGN: [Signature]				
24. SKETCH/PHOTO OF PART (show critical areas, location/orientation of defects) a) turbine burn out due to excess temperature b) Loss of material or broken blades. c) Cracks on the blade roots, leading and trailing blade edges DATE: 03/06/2018				
SEE APPENDIX 22				
25. EVALUATION - During inspection it was observed that there was complete loss or broken blades of both the power and free turbine blades - Recommendation for engine overhaul as per Turmo IVC MM.				
26. POST INSPECTION PROCEDURE - Fit the ignition plug to the access part. - Clean the engine ready for shipment to the dealer.				

Appendix 34: Photos of the broken Free Turbine Blades



BLADE ROOT

FREE TURBINE

STATOR

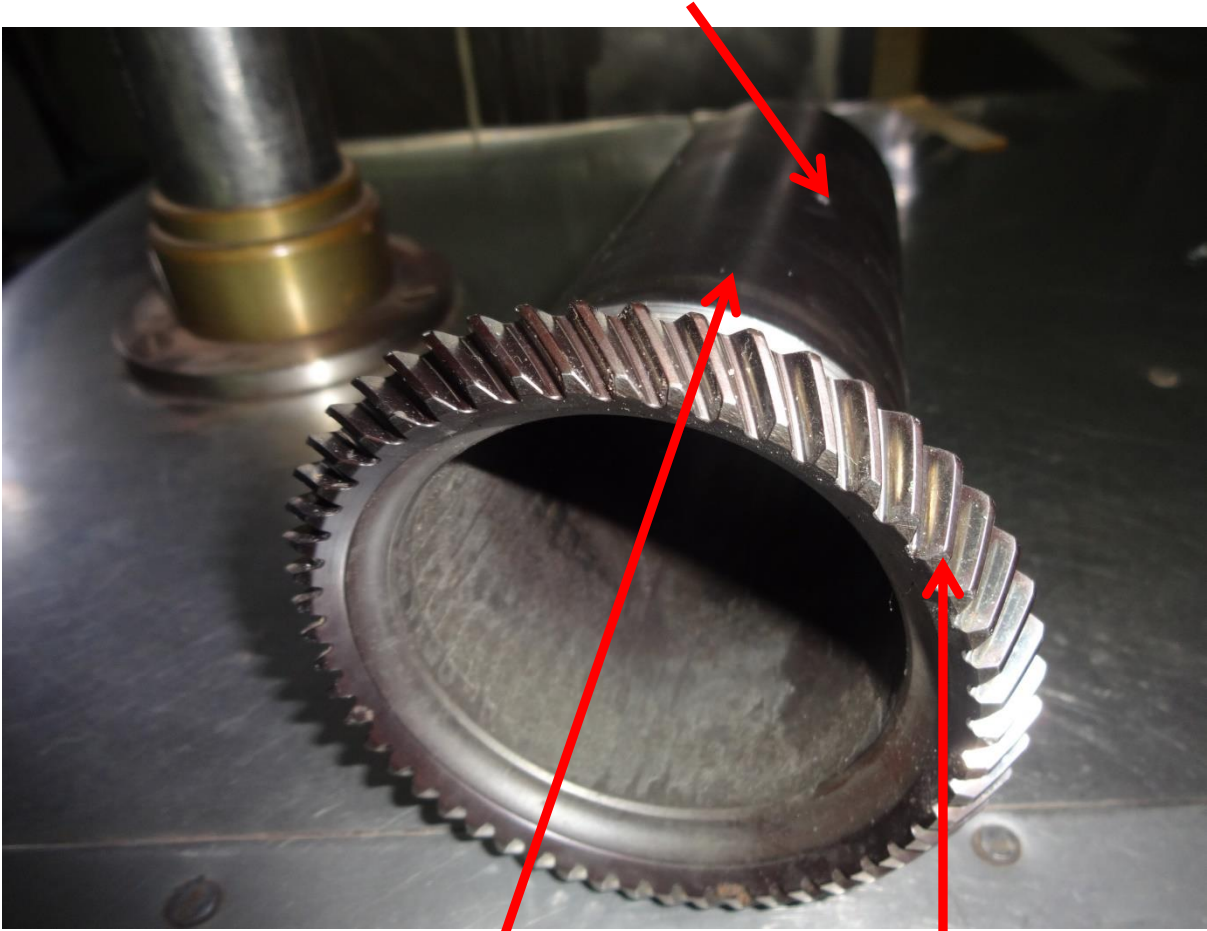
BROKEN TURBINE BLADES TIPS

Appendix 35: MPI of Engine Bevel Shaft Gear

NON-DESTRUCTIVE INSPECTION DATA					28
1. CONTROL NUMBER 03119			3. MDS		
4. NOMENCLATURE PTO DRIVEN BEVEL SHAFT GEAR			5. PART OR ASSEMBLY NO. 000J25-00390B		
6. TECHNICAL ORDER NO. 25-J25-9	PAGE NO. 5-5	FIGURE NO. 5-4	INDEX NO.	DATE OF ISSUE 10/11/2019	
7. NEXT HIGHER ASSEMBLY (noun or part No.) GEAR BOX		8. MFR SERIAL NO. (if applicable)		9. INITIATOR NAME & PHONE NO.	
10. DESCRIPTION OF DEFECT/CONDITION OR REASON FOR INSPECTION - ENGINE CEASED IN FLIGHT.					
11. PART - Removed		12. PART PREPARATION (Disassembly, cleaning and materials) - Loosen and disassemble the gear box from the engine. - Unsecure the the driver and driven gears			
MAGNETIC PARTICLE INSPECTION TECHNIQUE					
18. EQUIPMENT AND MATERIALS					
MANUFACTURER NAME GB Gould Boss	MODEL GB-3509A-01	NSN 6635-01366-6791	WET FLUORESCENT YES		
DRY POWDER MIA	VISIBLE DYE MIA	COLOUR Yellow Green	HOW APPLIED Flowing / Pouring		
19. INSPECTION METHOD (MAGNETIZING METHODS)					
<input checked="" type="checkbox"/> Continuous <input checked="" type="checkbox"/> residual <input checked="" type="checkbox"/> longitudinal d. AC <input checked="" type="checkbox"/> DC <input checked="" type="checkbox"/> circular					
AMPS OR AMP TURNS - 3,500 amps for circular and 8000 amps turns for longitudinal					
INSPECTION PROCEDURE (step by step description of inspection set up)					
- Magnetize the PTO driven bevel shaft gear circular by central conductor. - Magnetize and inspect for transverse cracks longitudinal magnetization. - inspect for transverse and longitudinal defects with fluorescent magnetic suspension and ultraviolet light. - Interpret the defects and record. - Demagnetize the shaft gear.					
24. SKETCH /PHOTO OF PART (show critical areas, location/orientation of defect etc.)			N.D.I. SECTION STATUS... Inspector SIGN... [Signature] DATE... 10/11/2019 APPENDIX 29		
a) Cracks on shaft splines b) Root of the bevel gears c) Bear of bevel gears					
25. EVALUATION - wear of bevel gears beyond limit thus need for replacement.					
26. POST INSPECTION PROCEDURE (DEMAGNETIZATION, POST CLEAN) Demagnetize PTO driven shaft gear to residual magnetism not to exceed 2 gauss using gauss.					

Appendix 36: Photos of PTO Driver Shaft Gear

HOLES ON THE SHAFT



THE SHAFT

BEVEL DRIVER GEARS

Appendix 37: Visual (Magnifying Glass) Inspection of Engine Exhaust Section parts

1					
NON-DESTRUCTIVE INSPECTION DATA					
1. control number 9/19			3.MDS		
4. NOMENCLATURE AFTER BURNER FLAME HOLDER			5. PART OR ASSEMBLY NO. 000J85-183901		
6. TECHNICAL ORDER NO. 2J-I85-98-2J-113		PAGE NO. 9-9	FIGURE NO. 9-5	INDEX NO.	DATE OF ISSUE 10/2/2019
7. NEXT HIGHER ASSEMBLY (noun or part No.) J85-GE-21 ENGINE			8. MFR SERIAL NO. (if applicable)		9. INITIATOR NAME & PHONE NO.
10. DESCRIPTION OF DEFECT/CONDITION OR REASON FOR INSPECTION - due to high Exhaust gas temperatures (High EGT)					
11. PART REMOVED			12. PART PREPARATION (Disassembly, cleaning and materials) - Carbon removal - cleaning I.A.W. To. 2J-1-13		
VISUAL (MAGNIFYING GLASS) INSPECTION					
20. EQUIPMENT USED Magnifying glass					
MANUFACTURE NAME: N/A		MODEL N/A		NSN N/A	
PROBE N/A	GUIDE TUBE USED (0) YES (1) NO 1		DIAMETER (mm) 8.0, 10.0, 13.0 15.0, 18.0, 20.0	TYPE MATERIAL 150-watt standard spot light x 10 power magnifying glass	
INSPECTION PROCEDURE (step by step description of inspection set up) - After cleaning the afterburner let it dry. - inspect cracks in white by use of 150 watt spot light and x10 magnifying glass power.					
24. SKETCH /PHOTO OF PART (show critical areas, location/orientation of defect etc.) a. Along all welded areas b. inner and outer shells c. Right and left vanes d. support arm e. Baffle plates and scoops, Engine deck and Cowling				N.D.I. SECTION STATUS: Inspector SIGN: [Redacted]	
25 EVALUATION 1. Loss of volume of material 2. Cracks originating from the edge of flame holder about 8mm - 20mm					
25. POST INSPECTION PROCEDURES. - Re-inspect the flame holder after welds repair					

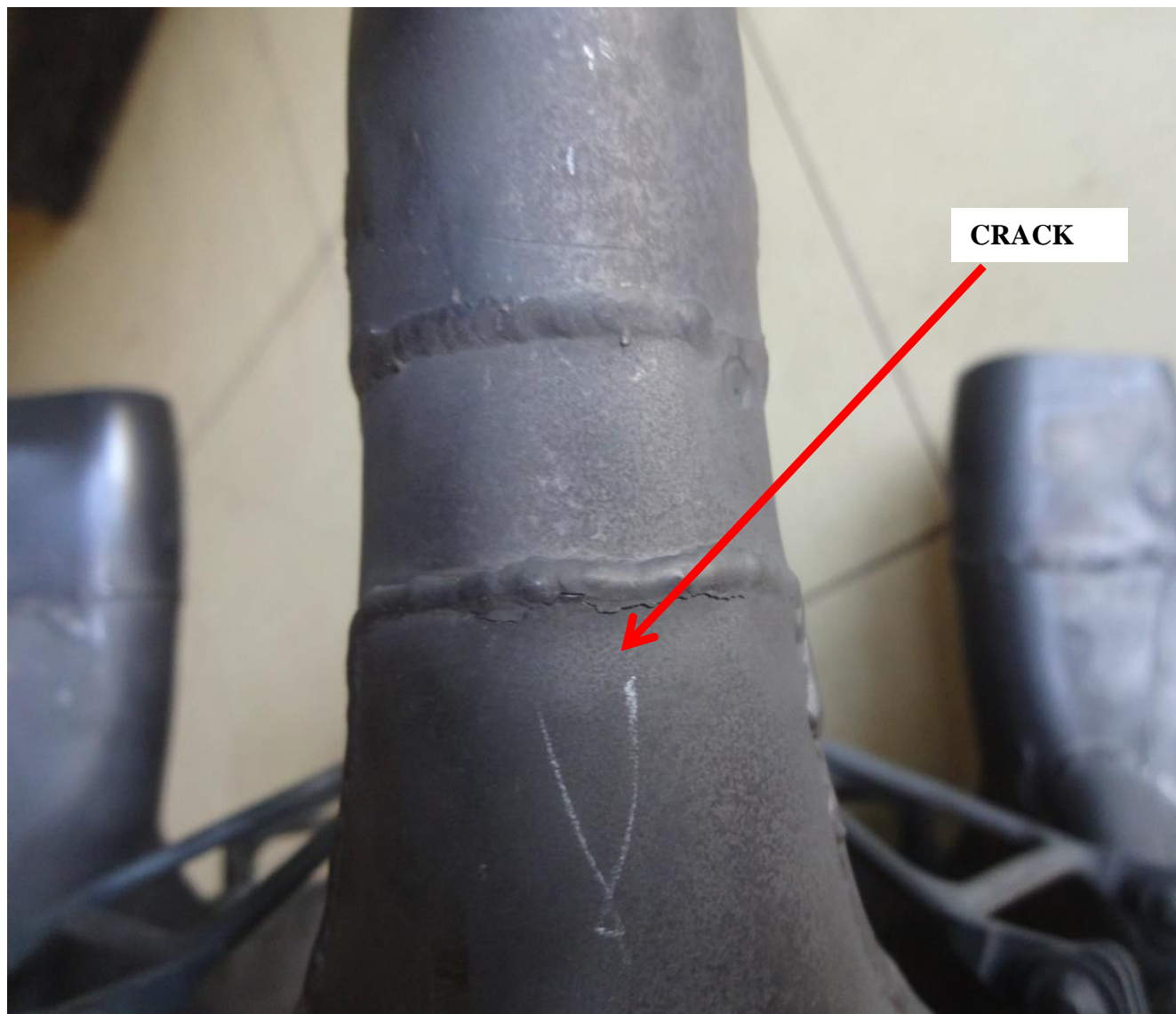
Appendix 38: Photos of Engine Cracked Flame Holder



Appendix 39: Photos of Engine Cracked Flame Holder along the Weld



Appendix 40: Crack on Engine Flame Holder Duct



Appendix 41: Visual (Magnifying Glass) Inspection of Engine Exhaust Section Parts

9				
NON-DESTRUCTIVE INSPECTION DATA				
1. CONTROL NUMBER 9118				3. MDS
4. NOMENCLATURE AFTER BURNER ASSEMBLY			5. PART OR ASSEMBLY NO.	
6. TECHNICAL ORDER NO. 25-585-94 25-1-13	PAGE NO.	FIGURE NO.	INDEX NO.	DATE OF ISSUE 9/7/2018
7. NEXT HIGHER ASSEMBLY (noun or part No.) J85-GE-21 ENGINE		8. MFR SERIAL NO. (if applicable)		9. INITIATOR NAME & PHONE NO.
10. DESCRIPTION OF DEFECT/CONDITION OR REASON FOR INSPECTION - High exhaust gas temperature and engine vibration				
11. PART - installed		12. PART PREPARATION (Disassembly, cleaning and materials) - Carbon removal - Cleaning I.A.W T.O 25-1-13 Process 6		
VISUAL (MAGNIFYING GLASS) INSPECTION				
20. EQUIPMENT USED magnifying glass				
MANUFACTURE NAME: N/A	MODEL N/A	NSN N/A		
PROBE N/A	GUIDE TUBE USED () YES <input checked="" type="checkbox"/> NO	DIAMETER 220mm	TYPE MATERIAL 150-watt standard spot light - X10 Power magnifying	
INSPECTION PROCEDURE (step by step description of inspection set up) - Clean the Afterburner by ice or sand blasting to remove carbon. - Inspect for cracks in white light through X10 magnifying glass - Mark the areas that have cracks.				
24. SKETCH /PHOTO OF PART (show critical areas, location/orientation of defect etc.) - Along all welded areas. See Appendix 10			N.D.I-SECTION STATUS: <u>Inspector</u> SIGN: <u>[Signature]</u> DATE: <u>9/7/2018</u>	
25 EVALUATION - A crack of twenty two centimetres (220mm) along the lower side of the weld was evidenced.				
25. POST INSPECTION PROCEDURES. - Re-inspect the area after TIG welding repair by fluorescent penetrant inspection.				

Appendix 42: Photos of Cracked Afterburner Assembly

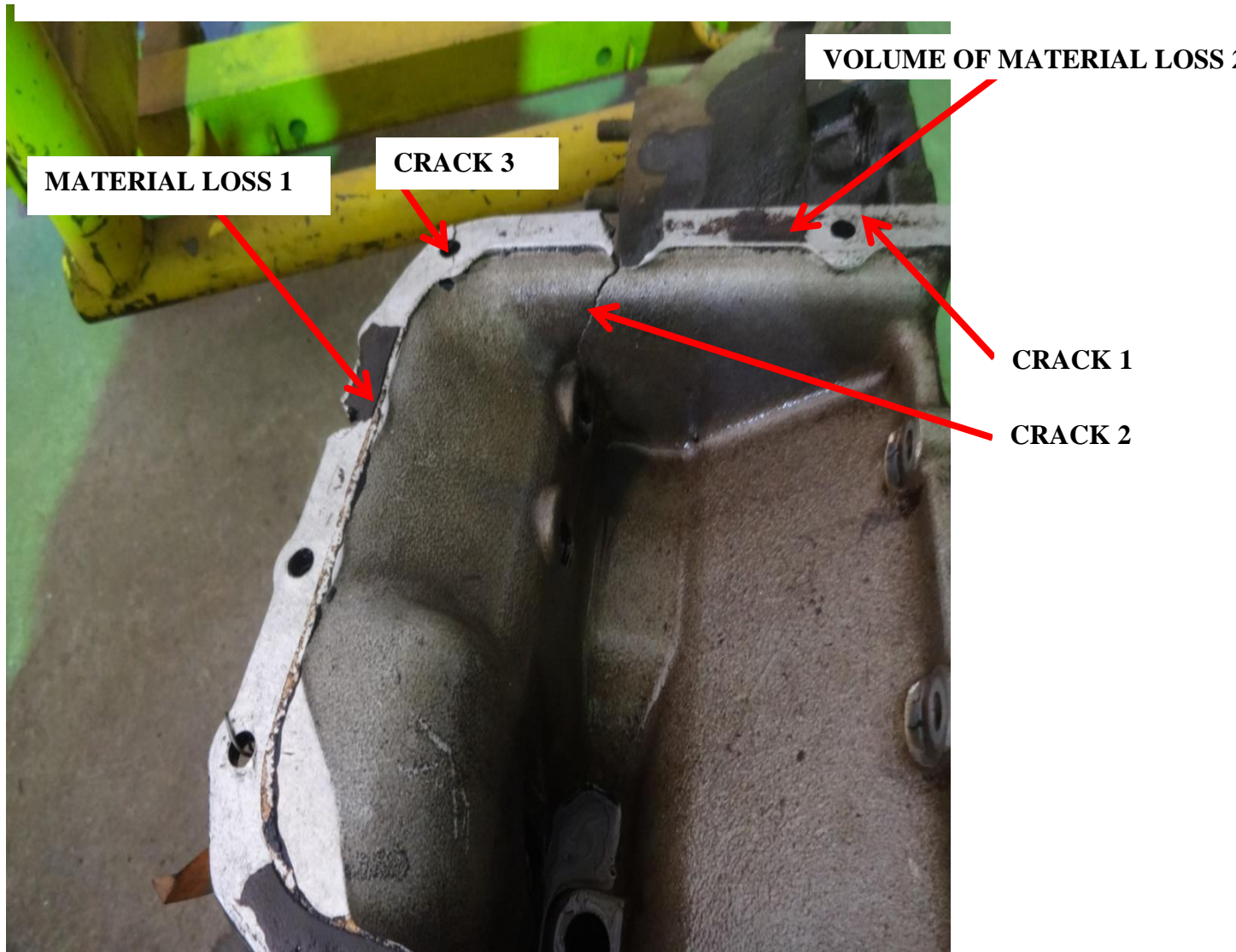
Crack along the weld



Appendix 43: Visual (Magnifying Glass) Inspection of other Engine Parts

NON-DESTRUCTIVE INSPECTION DATA				
1. control number 52/18				3. MDS
4. NOMENCLATURE Oil Sump and Crank case mating Surfaces			5. PART OR ASSEMBLY NO. 10-360-A1B6	
6. TECHNICAL ORDER NO. Overhaul manual 60247	PAGE NO. 8-31	FIGURE NO. 8-2	INDEX NO.	DATE OF ISSUE 15/2/2019
7. NEXT HIGHER ASSEMBLY (noun or part No.) Crank case Assembly		8. MFR SERIAL NO. (if applicable)		9. INITIATOR NAME & PHONE NO.
10. DESCRIPTION OF DEFECT/CONDITION OR REASON FOR INSPECTION → inspection after heavy aircraft landing.				
11. PART - removed		12. PART PREPARATION (Disassembly, cleaning and materials) - loosen the bolts and disassemble the oil sump - clean off the oils and greases by sand blasting.		
VISUAL (MAGNIFYING GLASS) INSPECTION				
20. EQUIPMENT USED Magnifying glass				
MANUFACTURE NAME: MIA		MODEL MIA	NSN	
PROBE MIA	GUIDE TUBE USED (0) YES (10) NO		DIAMETER (mm) 3.0, 5mm, 6.0 8.0, 22.0 25.0 25.5	TYPE MATERIAL 150-watt standard spot light X10 Power Magnifying
INSPECTION PROCEDURE (step by step description of inspection set up) a. open the oil sump and crank case mating surfaces. b. Wet sand blast the sump and surfaces to remove oils and greases c. Inspect the mating surfaces and the entire oil sump.				
24. SKETCH /PHOTO OF PART (show critical areas, location/orientation of defect etc.) 1. Cracks on the mating surfaces. 2. Cracks around the bolt holes. - see appendix B.			N.D.I-SECTION STATUS: Inspector SIGN: [Signature] DATE: 15/2/2019	
25 EVALUATION a. The crank case and oil sump mating surface lower flange had part of the material off. Cracks originating from the bolt holes. b. Cracks on the lower half of the oil sump c. Length of cracks on 3mm, 5mm, 6mm, 8mm, 22mm and 25mm				
25. POST INSPECTION PROCEDURES. The crank case part to be casted because it was beyond repair.				

Appendix 44: Photos of Oil Sump Crank Case Mating Surfaces (Interior surface)



- 1) Crack 1 Length is 5.00 mm
- 2) Crack 2 Length is 22.00 mm
- 3) Crack 3 Length is 6.00 mm
- 4) Material Loss 1 Length is 8.00 mm and Depth of 5.00 mm
- 5) Material Loss 2 Length is 25.00 mm and Depth of 20.00 mm

Appendix 45: Photos of Oil Sump Crank Case Mating Surfaces (Exterior surface)



Appendix 46: Visual (Magnifying Glass) Inspection of Engine Parts

NON-DESTRUCTIVE INSPECTION DATA					
1. control number 14/19					3. MDS
4. NOMENCLATURE DIFFUSER CASING			5. PART OR ASSEMBLY NO. 000J85-183901		
6. TECHNICAL ORDER NO. 21-J85-9 & 2J-1-13	PAGE NO. 9-3	FIGURE NO. 9-3	INDEX NO.	DATE OF ISSUE 26/3/2019	
7. NEXT HIGHER ASSEMBLY (noun or part No.) ENGINE		8. MFR SERIAL NO. (if applicable)		9. INITIATOR NAME & PHONE NO.	
10. DESCRIPTION OF DEFECT/CONDITION OR REASON FOR INSPECTION - High TS and Exhaust gas temperature					
11. PART - removed		12. PART PREPARATION (Disassembly, cleaning and materials) - Carbon removal - Cleaning IAW T.O 2J-1-13 process 6			
VISUAL (MAGNIFYING GLASS) INSPECTION					
20. EQUIPMENT USED Magnifying glass					
MANUFACTURE NAME: M/A		MODEL M/A	NSN M/A		
PROBE M/A	GUIDE TUBE USED () YES (x) NO		DIAMETER 0.0 mm	TYPE MATERIAL - 150-watt standard spot light - X10 Power magnifying	
INSPECTION PROCEDURE (step by step description of inspection set up) - The diffuser casing is cleaned by ice blasting or vapour blast to remove carbon - inspection carried out in white through X10 magnifying glass					
24. SKETCH /PHOTO OF PART (show critical areas, location/orientation of defect etc.) - seam welded areas - igniter boss weld area - forward and aft flanges - transition mount pads see appendix 8			N.D.I-SECTION STATUS... Inspector SIGN... [Signature] DATE... 26/3/2019		
25 EVALUATION - NO cracks found on critical areas as stated in section 24 above					
25. POST INSPECTION PROCEDURES. - Re-inspect the diffuser casing after weld repair has been done. but for these case no repair was done as there was no cracks.					